LISTE OF FIGURES

CHAPTER 5

LISTE OF TABLES

CHAPTER 1

INTRODUCTION

1.1 PROBLEM

1.1.1 General Problem

Dykes are described by Pollard (1987) as vertical, or nearly so, sheet intrusions (tabular bodies) that cut discordantly the host rocks and are used as conduits for molten rock involved in heat and mass transport throughout the crust (figure 1.1).

Figure 1.1: Simplified schematic image model showing the general context of the dyke emplacement (modify from Best, 2002).

Dyke swarms are defined as numerous coeval dykes emplaced during a single event and the number can vary from tens to hundreds. Dispersion

patterns vary according to the environment in which the dykes are emplaced in, and are controlled by different factors. These intrusions can occur in a wide variety of geologic and tectonic settings (i.e. divergent and convergent plate boundaries and intraplate environments) as in figure 1.2. Geometry and dispersion of the swarms, at the regional scale are controlled by the regional stress fields (Nakamura, 1977; Chadwick and Howard, 1991: figure 1.3) and gravitational stress in volcanic edifices (Fiske and Jackson, 1972).

Swarms can be irregular or they can follow a preferential orientation, where controlled by a horizontal stress field in extensional regimes, or as ring and radial dykes swarms where associated with sub-volcanic magma chambers related to volcanic edifices or central intrusive complexes (Ernst et al., 1995). Where related to volcanic edifices, some dykes are feeders to lava flows. They can be classified in three main patterns according to their topology, tectonic setting, and their composition: 1) regional or linear (figure 1.3A), 2) circumferential (figure 1.3B), and 3) radial (Acocella and Neri, 2009: figure 1.3C). The circumferential (concentric) and radial types of dykes swarms are documented in several studies, it occurs in the Slieve Gullion district in Ireland (Anderson, 1937), in the Fernandina volcano in Galapagos Islands (Acocella and Neri, 2009) and associated with an intrusive centre related to the Spanish Peaks, on Iceland (Gudmundsson, 1983). Even if the swarm is not presented as a radial and/or concentric pattern, they have an orientation associated with the structure of the intrusive centre (Ernst et al., 1995).

Figure 1.2: Schematic model that represents dyke emplacement in extensional and compressional regimes (modified from Best, 2002).

Figure 1.3: Patterns of dyke swarms: A) Linear (Regional) pattern in the Erta Ale rift zone, Ethiopia (Acocella and Neri, 2009); B) Radial pattern of Mackenzie dykes in the Northwest Territories, Canada (Ernst, et al., 1995); C) Concentric and radial pattern in Fernandina volcano, Galapagos Islands (Acocella and Neri, 2009).

Dykes may also form as a late magmatic stage commonly associated with mafic to granitic intrusions. This type of dyke is known as aplite, which are fine-grained to phaneritic leucocratic tabular intrusions associated with plutons. They are residual melts drawn into self-generated extensional fractures in the cooling and contraction within the intrusions (Best, 2002). Dyke morphology is controlled by 1) the elastic deformation of the country rock, and 2) the viscous resistance to flow which is also related to the fracture resistance of the host rock (Turcotte et al., 1987).

Textures, structures and the petrology of the dykes result of different factors. They are initially affected by the composition, the process of emplacement, characteristics of the host rock, and the tectonic environment. After emplacement, other contributing factors such as cooling rates, hydration, devitrification, hydrothermal alteration, and metamorphism may affect dykes. Detailed description of these features is used to determine the various processes involved during emplacement. The table 1.1 contains cited examples where distinct processes are interpreted from different types of textures and structures. It is also important to note that some of the features associated with dyke emplacement are analogous to textures observed during cooling of volcanic rocks.

Table 1.1: Textures and structures associated with dyke emplacement and later processes.

References	Davis and McPhie, 1996	Mueller and Donaldson, 1992	Dostal and Mueller, 1996	Hanson and Schweickert, 1982	Simons, 1962	Goto and McPhie, 1996
Location	Central Queensland, Australia	Hunter Mine Group South-central part of the Abitibi greenstone belt		Northern Sierra Nevada, California, USA	Klondyke quadrangle, Arizona, United States	Stanley dyke, Northwestern Tansmania, Australia
Article Description	Determine the textures and structures associated with quench and devitrification process of a rhyolitic dyke.	Describe textures formed during dyke emplacement		Describe peperite texture in a sill, and determine controlling factors	Determine texture formed during dyke emplacement	Describe peperite texture formed during the dyke emplacement into wet, poorly consolidated sediments
Composition	Rhyolite	Rhyolite		Rhyolite	Rhyolite	Basanite
Age	Late Devonian	Archean		Mesozoic	Late Cretaceous to early Tertiary	Miocene
Width/Length		1.5 km/2.5 km dyke swarm average			12 m/275 to 305 m	2 m/8 m minimum
Orientation	N-S strike	N-S strike		Subhorizontal		350 strike
Geologic Context	Dykes intruded into Silver Hills Volcanics, Drummond Basin	Dykes intruded in subaqueous volcanic rocks		Dykes intruded into welded sediments	Dykes intruded into welded vitrophyric welded tuff	Dyke intruded in to basaltic breccia
Cooling Products	Dispersed magnetite microlites and small spherulites accentuating a flow foliation. Long fractures perpendicular to the dyke margin (rapid chilling), and orthogonal fractures (further cooling) delimited by the long fractures.	Sinous, curvilinear, radial and straight columnar joints, and chilled margin (hyaloclastite)		Flow banding, flow brecciation, branching cracks and a spherulitic domain above the peperite borders	Fissures along the borders	Quenched glassy rims, jig-saw-fit textures, ellipsoidal vesicles and flow banding parallel to the contact
Hydration Products	Perlitic fractures due to the rapid cooling contraction and volume changes, delimited by the long and cross fractures.			Perlitic fractures		Perlitic fractures due to the rapid cooling contraction and volume changes
Devitrification Products	Axiolitic K-feldspar along the fractures and polygonal coarse grained quartz-oligoclase mosaic between the fractures.	Spherulites and orb texture in groundmass			Spherulite formation, in both dykes and host rock	
Hydrothermal Products		Sericite and Chlorite			Potassium bearing minerals	Carbonate fill the perlitic fractures
Metamorphic Facies	Prehnite-pumpellyite regional metamorphic facies, locally greenschist facies.	Greenschist regional metamorphic facies		Not described, but occurs and the textures are preserved		

Dykes are commonly associated with economic concentrations of metals. Dykes can play different roles in the mineralization process for distribution such as conduits, barriers, or as receptacles for hydrothermal fluids. According to the hydrothermal fluid source and the role of dykes for the mineralization, resulting deposits can be classified in three main types: 1) magmatic, 2) volcanogenic and 3) late. In deposits with complex geologic evolution, it can be difficult to attribute a main mineralization event due to superimposed processes. However, more important than the division itself, it is important to precise the role of the dykes in the mineralization processes. The main features for each type of deposit are summarized in table 1.2, with subsequent discussion below.

Table 1.2: Summary of dykes related deposits according to the hydrothermal fluid source and the role of dykes.

Type	Magmatic Porphyry Syenite	Volcanogenic		Later	Later (vein-type)
Occurrence	Canadian Malartic	Géant Dormant	Chevrier	Troilus	Sigma
Authors	Sansfaçon et al., 1987	Gaboury and Daigneault, 1999 Gaboury and Daigneault, 2000 Gaboury et al., 2000	Legault and Daigneault, 2006	Fraser, 1993 Goodman et al., 2005	Robert and Brown, 1986 Gaboury et al., 2001
Location	Piché and Pontiac groups at the south-eastern part of the Abitibi greenstone belt	Northern Volcanic Zone of the Abitibi Sub province	Chevrier volcanic center at the north-eastern part of the Abitibi Sub province	Frotet-Evans greenstone belt, Opatica sub province of the Superior province	Malartic group at Val d'Or area at the south-eastern part of the Abitibi greenstone belt
Age		U-Pb zircon 2722 ± 2 Ma for QFP	U-Pb zircon 2730 ± 10 Ma for rhyolite sill	U-Pb zircon 2791 ± 1.6 Ma for metadiorite	U-Pb age of 2694 ± 2 Ma for feldspar porphyry dykes
Dykes	Felsic (Syenite) and mafic (diorite) dyke swarm, porphyries or not	Plagioclase porphyry (FP) Quartz and plagioclase porphyry (QFP)	Quartz porphyry, Quartz and feldspar porphyry, and Feldspar porphyry	Aphanitic and foliated felsic dykes and weakly foliated mafic dykes	Feldspar porphyry dykes, and late diabase dykes
Host Rock	Komatiitic and basaltic lava flow intruded by syenite and diorite intrusions	Volcano-sedimentary sequence intruded by a calc-alkaline felsic complex	Felsic to intermediate volcanoclastic/lava flow cut by sills and dykes	Intermediate to mafic calc-alkaline metavolcanic rocks, intruded by diorite pluton, felsic and mafic dykes	Metavolcanic rocks intruded by porphyritic diorite, and undeformed feldspar porphyry dykes
Tectonic Context	NW Cadillac fault	Extensional Regime	NE trending deformation corridor	Thrust-bounded domain	
Depth	Shallow	~ 2 to 3 km	Shallow	Shallow	Medium
Metamorphic Facies	Lower Amphibolite facies	Greenschist facies	Greenschist facies	Upper greenschist to lower amphibolite facies	Greenschist facies
Deformation	NW-SE foliation	E-W volcanic strata strike, dip to south, sub vertical E-W regional schistosity	East-west foliation	Penetrative foliation dip steeply to the northwest	East-west foliation with average dip of 80° to north
Alteration	Quartz, carbonate (calcite and ankerite), sericite, chlorite, biotite and scheelite	Chlorite, sericite, tourmaline, calcite and actinolite	Carbonate (ankerite and calcite), sericite, and chlorite	Biotite; Albite-epidote-chlorite (propylitic), sericite, quartz and tourmaline	Biotite, chlorite, sericite, carbonate, quartz and tourmaline
Steps	Single event	3 different steps	Single event	2 - disseminated and vein-hosted mineralization	1 step of veins emplacement
Mineralization Style	Disseminated and quartz veins associated to the intrusions and the dykes at the shear fault contact between the Piché and Cadillac groups	Quartz-sericite flat veins stacked vertically along QFP dyke conduits in a volcanogenic and epithermal environment	Discordant quartz-carbonate veins and disseminated pyrite within melanocratic gabbro dykes. And concordant pyrite envelope associated with quartz-carbonate-pyrite veinlets	Disseminated grains, streaks along the foliation, and concordant and discordant veins and veinlets. Hosted at brecciated unit, amphibolite and felsic dykes, locally at the metadiorite and the mafic dykes	Stringer, sub vertical and flat veins associated to the shear zones, to the intrusion, and the feldspar porphyry dykes
Mineralization	Pyrite, pyrrhotite, chalcopyrite, galena, sphalerite, molybdenite, silver and gold	Pyrite, pyrrhotite, chalcopyrite, sphalerite, arsenopyrite, and gold	Pyrite and gold	Electrum and native gold, in association with pyrite, pyrrhotite, chalcopyrite, sphalerite, and telluride	Pyrite, pyrrhotite, scheelite and free gold
Dyke's Role	Both dykes, but mainly the mafic members are used as fluid conduits	QFP dykes are fluid conduits connected with a sub volcanic magma chamber	Quartz Porphyry dykes are fluid conduits connected with a sub volcanic magma chamber	Felsic dykes are passive barriers to fluid flow and conduits for hydrothermal fluids	Feldspar porphyry dykes used as host rock for the veins due the competence contrast

1.1.1.1. Magmatic deposits

This class constitutes a type of deposit where the metal source is magmatic as the intrusion-related deposits and the porphyries. The dyke swarms are usually associated with a central intrusion and represent conduits for hydrothermal fluids originating from the magma chamber. Mineralization usually occurs in quartz and carbonate veins within dykes and country rock, but also occurs as disseminated sulfide mineralization. Gold, silver, and copper are some metals that are commonly associated with this process. Lang and Baker (2001) classified this type as intrusion-related gold systems. In this classification, there is a distinct subgroup represented by the Au-Cu-Mo-W-Bi-(As-Te) Kidston mine in Australia, where the deposit is hosted in breccias associated with dykes and sills (Baker and Andrew, 1991). Another example is the Canadian Malartic mine (Sansfaçon et al., 1987) in Québec, Canada (table 1.2).

1.1.1.2 Volcanogenic deposits

Volcanogenic massive sulfides deposits (VMS) are the most studied type of this group, but it is not the only type. Another important type of mineralization is associated with dyke swarms related to volcanic centers. Mineralization is directly related to the dyke systems, which are conduits connected to the sub-volcanic magma chamber, serving as feeders for lava extrusion. Hydrothermal fluids rising from the chamber are commonly composed of mixed fluid sources that have both

magmatic and seawater signatures. Metals associated with these processes are generally gold, silver, copper, zinc, and lead. They usually occur hosted in quartz and/or carbonate veins and stringers around the dykes, but are also disseminated in the dykes and volcanic rocks. Two classical examples of this type are Géant Dormant mine and Chevrier deposit, both located in the Abitibi greenstone belt, Québec, Canada (table 1.2).

1.1.1.3 Late deposits

Late deposits represent all deposits that cannot be classified as magmatic or volcanogenic. In this class, dykes can exercise a different genetic role in the mineralization process. As example, the Sigma gold mine (table 1.2) in the Abitibi greenstone belt (also classifies as G-dyke style) have a system of flat veins, where dykes are the host rock. The hydrothermal fluids are commonly associated with late metamorphic events that remobilize metals. The competency contrasts between dykes and the country rock act as the control for fluid flow.

Another role attributed to late dykes is the barrier to contain and focus hydrothermal fluids in a preferential corridor. This was proposed at the Troilus gold mine (Goodman et al., 2005: table 1.2), where the hydrothermal fluids associated with a later metamorphic one percolated through the more permeable host rocks and stopped at the boundary with the less permeable dykes. As a result, dykes are both the footwall and the hanging wall for the mineralization.

In all these examples, the compositions of the dykes are clearly not a criterion for establishing mineralization origin. The most important components are the fluids, their source and geometry, as well as the texture and structure of the dykes. Additionally, the dyke components are linked with the environment in which these sheet intrusions are emplaced.

1.1.2 Specific Problems

Monsabrais is a volcanic centre located in the Blake River Group of the Abitibi greenstone belt in the Superior Province of Canada, where the regional metamorphism reaches subgreenschist facies (Powell et al., 1993). The volcanic sequences are dominated by submarine mafic to intermediate lavas, with massive to pillowed lavas, as well as volcaniclastic rocks (Ross et al., 2008), and intruded by the Monsabrais pluton. The units are crosscut by fine to medium grained gabbroic, monzogabbroic and dioritic ring dykes. These rocks are considered as the magmatic roots of a subaqueous summit caldera (Mueller et al., 2009).

Fieldwork and geochemistry indicates that the Monsabrais pluton is a multiphase intrusion ranging in composition from tonalite to quartz diorite with U-Pb zircon age of 2696.2 ± 0.9 Ma (Ross et al., 2008) and 2696.3 ± 1.3 Ma (Mueller et al., 2007). Geochemical analyses of the volcanic units indicate basaltic to andesitic composition with transitional to calc-alkaline characteristics, but there is no clear

field relationship between the volcanic facies and the intrusive units (Ross et al., 2008).

The geometry and cross-cutting relationships of the dykes and the pluton are thought to represent the feeder system and sub-volcanic magma chamber, respectively. No detailed studies have been done in the area to determine the relative chronology between the pluton, the dykes, and the extrusive rocks, as well as the role played by the dykes for the mineralization observed in the region. Similarities between Monsabrais and other mineralization sites (table 1.2) support the possibility of mineralization related to the intrusive rocks, and more specifically to the dykes.

Detailed studies regarding the dykes, the pluton, and the mineralization at Monsabrais need to be focused on field relationships, petrology and geochemistry. This analysis will allow for the establishment of the different phases of dykes, and how they are associated to the pluton, the construction of the volcanic pile and the mineralization. With this, it should be possible to determine the role of the dykes, such as primary conduits associated with the intrusion, with the volcanism, or just a physical barrier for late metamorphic fluids.

1.2 OBJECTIVE

The main objective of this project is to determine the different elements of magmatism, fracturing, and mineralization in the Monsabrais sector and place them in an appropriate metallogenic context. To achieve this it is necessary to:

1) Characterize dykes as families based on their specificities.

2) Establish the variety and characteristics of the mineralizations and hydrothermal alteration assemblages.

3) Determine the relative chronology for the dykes emplacement and mineralization episodes.

4) Place the mineralizations and the dykes in a metallogenic context.

The proposed specific objectives should provide the appropriate approaches to settle the problems. They are based on the compilation of older cases with similar geological problems.

1.3 METHODOLOGY

To accomplish the described objectives, it is necessary to define the methodological approach, which is described below and summarized in table 1.3. To establish the relationship between dykes, fractures, and mineralization at Monsabrais, it is necessary to divide the main objective in specific objectives and resolve each one with associated techniques. These techniques may be divided in 2 parts: 1) field work in the Monsabrais area and 2) laboratory and synthesis at UQAC.

The field work consists of systematic mapping and sampling of the Monsabrais sector. Geologic mapping is focused on textures, structures and crosscutting relationships between dykes, extrusive volcanic rocks and the Monsabrais pluton, as well as hydrothermal alterations and mineralization phases.

Laboratory work comprises distinct stages and different techniques. The first stage involves sample preparation including cutting, crushing and pulverizing, while the second stage consists of implementing the various analytical techniques described below. The petrography and the lithogeochemistry (major, trace and REE element) analysis are used to assign the dykes to different families, and characterize the mineralization and alteration phases. The methodology is led below, where the techniques are described in relation to specific objectives outlined for the project.

Table 1.3: Objectives and methodology.

Purpose	Objectives	Methodology	Equipment
The genetic role of dykes on the mineralization of the Monsabrais area	Characterize dykes as families based on their specificities	Mapping and systematic sampling	Field
		Petrographic and Mineralogic analysis	Petrographic Microscope (UQAC)
		Lithogeochemical analysis	ICP-MS and XRF (ALS-Chemex)
	Establish the variety and characteristics of the mineralizations and hydrothermal alteration assemblages	Mapping and systematic sampling	Field
		Petrographic and Mineralogic analysis	Petrographic Microscope (UQAC)
		Lithogeochemistry analysis	ICP-MS and XRF (ALS-Chemex)
		Sulfide elements analysis	LA-ICP-MS (UQAC)
	Determine the relative chronology for the dykes emplacement and mineralization episodes	Mapping and systematic sampling	Field
	Place the mineralizations and the dykes in a metallogenic context	Data integration	UQAC

1.3.1. Determination of different families of dykes

The first approach used in determining distinct families of dykes is field work. Important characteristics to observe are the mineralogy, where possible, primary

textures and structures usually at the borders, the dyke geometry, and the crosscutting relationships between them and the other units.

Subsequent petrographic observations with a microscope are important in classifying the different families according to primary mineral and hydrothermal alteration phases. Microscopic textures and structures can also reveal parameters about the emplacement and deformational history. Lithogeochemical analyses of major and trace elements analyzed by XRF and ICP-MS were performed by ALS-Chemex. Resulting data are used to determine the magma composition, affinity, and signatures of trace and REE elements in relation to tectonic setting. The lithogeochemistry and the mineralogical classification are complementary and permit a better division of dykes based on more than one characteristic.

1.3.2. Variety and characteristics of the mineralization and alteration assemblages

Geological mapping permits the determination of the characteristics and distribution pattern of the hydrothermal alteration and mineralization in the area. Field work is one of the most important components because observations can be used to determine which units are associated with mineralization. These observations are important criteria to determine if the mineralization is syn or post dyke emplacement. However, if the terrain is geologically complex, it is commonly necessary to use other techniques to establish these relationships.

Detailed description of the petrography and mineralogy is important to characterize the mineralization, such as 1) the sulfide composition, 2) alteration phases, and to establish, which metamorphic mineral assemblages are in equilibrium with the sulfides. Lithogeochemistry will be used to determine field anomalies, distribution patterns, and to characterize the composition of alteration and mineralization phases. Through these chemical analyses, it is possible to compare the least and most altered samples and determine what elements are defining the hydrothermal alteration and how this is reflected in the mineralogy.

Laser inductively coupled plasma emission mass spectrometry (LA-ICP-MS) is a tool for trace element analysis with a very low detection limits and good accuracy and precision (Rollinson, 1993) over a small sampling area. It is possible to quantify the trace elements in the sulfides and determine the signature of the mineralization.

1.3.3. Relative chronology for the emplacement and mineralization episodes

To determine the relative chronology between dyke emplacement and mineralization events, it is necessary to conduct a systematic mapping to determine the crosscutting relationships between the dykes, the pluton, the volcanic rocks, the mineralization and various structural elements. Observations of the geometry of the dykes and their border textures provide informations about emplacement processes, rheological regime and temperature exchange between

the dykes and the host rock. Additionally, the distribution pattern of sulfide mineralization associated with different units helps to understand their relationship.

1.3.4. Metallogenic context of the mineralization and the dykes

The last topic brings together all the other objectives, and constitutes a data compilation from the dykes, the other lithologies, the crosscutting relationships, the hydrothermal alterations, and the mineralizations resulting from observations made in the field, petrological descriptions, geochemical interpretations, and the established relative chronologies.

For this stage, the data provided from the different sources are compiled and contrasted, and a metallogenic history can be proposed. The evolution is explained according to the magmatic events that formed the dykes, the pluton, the volcanic rocks, the hydrothermal alterations and the mineralizations.

1.4 REGIONAL GEOLOGY

1.4.1 Abitibi Subprovince

The Abitibi Subprovince is an archean greenstone belt (Goodwin and Ridler, 1970) with a superficial area of 300x700 km (figure 1.4) divided in the northern (NVZ) and the southern volcanic zones (SVZ) and delimited by the east trend

major fault of Destor-Porcupine-Manneville (DPMFZ) (Muller et al., 1996). The Abitibi greenstone belt is composed by a volcano-sedimentary terrain associated to syn-volcanic and syn-tectonic intrusions, resulting from the collision of oceanic arcs with numerous arc-building and arc-fragmentation phases evolved during 2735 and 2670 Ma (Mueller et al., 2009).

The economic importance of the subprovince is related to the presence of several VMS deposits widely distributed in the Abitibi territory and the gold deposits located mainly along the major fault zones.

Figure 1.4: Geological map of the Abitibi greenstone belt (Daigneault et al., 2004).

1.4.2 Blake River Group

The Blake River Group, located within the southern volcanic zone of the Abitibi greenstone belt (figure 1.5), is constituted predominantly by mafic volcanic rocks, local felsic volcanic centers and a serie of plutons (Dimroth et al., 1982). The regional metamorphism that affects the supracrustal rocks (>2677 Ma) in the Rouyn-Noranda area varies from northwest to southeast as subgreenschist facies to greenschist-amphibolite facies transition respectively (Powell et al., 1993).

Pearson and Daigneault (2009) defined the Blake River Group as a megacaldera complex comprising three caldera events: 1) Misema; 2) New Senator; and 3) Noranda (figure 1.5). This interpretation is based on five main parameters: 1) radial and concentric dykes swarms distribution; 2) dome geometry from all the complex; 3) subaqueous volcaniclastic units on the periphery; 4) carbonate alteration distribution; and 5) syn-volcanic inner and outer ring faults.

Figure 1.5: Blake River Group geology with the syn-volcanic structures from Pearson and Daigneault (2009).

1.4.3 Monsabrais Volcanic Complex

The Monsabrais Complex (figure 1.6) is situated in the northwester part of the Blake River Group and is also denominated as Monsabrais Lake (Dimroth et al., 1982). This terrain is constituted by vesicular and plagioclase microphyric basalt and andesite flows with massive, pillow lavas and monolithic pyroclastic breccias facies (Dimroth et al., 1982). The volcanic sequence is cored by syn-volcanic tonalite to quartz diorite plutonic suite of Monsabrais and accompanied by ring dyke system of basaltic to andesitic composition (Dimroth et al., 1982; Ross et al., 2008; Pearson and Daigneault, 2009), and the stratigraphic sequence is subhorizontal (Castillo-Guimond, 2012). The metamorphic grade on these rocks is subgreenschist facies, locally higher at the proximity of the pluton (Powell et al., 1993).

U-Pb analysis from tonalite and leucotonalite phases of the Monsabrais pluton indicate crystallization ages of 2696.2 ± 0.9 Ma (McNicoll et al., in Ross et al., 2008) and 2695 ± 2.8 Ma (Mueller et al., 2012), reciprocally to the magmatic suite. A diorite phase and a pegmatoidal pocket of quartz-amphibole-plagioclase from the ring dyke system yield U-Pb ages of 2701.1 ± 1.2 Ma and 2698.7 ± 1.1 Ma respectively (McNicoll et al., in Ross et al., 2008).

Dimroth et al. (1982) interpreted the lava flows and the pyroclastic rocks of the Monsabrais and the Renault complexes as resulting from simultaneous subaqueous eruptions from two different volcanic centers. Ross et al. (2008) described the volcaniclalstic rocks as predominantly hyaloclastite and flow breccias. These rocks were recently interpreted as remnant summit calderas, in which the ring dykes are the roots of superficial aligned and overlapping summit craters (Mueller et al., 2009). According to Pearson and Daigneault (2009), the formation of the Monsabrais complex was simultaneous with the formation of the Misema caldera.

There are numerous showing of Cu-Zn-Au disseminated sulfide mineralizations occuring in the area and associated with dykes. This area is thus a natural laboratory to test the genetic link between dykes and mineralizations in a volcano-plutonic setting, overprinted by metamorphism and tectonic.

Figure 1.6: Geology of the area of Monsabrais area (Ross et al., 2008).

CHAPTER 2

LOCAL GEOLOGY

2.1 INTRODUCTION

The project terrain is a 1.7 km^2 area located at the Southwest of the Monsabrais pluton, situated at the Northwest border of the Blake River Group (BRG). The sector comprises a series of andesitic and basaltic volcanic rocks crosscut by the Monsabrais Pluton at north and a series of subvertical NS oriented dykes (figure 2.1).

This chapter presents and discusses the results of the field work, petrography and lithogeocheomistry of the dykes and the hydrothermal alteration. The volcanic units are part of the Master's project of Castillo-Guimond (2012) and are complimentary with the current project. An overview of these host rocks is essential to the full comprehension and later comparison with the intrusive units, although a detailed description and discussion is absent in this manuscript.

Figure 2.1: Geological map of the Monsabrais sector.

The Monsabrais area corresponds to a mafic to intermediate volcanic sequence formed by massive flow, pillow lavas and volcaniclastic rocks crosscut by two major gabbroic dykes. Those rocks are crosscut at the north by a gabbro to granodiorite magmatic suite named Monsabrais pluton and the felsic aplitic dykes associated with this. The dykes swarm crosscut all the others lithologies and are composed by equigranular and porphyritic dykes of gabbro to granodiorite composition.

Quartz-carbonate veins occur locally on the area, hosted in the volcanic rocks and bearing pyrite, pyrrhotite and chalcopyrite. These sulfides also occur as amygdules or disseminated in the volcanic sequence and some dykes. The hydrothermal alteration is weak, however present over all the lithologies. The hydrothermal overprint is characterized by the presence of albite, amphiboles (actinolite and hornblende), chlorite, epidote, quartz, white mica (sericite), and carbonate.

The figure 2.2 shows all the GPS point stations taken during the mapping. The outcrops without point were also mapped but the GPS points basically represent the dyke's occurrence. The figure 2.3 shows the location where samples have been subjected to further laboratory characterization.

Figure 2.2: GPS point stations distribution on the Monsabrais sector.

Figure 2.3: Sample distribution on the Monsabrais sector.

2.2 VOLCANIC ROCKS

The volcanic units are spread all over the studied area and represent the main rock pile exposed. Based on the lithogeochemistry, they are classified mainly as andesitic basalt to andesite. The presence of amygdules and microphenocrysts is common.

This section presents a brief and general description of the volcanic sequence. The extrusive rocks observed are subdivided in three facies based on their textural character: 1) massive flows; 2) pillow lavas; and 3) volcaniclastic rocks.

2.2.1 Massive flows

The massive flows (figure 2.4A) are the less outcropping of all the volcanic facies, appearing just in two northern locations near to the Monsabrais pluton border. They are basalt to andesitic basalt massive cores surrounded in both cases by pillow lavas. This facies is aphanitic and porphyritic to seriate and commonly amygdaloidal. The matrix is aphanitic to fine-grained, constituted by plagioclase, quartz, chlorite, epidote and smectite. The plagioclase crystals occur as laths and microlites.

The plagioclase phenocrysts are euhedral to subhedral (7-20%), with a sub-rounded shape forming clusters (figure2.4B). Some of those phenocrysts present concentric annular zonation (figure 2.4C). In some cases, the plagioclases are relicts and are partially to completely altered to epidote and white mica. The vesicles have rounded to sub-rounded shape and are filled by carbonate, epidote, chlorite and quartz (figure

2.4D). The chlorite is lamellar and may be found lined at the contact. The epidote is prismatic and the carbonate and the quartz are anhedral.

Figure 2.4: Massive flows. A) Mafic fine-grained macroscopic view (station LK-063); B) Cluster of plagioclase phenocrysts partially altered to epidote and white mica (sample LK-10-062); C) Plagioclase with annular zonation surrounded by the fine-grained matrix (sample LK-10-062); and D) Fine-grained matrix surrounding a rounded amygdule filled by chlorite and carbonate (sample LK-10-085).

2.2.2 Pillow lavas

The pillow lavas, of andesitic basalt to slightly andesitic composition, are stratigraphically situated between the massive and volcaniclastic facies and occur spread over the entire area. The pillows size range between 0.5 and 1m (figure 2.5A)

with common hyaloclastite pockets. Pillow breccia is also included into this facies due to the presence of thin metric levels of fragmental pillows in a continuous and thick pillow lavas facies.

The hyaloclastite occurs locally and are composed of sub-angular to angular clasts varying from milimetric to centimetric sizes with the same composition than the pillow lavas. The cement is predominantly carbonate and less recurrent silica. This facies is aphanitic to porphyritic/seriate (figure 2.5B) and commonly amygdaloidal. The amygdules are rounded to pipe shape and are filled by bladed carbonate (figure 2.5C), epidote, white mica and magnetite. The chlorite and quartz are locally present. It is common to observe the presence of spherulites, such as the coalescent albite spherulites from the figure 2.5D.

Figure 2.5: Pillow lavas. A) Pillow lavas pointing the top to south (station MONS-01); B) Phantom phenocrysts of plagioclase completely altered with the same microlitic texture of the matrix (sample LK-10-027); C) Rounded to sub-rounded amygdules filled by zeolites, chlorite and quartz (sample LK-10-023); and D) Coalescent albite spherulites with chlorite intergranular (sample LK-10-004).

2.2.3 Volcaniclastic rocks

The andesitic basalt to andesitic volcaniclastic deposits are the most common volcanic facies, bordering the pillow lava flows. This facies contains a high diversity of lithologies, which can comprises polymict and monomict fragments, varying in terms of texture, size and shape. The figure 2.6A shows a stratificated volcaniclastic rock with predominant rounded to sub-rounded and ameboidal fragments.

The fragments and the matrix have similar composition and textures. This facies is vesicular with trachyte (figure 2.6B) and porphyritic textures, locally granoblastic. The plagioclase phenocrysts, which constitute 5 to 15%, occur as clusters partially to completely altered to epidote and white mica. The other form of plagioclase occurrence is laths shaped in the groundmass, which are often recrystallized as albite.

The trachyte matrix is composed by the altered plagioclase laths surrounded by a groundmass of chlorite, epidote, white mica and quartz (figure 2.6C). Where the rock is highly altered, a granoblastic texture (figure 2.6D) completely overprints the original texture. The equidimensional crystals of epidote and quartz completely replace the original mineralogy. The vesicles are rounded to sub-rounded filled with anhedral quartz and euhedral epidote and chlorite.

Figure 2.6: Volcaniclastic rocks. A) Stratified volcaniclastic deposit with rounded to sub-rounded centimetric clasts (station LK-SUD-02); B) Trachytic matrix composed by plagioclase laths surrounded by a chlorite groundmass and rounded quartz and chlorite amygdules (sample LK-10-014); C) Overview of a fragment with intergranular texture constituted by chlorite, albite and epidote (sample LK-10-005); and D) Granoblastic texture constituted by epidote and quartz from a volcaniclastic matrix (sample LK-10-005).

2.3 MONSABRAIS PLUTON

The Monsabrais pluton is a magmatic suite crosscutting the volcanic sequence of Monsabrais. Its occurrence is restricted to the north of the studied area. This unit is a magmatic suite of gabbro to granodiorite which varies from a fine-grained to pegmatoidal-grained size (figure 2.7A and B). This unit is commonly porphyritic with

granular and seriate texture characterized by plagioclase laths with intergranular fine-grained size groundmass (figure 2.7C).

The phenocrysts present on the samples can be plagioclase and pyroxene relict crystals, either occurring alone or associated. The plagioclase phenocrysts constitute 25 to 35% of the rock and are usually grouped as cluster of euhedral to subhedral crystals with a prismatic shape, now recrystallized to albite and partially to totally altered to epidote and white mica in distinct proportions (figure 2.7D). The pyroxenes are subhedral to anhedral prismatic shape phenocrysts which compose 10% modal of the rocks. These phenocrysts actually occur completely altered to actinolite and chlorite (figure 2.7E) with some pyroxene relicts preserved on these pseudomorphs.

The matrix is composed of subhedral plagioclase laths (tabular shape) commonly recrystallized to albite and partially to completely altered to epidote and white mica (figure 2.7F). The intergranular groundmass is predominantly constituted by fine-grained size chlorite, epidote, actinolite, quartz and white mica and carbonate are minor minerals constituents. The carbonate usually fills intergranular porosity or some apophyses and may constitute a late magmatic event. The occurrence of smectite is resulting of the weathering due to the surface exposure to meteoric water.

Figure 2.7: Monsabrais pluton. A) Medium-grained sized macroscopic sample (sample LK-10-093b); B) Granular texture composed by plagioclase pseudomorphs with reaction border, quartz and actinolite (sample LK-10-094); C) Overview of the matrix composed predominantly by plagioclase and chlorite (sample LK-10-094); D) Clusters of plagioclase phenocrysts completely altered surrounded by the matrix (sample LK-10-016); E) Pseudomorph of pyroxene completely altered to chlorite surrounded by an albite and chlorite predominant matrix (sample LK-10-019); and F) Overview of the matrix composed by plagioclase, epidote, albite and actinolite (sample LK-10-019).

2.4 DYKES

The dykes appear on the entire sector crosscutting all the other lithologies in the Monsabrais area and occur as an intricate network in which all the different families crosscut each other at some points. The stereogram from the figure 2.8 indicates a dominant strike orientation of N20°E and N45°E. This trend is consistent with a radial organization of the dykes, as described in chapter 1; since the studied area is locate at the south of Monsabrais pluton.

The figure 2.9 shows the dip frequency of the dykes and confirm that the major part is subvertical, varying predominantly from 70° to 90°. The thickness of the most part of the dykes is centimetric to a few meters, as illustrated in the figure 2.10, where most part of dykes are inferior to 3m. There are two major dykes that crosscut the area, with 100 to 200m of thickness, as mapped on the figure 2.1. Statistically, there is no relationship between dyke thickness and strike (figure 2.11).

Figure 2.8: Stereogram of the strike orientation of the dykes.

Figure 2.9: Diagram of dip frequency.

Figure 2.10: Diagram of thickness frequency.

Figure 2.11: Diagram of thickness versus strike direction.

The variation of thickness, strike, and dip is just some of the main characteristics of a dykes swarm. There is a wide range of distinct features which can be used to divide the dykes in different families. In this section the dykes are classified in families based on their textural features through the petrographic description.

2.4.1 Major Dykes

These dykes are individualized based on their thickness and lateral continuity. They are two gabbroic dykes with thickness of 100 to 200 m crosscutting all the volcanic facies in a NS orientation (figure 2.1). The contact with the pluton is not visible, although it is possible to establish through field observations and U-Pb data that the dykes were earlier than the pluton. The West and East Major Dykes are described separately below because of their distinct mineralogy.

2.4.1.1 West Major Dyke

The West Major Dyke is a NS oriented intrusion with fine-grained granulometry and a massive appearance (figure 2.12A), which occurs at the central west part of the sector (figure 2.1). Its texture is seriate to slightly porphyritic characterized by 10 to 15% of anhedral hornblende phenocrysts recrystallized to actinolite (figure 2.12B and C) with some relicts of pyroxene. Those phenocrysts are locally altered to chlorite.

The matrix of this unit is composed by plagioclase laths recrystallized to albite and commonly altered to epidote/clinozoisite and white mica (figure 2.12D). The

intergranular material is an altered mafic groundmass constituted predominantly by chlorite and actinolite. The quartz is recurrent as a minor intergranular component. The smectite can occur disseminated as a result of the surface weathering.

Figure 2.12: West Major Dyke. A) Macroscopic view of the West Major Dyke (sample LK-10-035); B) Hornblende phenocrysts with recrystalization border of actinolite (sample LK-10-035); C) Hornblende phenocrysts with recrystalization border of actinolite (sample LK-10-035); and D) Matrix composed predominantly by plagioclase and chlorite (sample LK-10-035).

2.4.1.2 East Major Dyke

The East Major Dyke is a N20^{o}E striking intrusion located on the extreme east of the sector. It is a massive, fine-grained and dark coloured dyke, similar to the west dyke. Its texture is porphyritic to intergranular and locally micrographic.

The larger crystals have almost the same size than the rest of the matrix and can own a poikilitic to subpoikilitic texture (figure 2.13A), enveloping the plagioclase crystals. The phenocrysts compose up to 25 to 30% of this unit and are considered pseudomorphs of the primary pyroxenes, which occurs locally as relicts, partially recrystallized to hornblende and actinolite. In some crystals, the pyroxene is intensely hydrated resulting in the formation of chlorite and epidote (figure 2.13B).

The intergranular texture (figure 2.13C) is characterized by the presence of plagioclase crystals surrounded by a mafic groundmass composed by chlorite, actinolite, epidote and clinozoisite. The plagioclase laths are constantly recrystallized to albite and altered to epidote and white mica. The presence of medium-grained size quartz is due to a late silicification. The quartz and the feldspar occur mutually in the form of micrographic texture (figure 2.13D) in some samples.

Figure 2.13: East Major Dyke: A) Hornblende phenocrysts with actinolite border surrounded by the fine-grained matrix of actinolite, chlorite, plagioclase and quartz (sample LK-10-084); B) Subhedral quartz crystals surrounded by intensely altered actinolite (sample LK-10-092); C) Matrix composed predominantly by chlorite, actinolite and plagioclase laths (sample LK-10-090); and D) Micrographic texture of quartz and plagioclase and relict crystal of pyroxene (sample LK-10-092).

2.4.2 Equigranular dykes

This unit comprises all the dykes with no phenocrysts and aphanitic to medium-grained granulometry, corresponding to the greatest number of mapped dykes. Those dykes are distributed all over the area crosscutting the pluton, the volcanic sequence and other dykes with a NE strike trend. However, some porphyritic dykes also cut those dykes, hence adding complexity to the relative chronology. In this section, dykes are

subdivided in 1) aphanitic (up to fine-grained size) and 2) phaneritic, to simplify the description of this embracing unit.

2.4.2.1 Aphanitic equigranular dykes

The aphanitic equigranular dykes vary from aphanitic to slightly fine-grained, with a gabbroic to dioritic composition characterized by a microlitic texture formed by plagioclase laths surrounded by a mafic groundmass. The plagioclase is often recrystallized to albite, epidote and white mica. The matrix is completely recrystallized to chlorite, epidote, clinozoisite and quartz. Low temperature garnet, probably grossular (figure 2.14A), pervasive carbonate, quartz and intense albitization (figure 2.14B) occur probably as the result of hydrothermal alteration.

The amygdules are a recurrent feature of this type of dyke. They constitute 5% to 10% modal, are rounded to sub-rounded and are usually filled by quartz and chlorite and less commonly by epidote/clinozoisite and smectite. Prehnite (figure 2.14C) is an important minor component, which indicates a specific metamorphic facies.

Figure 2.14: Aphanitic equigranular dykes. A) Poikilitic texture formed by sub-rounded grossular surrounded by quartz and carbonate groundmass (sample LK-10-053); B) Altered matrix composed by albite, quartz and actinolite (sample LK-10-077); C) Altered matrix composed by prehnite with radial crystal shape and quartz (sample LK-10-053); D) Macroscopic view of the dyke with pinch and swell geometry (station MONS-13); E) Chilled border and border zonation characterized by amygdules concentration levels (sample LK-10-001); and F) Trachytic texture characterized by the plagioclase laths and chloritized aphanitic matrix and amygdules filled with quartz and chlorite (sample LK-10-072).

In the field, pinch and swell geometries, chilled borders and amygdular zonated borders are common. However, they also occur in the others dykes. The figure 2.14D shows a pinch and swell structure in a dyke emplaced in the pluton at the extreme west of the area. The chilled border (figure 2.14E) is the result of thermal shock cooling during the emplacement. It is characterized as a glass and aphanitic mineral rim varying from some millimeters to few centimeters, frequently developed in dykes intruding volcaniclastic rocks. The amygdular zonation occurs commonly associated to the chilled borders and manifests a quick cooling (figure 2.14F).

2.4.2.2 Phaneritic equigranular dykes

The phaneritic equigranular dykes (figure 2.15A) are gabbroic to dioritic intrusions of fine-grained to medium-grained size granulometry. They are predominantly thicker than the other equigranular dykes. Their larger size granulometry is probably related to their larger thickness, as a larger volume of magma is longer to cool.

The texture is predominantly granular to slightly porphyritic. The major components are actinolite and plagioclase, forming locally subpoikilitic to poikilitic textures (figure 2.15B) of actinolite enveloping the plagioclase crystals. The actinolite occur zonated (figure 2.15C), which represent at least two generations of these minerals.

The pyroxene relicts occur locally recrystallized to actinolite and also to chlorite and epidote when more hydrated (figure 2.15D). The plagioclase is often recrystallized to albite and also to epidote/clinozoisite and white mica. The quartz is a minor component

of the whole rock and occurs intergranular. The smectite is a weathering mineral also present as a minor constituent.

Figure 2.15: Phaneritic equigranular dykes. A) Macroscopic view of the dyke (station LK-013); B) Matrix composed of epidote, chlorite and actinolite (sample LK-10-067); C) Pyroxene crystal partially altered to hornblende and actinolite surrounded by a chlorite and epidote matrix (sample LK-10-067); and D) Pseudomorph crystals of pyroxene completely altered to actinolite and chlorite (sample LK-10-018).

2.4.3 Porphyritic dykes

The porphyritic dykes are together with the equigranular dykes the most common of all the dyke units. Both occur mutually crosscutting each other. They also occur

distributed throughout the area, crosscutting the pluton, the volcanic sequence and the two major dykes.

This unit occurs as a dark, porphyritic and massive rocks as exposed on the figure 2.16A, with gabbroic to granodioritic composition. Their slightly more felsic composition compared to the equigranular dykes are probably due to a higher concentration of plagioclase phenocrysts for some samples. Chilled borders, as in the figure 2.16B, occur frequently where the volcaniclastic are the host rock.

The porphyritic texture is characterized by the presence of pyroxene and plagioclase phenocrysts occurring together or alone. These phenocrysts appear as phantom textures (figure 2.16C and D) in rocks intensively recrystallized. Both types of phenocrysts can appear in clusters. The plagioclase phenocrysts (figure 2.16E) can vary from 2 to 50% modal and are occasionaly recrystallized to epidote, white mica and quartz. The pyroxene phenocrysts (figure 2.16F) represent 2 to 15% modal and frequently occur recrystallized to hornblende, actinolite or chlorite and epidote.

The matrix have a trachytic texture constituted by plagioclase laths partially to completely recrystallized to albite, epidote and white mica embedded in a mafic groundmass composed by chlorite, epidote/clinozoisite and ocasionally actinolite. Carbonate and quartz occur in some members which were exposed to intense leaching, not only replacing the phenocrysts. Rocks with intense albitization may produce a granuloblastic texture that overprints the primary texture. The smectite can occur i small percentages.

Figure 2.16: Porphyritic dykes. A) Macroscopic view from a porphyritic dyke (sample LK-10-002); B) Chilled margins of a porphyritic dyke emplaced in volcaniclastic rocks (sample LK-10-072); C) Phantom plagioclase phenocrysts completely absorbed by the plagioclase and chlorite matrix (sample LK-10-071); D) Phantom actinolite phenocrysts partially absorbed by the plagioclase and chlorite matrix (sample LK-10-030); E) Chlorite and epidote matrix and saussuritized plagioclase phenocrysts clusters (sample LK-10-073); and F) Actinolite phenocrysts surrounded by trachytic matrix characterized by altered plagioclase laths and aphanitic groundmass of chlorite and epidote (sample LK-10-009).

The amygdules constituting 2 to 15% modal, are rounded to sub-rounded and are usually filled by quartz and chlorite, and ocasionally by epidote, clinozoisite, carbonate and actinolite.

2.4.4 Aplitic dykes

The aplitic dykes (figure 2.17A) have their occurrence strictly related to the Monsabrais pluton and occurring only at the southern border of the pluton. Those intrusions are emplaced in the pluton and in some facies of the volcanic sequence. The litogeochemical analyses (chapter 3) characterize those dykes as granodiorite to granite.

These dykes are predominantly fine to medium-grained with a granular texture composed by actinolite, feldspar and quartz crystals (figure 2.17B). The quartz and feldspar presents intergrown boundaries between their crystals. The actinolite is often present as phenocrysts composing up to 5% modal. Those phenocrysts occur zonated characterizing two generations of this mineral as show on the figure 2.17C.

The actinolite may happens recrystallized to chlorite and epidote and the feldspar may occurs recrystallized as epidote/clinozoisite and white mica. The carbonate occurs as trace.

Figure 2.17: Aplitic dykes. A) Outcrop with aplitic dykes oriented to 055°/90° (sample LK-10-026); B) Granular texture typical of the aplitic dykes composed by quartz, plagioclase and actinolite (sample LK-10-026); and C) Actinolite phenocrysts surrounded by the matrix of albite, quartz, epidote and chlorite (sample LK-10-63).

2.5 VEINS

The quartz-carbonate veins are described in two locations and in only one, the strike and dip are clear (045°/90°). Both occurrences have trace to low concentrations (4%) of pyrite and chalcopyrite, as trace of malachite and azurite. One of the occurrences is on the northwest of the area intruding the Monsabrais pluton. The other occurrence is on the central part and emplaced in the volcaniclastic rocks.

The figure 2.18A shows the vein with two distinct compositions, which clearly manifest two pulses of hydrothermal fluids. The inner ribbon (figure 2.18B) is composed by quartz, carbonate, grossular (garnet), pyrite and chalcopyrite and the outer ribbon (figure 2.18C) is composed by quartz, pyrite and chalcopyrite.

Figure 2.18: Quartz-carbonate veins. A) Microscopic view from quartz-carbonate ribbon inside a quartz vein (sample LK-10-044); B) Inner ribbon of the vein composed by quartz, carbonate, grossular, pyrite and chalcopyrite (sample LK-10-044); and C) Outer ribbon of the vein, composed by quartz, pyrite and chalcopyrite (sample LK-10-044).

2.6 HYDROTHERMAL ACTIVITY

Archean pluton-volcanic environments are potential host of VMS (Volcanogenic massive sulfides) deposits, especially in the Abitibi subprovince. The compilation of Galley et al. (2007) shows that the Abitibi province in Ontario and Québec own 42% of the VMS deposits in Canada, corresponding to a total tonnage of 600 Mt.

The alteration zones are important guidelines to the exploration of this type of mineralization because they form larger halo than the sulfides deposits. Numerous publications have characterized these alteration zones in terms of their distribution, mineralogy and petrography. Hannington et al. (2003) characterized the hydrothermal alteration at the Blake River Group as a series of secondary minerals.

The secondary minerals observed in the Monsabrais area are: albite, amphiboles (actinolite and hornblende), chlorite, epidote, silica (quartz), white mica (sericite), carbonate and sericite. This section characterizes the spatial distribution for the following minerals: chlorite, epidote, quartz, white mica and carbonate (figure 2.19).

These minerals are main components of alteration zones intimately related to the VMS occurrence. Tracing their distribution and characterizing their mineralogical association are important to determine the mineralization potential of Monsabrais.

Quartz

A

Epidote

B

Chlorite

C

Figure 2.19: Maps of mineral percentages as defined in thin sections. A) Quartz; B) Epidote; C) Chlorite; D) White mica; and E) Carbonate.

2.6.1 Quartz

The silicification occurs as a pervasive alteration in the form of quartz in the volcanic pile and locally in dykes. The figure 2.19A shows a random pattern of distribution of the

quartz at Monsabrais, which highlights some pluton facies as expected, due to the primary silica content. There are also slight elevated presences of silica in the volcanic piles at west of both major dykes.

The figure 2.20A is an example of the silica alteration. The porphyritic dyke shows an intense silicification. The quartz replaces all the primary minerals from the matrix, forming a granoblastic texture that completely overprints the primary texture. The chlorite occurs also filling the vesicles.

Other common occurrence of quartz is associated with carbonate as a major constituent of the veins, although those just occur in two locations all over the Monsabrais sector.

2.6.2 Epidote

The epidote percentage is determined from the presence of epidote and clinozoisite. Its distribution in Monsabrais is illustrated on the figure 2.19B, which shows a random spreading occurrence in the pluton, in the volcanic pile and in the major dykes. The pluton is slightly more felsic than the other rocks and the epidote presence is associated to white mica as result of the plagioclase recrystallization.

Excluding the pluton, the higher concentration of this mineral is on the west contact of the volcanic sequence and the major dykes, in both lithologies. This distribution is similar to the silica occurrence.

Figure 2.20: Hydrothermal alteration. A) Pervasive silification of the matrix (sample LK-10-032); B) Granoblastic texture characterized by the epidote (sample LK-10-005); C) Intense chloritization of the matrix (sample LK-10-003); D) White mica due to an intense hydration (sample LK-10-028); E) Equigranular quartz and carbonate in a vein (sample LK-10-044); and F) Granoblastic texture characterized by the albite crystals (sample LK-10-041).

This mineral occurs associated with white mica (phengite) replacing plagioclase, usually when plagioclase occurs as phenocrysts. Epidote is also a major component of the matrix associated with chlorite. In some rocks, where this alteration is more intense,

the epidote appears as principal constituent in a granoblastic texture (figure 2.20B) which overprints the protolith texture. Amygdules with epidote, chlorite and carbonate filling are frequent.

2.6.3 Chlorite

The chlorite is the secondary mineral having the highest percentage in the Monsabrais area, related to the mafic to intermediate composition of the rocks. For this reason, the chlorite appears as principal constituent even in rocks with no alteration. The figure 2.19C shows that the chlorite content is higher in all the volcanic sequence and in the West Major Dyke. The lower concentration of this mineral is on the East Major Dyke and in the pluton.

This mineral is abundant in the matrix of all the dykes and volcanic facies, commonly associated to plagioclase laths (figure 2.20C). The second and also frequent form of occurrence is associated to epidote and actinolite replacing the pyroxene phenocrysts. The least recurrent occurrence is filling the amygdules, which can be associated with a large range of minerals, but more frequently with epidote, and white mica

2.6.4 White mica

The white mica observed in the Monsabrais rocks is mostly described as sericite. Its occurrence is not restricted to any unit as illustrated by the figure 2.19D. The higher

concentrations occur in the western part, near the intrusive members. The figure 2.20D shows a pervasive alteration of sericite. The sericite is associated to the epidote/clinozoisite when resulting from the recrystallization of plagioclase phenocrysts. The sericite also occurs with chlorite as major constituent of the altered matrix.

2.6.5 Carbonate

The carbonate alteration is only weakly developed in the Monsabrais rocks. Its occurrence is in quartz-carbonate veins (figure 2.20E), that occurs at the form of two individual lodes. The carbonate also occurs disseminated as a minor constituent of the dykes and within all the volcanic facies or as cement in some volcaniclastic rocks and hyaloclastites associated with pillow lavas. The figure 2.19E shows a random distribution with no distinct geological meaning.

2.6.6 Other secondary minerals

Albite, amphiboles (hornblende and actinolite) and smectite are the other secondary minerals present in the sector. Some of their particularities are described below.

The albite appears in almost all the rocks, as result of the recrystallization of the primary volcanic plagioclase to a more stable form. However, albite occurs in anomalous concentration in some porphyritic dykes as on the figure 2.20F, where a pervasive albitization with granoblastic texture overprints the original texture.

The hornblende and the actinolite occur commonly as the result of the recrystallization of primary pyroxene phenocrysts. The presence of both minerals or two generations of actinolite can occur mutually, refining a crystal zonation common on the porphyritic rocks. The actinolite is also associated to the chlorite as an intergranular mineral in samples from the Monsabrais pluton. Actinolite is not present as a major constituent of the other rocks.

The smectite occurs distributed over all the area, disseminated as a trace or minor mineral constituent from the groundmass of the volcanic sequence and all dykes. For this reason, its distribution is not considered here.

2.7 DISCUSSION

The secondary minerals occur, globally, in all the lithologies, varying where the abundances is function of the chemical composition of the rock. The use of petrography enables the identification of a wide range of secondary and primary minerals that through the observation of their inter-relationships are classified as metastable or unstable phases. The identification of the stable mineral assemblage is fundamental to determine the metamorphic facies of the rocks.

The metastable phases are minerals belonging to mineral assemblage in equilibrium between them. This assemblage is formed by: chlorite, actinolite, epidote/clinozoisite, plagioclase (albite), white mica (sericite and phengite) and quartz, prehnite, garnet (grossular) and carbonate (calcite).

Unstable phases are minerals not in equilibrium with the main mineral assemblage, occuring as relicts or presenting any type of recrystalization. Those minerals are: clinopyroxene (augite), hornblende, actinolite (with more Fe content), plagioclase (more calcic), zeolites and smectite.

Stable mineral assemblages are used to determine the metamorphic degree facies. Yardley (1990) present a compilation using Humphris and Thompson (1978) data, classifying the metamorphic facies according to the occurrence of a range of minerals. Thus, the presence of prehnite, chlorite, calcite and epidote characterized a prehnite-pumpellyte metamorphic facies. However, the presence of actinolite, albite, chlorite, epidote, quartz and even hornblende are more compatible with a greenschist metamorphic facies. This coexistence is explained by the location of Monsabrais close to the limit between prehnite-pumpellyite and greenschist metamorphic isograds defined by Powell et al. (1993). Hannington et al. (2003) also described the occurrence of indicative minerals of both facies at the New Insco VMS deposit which is close to Monsabrais.

The presence of hornblende, a characteristic of high temperature zone in green schist facies, can be explained by a geothermal anomaly caused by the intrusion of the Monsabrais pluton prior to the regional metamorphism; explaining the recrystallization of hornblende to actinolite.

The textures present in the volcanic facies characterized by Castillo-Guimond (2012) are typical of extrusive rocks and are widely described on the literature. The predominant equigranular texture of fine to medium-grained size rocks from the

Monsabrais pluton is also typical of slow cooling intrusive igneous rocks. The West and East Major Dykes have a fine-grained size granulometry and equigranular to porphyritic texture consistent with their large volume.

The equigranular dyke textures vary according to their thickness. The thinner dykes present an aphanitic to fine-grained size granulometry with a microlitic to trachytic textures. Furthermore, thicker dykes have fine to medium-grained size granulometry with a slightly porphyritic texture. The grain-size variation is function of the volume to cool. Consequently faster heat exchange with the host-rock results in a quicker cooling inhibiting the formation of larger crystals. In contrast, the thicker and more voluminous dykes have a slower cooling rate allowing the crystallization of larger minerals.

The matrix of the porphyritic dykes passes through a similar process of cooling as described for the equigranular dykes, where the grain-size is function of the thickness. However, the phenocrysts are explained by a polygenetic process described by Best (2002) which involves a two-stage cooling for the magma. The first stage occurs in an insulated environment that provides slow cooling resulting in small nuclei generating the phenocrysts and a second stage of fast heat loss which produce the matrix. The first process can occur in the magma chamber or in a sub-chamber and the second process occurs during the emplacement of the dykes in shallow depth.

The aplitic dykes are interpreted as a later magmatic pulse of the Monsabrais pluton, composed of residual magma with high volatile content. This interpretation is based on the more felsic composition and the larger size crystals than the rest of the magmatic suite.

The hydrothermal alteration textures and mineralogy involve a pervasive replacement of the protoliths. According to the figure 2.19 the rocks present different degrees of alteration. Galley (1993) characterized semi-comfortable alteration zones associated to base-metals deposits occurring in subaqueous volcanogenic environment. These are resulting from simultaneous and successive metasomatic reactions between seawater and the volcanic pile in a convective system.

The chloritization, spilitization (albitization), silicification, epidotization, sericitization and carbonation are the products of such syn-volcanic convective hydrothermal systems. However, the punctual and random distributions of altered rocks at Monsabrais suggest a diffuse, rather than a well focalised and hydrothermal system.

CHAPTER 3

LITHOGEOCHEMISTRY

3.1 INTRODUCTION

The geochemistry is a useful tool for the comprehension of a geological environment, based on the characterization of the major and minor elements behaviour. This project uses the lithogeochemistry as tool to characterize the intrusive lithologies, their relation with the volcanic sequence and the signature of the hydrothermal process.

A total 67 samples were analyzed. The selection criteria for samples are in the following order:

1. Distinct dykes;

2. Distinct pluton facies;

3. Main volcanic facies for comparison;

4. Hydrothermal alteration.

The samples were cut at the laboratory of the *Université du Québec à Chicoutimi* (UQAC). The fragments were selected to avoid the presence of

alteration and/or weathering and were sent to the ALS CHEMIX laboratory in Val d'Or. The selected samples were divided in three different batches analyzed by distinct methods (appendix 3).

The major element oxide values used in this chapter were acquired by XRF (X-ray fluorescence) for the first batch and ICP-AES (inductively coupled plasma-atomic emission spectrometry) for the second and third batches. The 38 minor elements, which include the REE (rare earth elements) used in the calculus and diagrams were acquired by ICP-MS (inductively coupled plasma-mass spectrometry). The elements with values under the detection limit were considered zero for the calculation processes.

This chapter is subdivided in six parts following the lithogeochemistry use: A) rock classification; B) magmatic affinity; C) spidergrams; D) discrimination diagrams; E) hydrothermal alteration and F) discussion.

3.2 ROCK CLASSIFICATION

The rock classification is based on the use of less mobile elements to generate information from the protolith. For this reason, the use of major elements was mainly avoid in this work. This is a fundamental choice for an archean geological environment as the Monsabrais is described in the literature as the result of

subaqueous volcanism, exposed to the circulation of a high volume of hydrothermal fluids.

The figure 3.1 presents the classification of Winchester and Floyd (1977) for volcanic rocks based on the ratios Zr/TiO_2 and Nb/Y. All the units are sub-alkaline in the rock sequence plotted on this diagram, including the intrusive members for comparison purpose. The Monsabrais rocks have basalt to rhyodacite trend composition, which is shared between the intrusive and extrusive lithologies. However the majority has basaltic to andesitic composition.

Figure 3.1: Compositional classification Nb/Y vs Zr/TiO_2 from Winchester and Floyd (1977).

3.3 MAGMATIC AFFINITY

The figure 3.2 presents several diagrams used by Barrett and MacLean (1993; 1999) to attempt to determine the syn-magmatic provenance of rocks from a same district through the characterization of immobile element content.

The figure 3.2A shows an evolving trend from the more mafic samples near the origin toward the felsic pole further from the origin, forming a fan shape distribution. This fan variation can be the result of Zr and Y mobilities in response to the hydrothermal alteration. The diagram Al_2O_3/TiO_2 (figure 3.2B) shows the dykes, the plutonic and volcanic rocks plotting along a fractionation trend, indicating a co-magmatic origin for all the samples. Samples distributed along alteration lines manifest some hydrothermal alteration overprint, due to mass gains.

The figures 3.2C and D, in addition to highlight the typical co-magmatic character of the samples, also indicate a predominant transitional magmatic affinity of the rocks. The figure 3.3A from Barrett and MacLean (1999) supports the dominant transitional character. However, the ratio Th/Yb (figure 3.3B) plots half of the samples as calc-alkaline. Those diagrams were designed to treat a large volume of data, highlighting the preferential trend of the dataset. However, the spidergrams provide a better characterization.

Figure 3.2: Co-magmatic diagrams from MacLean and Barrett (1993); 1999).

Figure 3.3: Magmatic affinity diagrams from Barrett and MacLean (1999).

3.4 SPIDERGRAMS

This section presents the behaviour of the trace elements including the REE. The elements abundances are displayed in the form of spidergrams, in which the values are normalized by the Primitive Mantle from Sun and McDonough (1989) for a better comparison between them.

The figure 3.4 presents the spidergrams of the REE abundances. It is possible to describe the samples as having a uniform REE behaviour with a REE fractionation slope characteristic of transitional magmatic affinity, with variable Eu (Europium) anomalies. The moderate slopes of the REE profile are similar for the majority of the rocks, but defined by variable element abundances.

The sample LK-10-017 is from an intensely epidotized porphyritic dyke (figure 3.4D). Its REE signature is typical of tholeitic magma, diverging from the rest of the REE patterns. However, the depletion in light REE may be related to the intense hydrothermal alteration, which leached those elements.

Figure 3.4: REE diagrams normalized by the primitive mantle from Sun and McDonough (1989). A) Samples of major dykes, Monsabrais pluton and aplitic dykes; B) Samples of massive flows, pillow lavas and volcaniclastic rocks; C) Samples of equigranular dykes; and D) Samples of Porphyritic dykes.

The figure 3.5 compares values from normalized Eu with Eu*. The Eu* is calculated from the interpolation of normalized Sm (Samarium) and Gd (Gadolinium) through the equation $\sqrt{[(Sm_N)x(Gd_N)]}$ of Taylor and MacLennan (1985) in Rollinson (1993). The Eu/Eu* ratio shows a dominant trend along line of m=1 and some dispersed values characterizing both negative and positive anomalies. The positive anomalies are usually related to the presence of abundant plagioclase in the rocks, which is related to the divalent state of this element being compatible with feldspar (Rollinson 1993). Conversely, negative anomalies in plagioclase rich rocks are commonly interpreted as the result of hydrothermal leaching of Eu^{3+}.

The figure 3.6 shows the REE patterns grouped according to their La/Yb ratios, attempting to quantify the variation of heavy REE in relation to light REE, in order to optimize the description of their behaviour. The majority of the samples are characterized by a ratio varying from 3 and 6 and their grouping does not reflect the compositional or the unit classification, previously established on field characteristics.

The figure 3.7 presents multi-elemental diagrams constituted by 12 of the REE and 7 HFS (High field strength elements): Th, Nb, Ta, Zr, Hf, Ti and Y. The Y is placed on the Ho position on the diagram. Ho and Y have similar ionic radius (Rollinson, 1993). The multi-elemental diagrams expose a relative homogeneous signature without significant variation between the samples. The signature is

characterized by moderate negative anomalies in Nb and Ta, low positive anomalies in Zr and Hf and high negative anomaly in Ti.

As an exception, the sample LK-10-017 (intensely epidotized porphyritic dyke) own a distinct multi-elemental profile characterized by a low negative anomaly in Nb and low to moderate positive anomalies on the other HFS elements. This may be related to the intense epidotization.

Figure 3.5: Diagram of calculated Europium (Eu*) versus analyzed Europium, values in ppm.

Figure 3.6: REE diagrams normalized by the primitive mantle from Sun and McDonough (1989): A) All the samples; B) 3>La/Yb; C) 3>La/Yb>6 and D) La/Yb>6.

Figure 3.7: Spidergrams normalized by the primitive mantle from Sun and McDonough (1989). A) Samples of major dykes, Monsabrais pluton and aplitic dykes; B) Samples of massive flows, pillow lavas and volcaniclastic rocks; C) Samples of equigranular dykes; and D) Samples of Porphyritic dykes.

3.5 DISCRIMINANT DIAGRAMS

Discriminant diagrams are a statistical technique used for classifying samples into predefined groups (Rollinson, 1993). Thus, the discrimination diagrams on figures 3.8 and 3.9 are designed to interpret the tectonic environment for the magma generation. The Monsabrais area belongs to a regional magmatic event in which the tectonic environment, as well other magma features are well described in the literature. Thus, the following observations serve to determine if the Monsabrais area agrees with the regional model.

The discriminant diagrams from Gill (1981) on the figures 3.8A and B use immobile elements to determine the magma source. On both graphics, the samples have a fan shape spreading; however they are not plotted on the same fields on the diagrams. On both diagrams, half of the samples are classified as orogenic andesites, but on the figure 3.8A the other half of the samples are classified as N-MORB, whereas in the figure 3.8B, it is E-MORB. This discrepancy is easily explained by superimposed hydrothermal processes typical of archean terrains, rather than indication of complex magma mixing.

Figure 3.8: Discriminant diagrams from Gill (1981): A) Nb/La and B) Th/La.

The discrimant diagram from Wood (1980: figure 3.9) is primary designed on the immobile HFS elements Th-Hf-Ta. However, due to the low concentrations of Hf and Ta, these are replaced by Nb and Zr as proposed by Rollinson (1993). The samples plot predominantly in the arc-basalts field. The samples plotting in other fields are interpreted as resulting of the slight mobility character of Th under hydrothermal alteration. This interpretation is based on the observation of Rollinson (1993) about the Th uncertainty mobility in altered basalts.

Figure 3.9: Discriminant diagram from Wood (1980).

3.6 HYDROTHERMAL ALTERATION

In an attempt to draw a pattern of the main alteration on the sector, the lithogeochemical results were treated by the software NORMAT developed by Piché and Jébrak (2004). It is a technique for quantifying hydrothermal alteration in greenschist facies rocks using normative mineral ratios.

The tables with the values calculated by the software are presented in the appendix 4. Results are distributed spatially in the area as seen on the figure 3.10. The IFRAIS is defined by Piché and Jébrak (2004) as a measure of the global alkali element depletion and represent how preserved is the rock. The ISER and IPARA respectively represent sericitization and paragonization indexes. The chlorite is a normative value of chlorite calculated from Fe, Mg and Al, that may be the result of hydrothermal alteration or metamorphism.

The value corresponding to this chlorite index (ICHL) determined by NORMAT did not show any significant variation and it was not used. Rather, it was the chlorite concentration (figure 3.10A), which is higher on the west and south of the area and lowest on the east of the sector. The ICHL correspond exclusively to hydrothermal chlorite (higher Fe) and the chlorite percentage corresponds to the total chlorite (high Fe or high Mg).

The paragonization and sericitization indexes (figures 3.10B and C) have a similar distribution pattern, which is stronger on the west and weaker on the east

side. The IFRAIS distribution (figure 3.10D) shows an inverse relationship to the other normative indexes agreeing with the interpretation of a higher hydrothermal alteration on the central to west part of the area.

Figure 3.10: Maps with the concentration of alteration minerals from normative calculation. A) Normative chlorite mineral; B) Sericite alteration normative index (ISER); C) Normative paragonite alteration index (IPARA); and D) Index of relative alteration intensity (IFRAIS).

3.7 DISCUSSION

The lithogeochemistry leads to the interpretation of a unique magmatic source for the dyke families, volcanic sequence and the pluton. This magmatic source has a predominant transitional magmatic affinity. The small variations in relative abundance of REE and HFSE can be interpreted as the result of a slight process of partial melting from the source, which is plausible considering the magma chamber is constantly feed with melt injections.

The REE and multi-elemental spidergrams present a profile typical of rocks that experienced the crystal fractionation process. This interpretation is based on the constant correlation between the light REE and heavy REE on the majority of the samples.

The distinct degrees of fractionated crystallization in a same unit indicate a magmatic event resulting of multiple phases. Therefore, different lithologies with the same degree of crystal fractionation can be genetically related. However, this can be also explained by the existence of multiple magma chambers in which the magma evolve. Nevertheless, even with the slight REE pattern variations, a co-genetic magmatism is prefered than a multiple source magmatic system, because the field and petrographic observations do not support this interpretation.

The Eu anomalies just represent the feldspar content from the samples, having positive anomalies for samples with the high content of plagioclase, and a negative anomaly for rocks that experienced some degree of hydrothermalism.

The discriminant diagrams were selected because of their use in basaltic and andesitic sequences. The result indicates a magmatic arc event that agrees with the regional model. Negative anomalies in Nb, Ta and Ti are indicators of continental crust contribution in the magma source (Rollinson, 1993), supporting the magmatic arc model.

The weak and diffuse hydrothermal alteration characteristic of the system is expressed in the binary diagrams from the figure 3.2 and also highlighted by the NORMAT indexes. However, the maps with the normative minerals and indexes (NORMAT) are not consistent with the maps of distribution of alteration minerals based on the petrographic observations. This discrepancy is probably due to the low intensity of the hydrothermal alteration, which can also happen overprinting each other.

CHAPTER 4

SULFIDE MINERALIZATION

4.1 INTRODUCTION

The sulfides characterization is important to determine the metalogenic evolution of Monsabrais. The distribution, the form of occurrence and the geochemical signature are the parameters used in this study. The distribution of the sulfides was noted during the field work. The form of occurrence was also observed during the field and described with more details through the petrography of 13 polished thin sections. The geochemical signature was characterized using the LA-ICP-MS (Laser ablation inductively coupled plasma-mass spectrometry).

The sulfides are pyrite, chalcopyrite and pyrrhotite, all three can occur associated. The pyrite and pyrrhotite were analyzed with the LA-ICPMS and results were compared to other selected pyrite and pyrrhotite occurrences.

4.2 DISTRIBUTION

The sulfide occurrences are spread over the sector and found in all the lithologies in variable quantities. The figure 4.1 illustrated the mapped distribution of pyrite, pyrrhotite and chalcopyrite on the sector. The pyrite has the wider distribution and occurs all over the sector. The pyrrhotite is the second most abundant sulfide and its distribution is more restricted. The chalcopyrite is the least abundant and occurs only locally, usually associated with one of the other sulfides.

Sulfides occur as: 1) amygdular; 2) disseminated and 3) disseminated in quartz-carbonate veins. The figure 4.2 represents the form of occurrence plotted on the sector map.

The sulfides occur mostly as amygdule filling in the volcanic sequence and in some amygdular dykes emplaced in extrusive rocks. This type of mineralization occurs usually where the volcanic rocks (figure 4.3C and D) are at the proximity of dyke swarms.

The disseminated form is the most recurrent, tending to occur more often in the volcanic pile (figure 4.3A and B) and in the dyke swarms as the amygdular occurrence.

Figure 4.1: Map of the sulfide distribution.

Figure 4.2: Map of the form of occurrence of sulfides.

Figure 4.3: Form of occurrence of the sulfides. A) Disseminated pyrite and chalcopyrite in a volcaniclastic rock (sample LK-10-004); B) Microscopic view (reflected light) of disseminated pyrite and chalcopyrite in a volcaniclastic rock (sample LK-10-005); C) Amygdular pyrrhotite in a massive flow (sample LK-10-085); D) Microscopic view (reflected light) of amygdular pyrrhotite in a massive flow (sample LK-10-085); E) Disseminated pyrite in a quartz-carbonate vein (sample LK-10-043); and F) Microscopic view (reflected light) of disseminated pyrite in a quartz-carbonate vein (sample LK-10-043).

The vein-bearing are the least common form of sulfides occurrence and it is developed only in two locations. Those quartz-carbonate veins were already described at the chapter 2, hosting disseminated pyrite and chalcopyrite (figure 4.3D and E).

4.3 PETROGRAPHY

The pyrite, pyrrhotite and chalcopyrite are characterized based on their textures, shape, size and mineral assemblages. The main features from the sulfides are presented in the figure 4.4 and are described below.

The pyrite is the most common sulfide, occurring in the veins, disseminated in the rocks and as amygdule filling. It is possible to recognize two distinct pyrite families based on their textural features. The first family (figure 4.4A) denominated pyrite 1 (Py1) has a spongy aspect, subhedral to anhedral crystal shape, presenting fractures and silicate mineral inclusions. The second family (figure 4.4B), pyrite 2 (Py2) occurs as euhedral to subhedral, weakly fractured crystals, with less common inclusions of silicate minerals. Locally, primary Py1 crystals are surrounded by rims of Py2.

The two pyrite families are disseminated in the whole rocks, in the quartz-carbonate veins and filling vesicles. They commonly occur together, as noticed in some samples from the quartz-carbonate veins.

Pyrite - Family 1

Spongy, anhedral to subhedral and fractured crystals with local inclusions of silicate minerals.

It occurs disseminated in the whole rock, disseminated in veins and filling amygdules.

Pyrite - Family 2

Subhedral to euhedral crystals, locally fractured with inclusions of silicate minerals.

It occurs disseminated in the whole rocks, disseminated in veins and filling amygdules.

Pyrrhotite

Spongy, anhedral and fractured crystals with inclusions of pyrite and silicate minerals.

It occurs disseminated in the whole rocks and filling amygdules.

Chalcopyrite

Anhedral and fractured crystals with inclusions of silicate minerals.

It occurs disseminated in the whole rocks and disseminated in veins.

Figure 4.4: Reflected light photomicrography of sulfides and their classification based on petrography. A) Pyrite 1 (sample LK-10-023); B) Pyrite 2 (sample LK-10-43); C) Pyrrhotite (sample LK-10-085); and D) Chalcopyrite (sample LK-10-87).

The pyrrhotite (figure 4.4C) varies from crystals size < 0.5mm up to 8 mm. These crystals have subhedral to anhedral crystal shape, a spongy texture and are frequently fractured. The occurrence of this sulfide is almost restricted to the amygdules, usually in the volcanic rocks and less commonly in some dykes.

The chalcopyrite crystals (figure 4.4D) are anhedral, varying from less than 0.1mm up to 2mm. The crystals are usually fractured with inclusions of quartz. They occur associated with pyrite when disseminated in the whole rocks and in quartz-carbonate veins. The sulfide crystals can also appear as inclusions in pyrrhotite crystals in the amygdules.

4.4 LA-ICP-MS

4.4.1 Methodology

The sulfide analyses by the LA-ICP-MS method were used to characterize their chemical signature, with the aim of determining if sulfides with distinct petrographic features belong to one or more hydrothermal events. It is also possible to compare the results with other selected sulfides from well known setting. Twelve polished thin sections of 30 μm were analyzed, eight thin sections containing pyrite and five containing pyrrhotite.

The equipment used is the model M-50 resolution Excimer (193nm) ArF resonetics and an Agilent 7700x mass spectrometer from the LabMaTer (Earth's Materials Laboratory) of UQAC. The lines ablated on the sulfides had distinct length and were performed with a beam size of 43 μm, a laser repetition rate of 15 Hz, rastering at 7.5 μm/s and laser energy of 4 mj/cm^2. The data produced by the technique were treated on the software IOLITE 2.15. The blank sample GSE-1 (29 analyses) and the standard PS-1 (34 analyses) were used respectively for calibration and control in the ablation and during the data treatment. The standard and blank samples were analyzed before and after the change of each thin section. The Fe was the element selected for the stoichiometric reduction of both pyrite and pyrrhotite; the values utilized are Fe=46,55% and Fe=62,33%, respectively.

A total of 30 elements was analysed: ^{33}S, ^{34}S, ^{51}V, ^{52}Cr, ^{53}Cr, ^{55}Mn, ^{59}Co, ^{60}Ni, ^{65}Cu, ^{66}Zn, ^{71}Ga, ^{72}Ge, ^{75}As, ^{82}Se, ^{95}Mo, ^{98}Mo, ^{107}Ag, ^{111}Cd, ^{115}In, ^{118}Sn, ^{121}Sb, ^{125}Te, ^{182}W, ^{184}W, ^{195}Pt, ^{197}Au, ^{200}Hg, ^{202}Hg, ^{208}Pb, ^{209}Bi. However, only 22 elements are displayed in the elemental diagrams of their signature, as: ^{51}V, ^{52}Cr, ^{55}Mn, ^{59}Co, ^{60}Ni, ^{65}Cu, ^{66}Zn, ^{71}Ga, ^{72}Ge, ^{75}As, ^{82}Se, ^{95}Mo, ^{107}Ag, ^{111}Cd, ^{115}In, ^{118}Sn, ^{121}Sb, ^{125}Te, ^{197}Au, ^{200}Hg, ^{208}Pb, ^{209}Bi. The results are presented in the following section.

4.4.2 Trace element signatures

Huston et al. (1995) separated the elements in pyrite in three groups based on their predominant form of occurrence. The group 1 is constituted by elements that occur as inclusions: Cu, Zn, Pb, Ba, Bi, Ag and Sb. The group 2 is constituted by elements that occur as nonstoichiometric substitution in the lattice: As, Tl, Au and possibly Mo. The group 3 is composed by the elements involved in stoichiometric substitutions: Co and Ni for Fe and Se for S. The elemental signature displayed in the figure 4.5 present these elements and other.

The two textural distinct pyrite families have a similar elemental signature (figure 4.5). The abundance of the majority of the elements are similar and do not vary more than one order of magnitude. The more discrepant values are the Zn and Cd abundances, which are not relevant to distinct the pyrites as two different families. Hence, the textural subdivision is not manifested by a significant chemical difference.

It is important to highlight the higher value from V, which is not expected in this sulfide. However, V has numerous valence state (+2, +3, +4, +5) and its abundance in these pyrites may be related to a specific condition of the hydrothermal system or the result of contamination, because the blank sample GSE-1 presents higher values than expected for this standard. Elements as Co, Ni, Cu, Zn have elevated values in the pyrites and the pyrrhotites. In contrast, Au

is an extreme negative anomaly, as the values are often under the detection limit.

The elemental pyrrhotite signature is displayed on the figure 4.6. The results form a similar pattern of those of the pyrite. The figure 4.7 shows the elements abundance of pyrite and the pyrrhotite together. There is a noticeable enrichment of Cu and depletion of Se in pyrrhotite relative to pyrite.

Figure 4.5: Trace element signatures of the two families of pyrite from Monsabrais.

Figure 4.6: Trace element signature of pyrrhotite from Monsabrais.

Figure 4.7: Comparison between the trace element signatures of the pyrites Py1 - Py2 and the pyrrhotite from Monsabrais.

4.5 DISCUSSION

The aim of analyzing sulfides is to determine if these minerals are originating from a singular or multiple hydrothermal events. The similarity of the metal signature supports a unique formation process for the pyrite and pyrrhotite. The punctual variations of some elements remain within one order of magnitude, which is considered insignificant for defining multiple events.

Thin sections of pyrites from Bouchard-Hébert and Chadbourne deposits (provided by Damien Gaboury) were analyzed concomitantly to the Monsabrais sulfides. Two ablations were performed on the pyrite from the Bouchard-Hébert deposit and 4 ablations on the pyrite from the Chadbourne deposit. Bouchard-Hébert mine, also known as Mobrun mine is a polymetallic deposit (Cu, Zn, Ag and Au) situated near the Rouyn-Noranda city and hosted in the volcanic complex of Mobrun (Barret et al., 1992). The massive sulfides are hosted by variably deformed bimodal volcanic sequence constituted by coherent and brecciated flows (Barret et al., 1992). Chadbourne was a gold deposit located in the middle of the Noranda town. Chadbourne is characterized by Walker and Cregheur (1982) as a gold deposit hosted in an andesitic breccias pipe in gradational contact with an andesitic flow intruded by a syenite intrusion. The hydrothermal source is interpreted as originating from the syenitic intrusion, analogous to shallow hot spring activity.

The pyrite from Bouchard-Hébert (figure 4.8) has lower values of Ni, Cu and higher values of Zn, Ga, Se, Ag, Cd, In, Sn, Sb and Te. It is important to highlight that the pyrite analyzed is massive and the pyrite from Monsabrais occurs disseminated and in lower percentage. The Chadbourne pyrite has a more similar signature to the Monsabrais pyrite; the distinctions are restricted to the lower abundance of Ni, Cu, Zn and Ga. The two signatures present variation in some elements, which are interpreted as inherent of distinct geological contexts. However, it is possible to underline a similar pattern of element abundance, which can be attributed, at different degrees, to a volcanogenic hydrothermal system.

Additionally with those complementary pyrites, the Monsabrais pyrite was compared with pyrite from distinct geological environments. The author utilized already published results. The pyrite values are from Lac Line (Côté-Mantha, 2009) and Cap d'Ours (Genna, 2009) mineralizations and Wona gold deposit (Augustin, 2011). The diagrams from the figures 4.9, 4.10 and 4.11 display a reduced number of elements, because the diagrams were constructed with the available elements from the literature.

The Lac Line is an archean polymetallic mineralization (Au, Ag and Cu) located north of the Chibougamau city, hosted in a mafic to intermediate volcano-sedimentary sequence and intruded by a tonalitic stock, both weakly metamorphized (Côté-Mantha, 2009). The mineralization is interpreted as resulting from a sea-floor hydrothermal event with a possible contribution from

magmatic fluids from the intrusions. The figure 4.9 shows the comparison between the pyrite from Monsabrais and Lac Line. The elements Co, As, Pb and Bi are higher on the Lac Line and the elements Cu and Ag are lower. Higher values from As are expected from a gold bearing mineralization, but the signatures are similar.

The mineralization of the Cap d'Ours is situated near the Horne mine in the city of Rouyn-Noranda and it is described by Genna (2009) as a pyrite occurrence hosted in a felsic volcanic sequence and associated to quartz-plagioclase porphyritic dykes. Three types of pyrite were individualized Py1 (volcanogenic), Py2 (metamorphic) and Py3 (volcanogenic with metamorphic borders). The figure 4.10 compares the elements abundance from Monsabrais and Cap d'Ours pyrites. Results are different even if both sites have similar geological context. However, the felsic composition of the volcanic sequence from Cap d'Ours compared to the mafic to intermediate composition from the volcanic sequence from Monsabrais are interpret as one of the factor accounting for this discrepancy.

The Wona deposit is a major gold deposit situated in the Burkina Faso country, hosted in the poly deformed and metamorphized paleo-proterozoic mafic volcano-sedimentary rocks from the Houndé greenstone belt (Augustin, 2011). The same author separated the pyrite in three families, primary (hydrothermal), metamorphic and hydrothermal, which both hydrothermal events are interpreted as associated to an orogenic system. The figure 4.11 plots the

pyrites from the Monsabrais with the pyrite families, from the Wona deposit. Results show a low degree of correspondence between them. The distinct elemental signatures clearly reflect the distinct geological context and different hydrothermal processes.

Globally, the Monsabrais pyrites share similar trace elements signature with the pyrites described by Côté-Mantha (2009) from the polymetallic deposit of Lac Line. The Lac Line mineralization is characterized as an atypical Au-Ag-Cu hosted in an archean volcano-sedimentary and plutonic sequence weakly metamorphosed. The mineralization is interpreted as resulting of a sea-floor syn-volcanic hydrothermalism with hydrothermal contribution from the pluton emplacement.

For pyrrhotite comparisons, three complementary analyses were performed in pyrrhotite occurring in hyaloclastite pillow lava rim from the Géant Dormant deposit (provided by Damien Gaboury). This deposit is described by Gaboury and Daigneault (1999) as an archean vein-type gold deposit generated by a multiple stage mineralization centered on a felsic complex intruding in volcano-sedimentary sequence. The pyrrhotite is associated to the first mineralization event related to sea-floor hydrothermalism. The figure 4.12 presents the pyrrhotite signatures from Monsabrais and Géant Dormant. The results are very similar, except for a small variance of Cr, Zn, Ga and Sb. The author recognizes the small quantity of available data of pyrrhotite to compare the mineralizations. However, the similarity of the analyzed elements supports the interpretation that

Monsabrais sulfides result from a sea-floor volcanogenic system, with a possible magmatic input from the adjacent pluton.

Figure 4.8: Comparison between the trace element signatures of the pyrites from Monsabrais and the pyrites from Bouchard-Hébert and Chadbourne deposits.

Figure 4.9: Comparison between the trace element signatures of the pyrites from Monsabrais and the pyrites from Lac Line deposit (Côté-Mantha, 2009).

Figure 4.10: Comparison between the trace element signatures of the pyrites from Monsabrais and the pyrites from Cap d'Ours (Genna, 2009).

Figure 4.11: Comparison between the trace element signatures of the pyrites from Monsabrais and the pyrites from Wona deposit (Augustin, 2011).

Figure 4.12: Comparison between the trace element signatures of the pyrrhotite from Monsabrais and the pyrrhotite from Géant Dormant deposit.

CHAPTER 5

DISCUSSION

5.1 SYNTHESIS OF RESULTS

The previous chapters applied a range of methods in order to characterize the studied area. From these techniques, results were generated to answer the problematic presented by this project. The results were generated by: 1) field observations; 2) petrography; 3) lithogeochemistry; and 4) sulfide composition. The main results are presented below and discussed in the light of similar studies.

5.1.1 U-Pb ages

Previous studies indicate U-Pb ages of 2696.2 ± 0.9 Ma and 2695 ± 2.8 Ma ((McNicoll et al., in Ross et al., 2008; Mueller et al., 2012) to the plutonic suite of the Monsabrais and ages of 2701.1 ± 1.2 Ma and 2698.7 ± 1.1 Ma (McNicoll et al., in Ross et al., 2008) for the ring dykes system, which is part of the major dykes, as referred in this study.

5.1.2 Field observations

The field observations are the main method to determine the relative chronology between the rocks. The volcanic pile has subhorizontal stratigraphy $(20°-30°)$ without ductile deformation, characterizing the volcanic sequence as homoclinal. The contact between the major dykes and the volcanic sequence is locally described as transitional indicating a feeder role for these intrusive rocks. The Monsabrais pluton clearly crosscuts the volcanic sequence and the major dykes. The equigranular and porphyritic dykes crosscut the previously described lithologies, and occur as synchronous intrusions, sharing occasionally the same weakness planes.

The presence of pinch and swell geometries along some equigranular and porphyritic dykes hosted in the volcanic sequence and within the Monsabrais pluton indicates that the emplacement of the dykes was within hot and unconsolidated rocks. Otherwise, chilled margins are frequently observed where the equigranular and porphyritic dykes are hosted in the volcanic sequence, indicating an emplacement in an already cooled rock. Those evidences indicate that these dykes are syn-volcanic and syn-pluton emplacement. The aplitic dykes are hosted in the Monsabrais pluton or in volcanic rocks near the pluton border. They are characterized by sharp contacts with the host rocks.

5.1.3 Petrography

The occurrence of phenocrysts points to a polygenetic process involving two-stage of cooling for the magma (Best, 2002). The first stage can occur in the magma chamber or in sub-magma chamber and the second stage can occur during the emplacement of the dykes at shallow depth from the surface.

The presence of zeolites in some amygdules is indicative of a primary low grade metamorphic event, which can be related to the sea-floor metasomatism. The relict crystals of hornblende indicate the existence of a geothermal anomaly, which could be related to the Monsabrais plutonic suite emplacement. The two metastable mineral assemblages, one characteristic of prehnite-pumpellyite facies and the other of low greenschist facies indicates a progressive metamorphic event that agrees with the regional metamorphism (Powell et al., 1993).

The chloritization, spilitization (albitization), silicification, epidotization, sericitization and carbonatization are interpreted as semi-conformable alteration zones produced by the leaching of the rock pile as the result of the percolation of hydrothermal fluids associated to a syn-volcanic convection system. The pyrites from the quartz-carbonate veins have the same signature than the pyrite associated to the hydrothermal alteration, leading to the interpretation of a same formation processes for both. The lack of a well focalised hydrothermal system limits further discussion.

5.1.4 Lithogeochemistry

The lithogeochemistry indicates a co-magmatic source for the dykes, volcanic pile and pluton with an arc basalt and andesite signature. Those lithologies present a limited range composition with local rhyodacite, with a predominant transitional magmatic affinity. Samples with tholeitic and calc-alkaline magmatic affinities are reported, but this variation does not agree with the textural and field characteristics. Consequently, all rocks are considered similar geochemically. The variation of the trace element profiles is interpreted as the result of a slight partial different melting or a moderate process of crystal fractionation in the magma chamber. The process of hydrothermalism and metamorphism do not affect significantly the immobile elements, in accord with the low hydrothermal alteration and a low grade metamorphism as established from petrographic observations.

5.1.5 Sulfides

The similar element signatures from both families of pyrite and pyrrhotite indicate a unique hydrothermal event for their genesis. The element signatures support a volcanogenic hydrothermal system for the sulfides origin, based on the comparison with sulfides from other known environments. The textural difference between the Pyrite 1 and the Pyrite 2 can be result of a weak increase of the geothermal gradient in the sector.

5.2 EVOLUTION MODEL

The evolution model is based on all the results presented in this manuscript. The figures 5.1 display three distinct increments of the geological evolution proposed for the studied area. The model extends the interpretation to the entire Monsabrais volcano-plutonic complex.

The figure 5.1A shows a large magma chamber of basaltic to andesitic composition corresponding to the magma source for the volcanic and the plutonic event. The smaller sub-magma chamber is the early Monsabrais plutonic suite. During this period, some growing of the phenocrysts occur in the magma chamber. This process is continuous during the entire magmatic event. On the surface, there is the formation of annular and concentric fractures induced by magma pressure.

The figure 5.1B is the most relevant because it represents a series of key events. The volcanism is active and it is fed by their major dykes that are used as magma conduits. Those same dykes also transport heated metal-bearing hydrothermal fluids. This fluid originated from the mixing of volcanogenic fluids and sea-water infiltrated along the peripheral fault system. This process of fluids percolation produced semi-comfortable hydrothermal zones and the discharge of these fluids along the dykes precipitating the metals. This same process is

responsible for the quartz-carbonate vein formation. On shallow levels, the crystallization of zeolites occurred in the vesicles of the volcanic rocks.

The progressive emplacement of the Monsabrais plutonic suite towards the surface produced a local increase of the geothermal gradient, causing the recrystallization of the clinopyroxene in hornblende. During the entire process of extrusion and plutonic emplacement, the equigranular and porphyritic dykes had been emplaced, sourced from distinct positions within a same magmatic chamber. The aplitic dykes are the last unit to be emplaced in Monsabrais, representing the residual melt on the sub-magma chamber.

The process of regional metamorphism is posterior to the entire magmatic event, being responsible to the recrystallization of minerals from the rock pile, and partially overprinting other thermal events.

The figure 5.1C represents the actual stage of the Monsabrais Volcanic Complex, after being covered by younger sediments and eroded by the glaciers, exposing what is considered the roots of an archean volcano-magmatic center.

Figure 5.1: Evolution model for the Monsabrais sector divided into 3 development phases.

The Monsabrais sector mapped in this project is part of the Blake River Group. Pearson and Daigneault (2009) interpreted the Blake River Group as a subaqueous megacaldera complex, in which the Monsabrais Volcanic Complex, like other volcanic complexes, is interpreted as the subaqueous summit calderas associated to the Misema caldera event (Mueller et al., 2009). The Monsabrais magmatic system presents evidences agreeing and disagreeing with the interpretation of a subaqueous summit caldera.

Evidences in support of the regional model are: 1) Mafic to intermediate dykes swarm in a radial organization, characterized by a N to NE orientation on the south/southwest of the centered plutonic suite of Monsabrais; and 2) weak carbonate alteration associated mainly with the pillow lavas and the volcaniclastic units.

According to the evidences enumerated in this manuscript, the Monsabrais Volcanic Complex is interpreted as a subaqueous volcanic center with polyphase, complex and long evolution magmatism. However, the small area of study does not permit a larger contribution to the summit caldera model for the Monsabrais Volcanic Complex.

CHAPTER 6

CONCLUSION

The Monsabrais Volcanic Complex is located in the important mining camp of Noranda. The new insights about the Blake River Group, interpreted as a megacaldera complex (Pearson and Daigneault, 2009), opened new perspectives for exploration. The gap of information about the relationship between lithologies, alteration and mineralization turned the Monsabrais Complex as an interesting area of research.

The objective of determining the genetic role of the dykes for the mineralization was specified according to the problems presented by the area, such as the abundance of various dykes with sulfides along them. For the accomplishment of the general objective, four specific objectives were fixed. To attempt to reach the goal, several methods were applied and the results of each objective are presented below.

6.1 DISTINCT FAMILIES OF DYKES BASED ON THEIR SPECIFICITIES

The dykes are the most important part of this project. The primary identification of dykes and the determination of the relative chronology between them and the other lithologies were achieved during the mapping through the field observations. The petrography was the most important method for the dyke classification in different families. The textural characterization was used as an essential tool for

this distinction. The textures and the mineralogy description were employed to infer the emplacement process and the metamorphic events.

The lithogeochemistry was used with precaution, as the archean rocks usually experiment several geothermal events that can modify the chemical composition of the rocks and in consequence mask the protolith signature. To avoid those interferences, least mobile elements as the REE and HFSE were used. It was possible to determine the co-magmatic character of all the lithologies, magmatic features and process from the sector.

6.2 VARIETY AND CHARACTERISTICS OF THE MINERALIZATIONS AND HYDROTHERMAL ALTERATION ASSEMBLAGES

The field observations were useful to determine the sulfides presence on the outcrops. However, the alteration zones are not as well recognizable at the same scale. The sulfides and the alterations seem to follow a random pattern. The petrography was crucial to characterize the alterations. Using mineralogy and textures descriptions, it was possible to determine their type.

The lithogeochemistry study provided answers about the chemistry behavior during the hydrothermalism process. The normative minerals (NORMAT) were used as a complementary technique to determine a pattern for the alterations. However, this technique did not contribute for the comprehension of the area as expected. LA-ICP-MS analyses on the pyrite and the pyrrhotite support the

interpretation of a unique genesis process for both sulfides, similar to other known volcanogenic mineralizations.

6.3 RELATIVE CHRONOLOGY FOR THE DYKES EMPLACEMENT AND MINERALIZATION EPISODES

The most efficient methodology to determine the relative chronology on Monsabrais was the crosscut relationships between the dykes and the other units on the field. No others techniques were applied complementary to this. It appears that the mineralization was synchronous with dyke emplacement.

6.4 MINERALIZATIONS AND DYKES IN A METALLOGENIC CONTEXT

The proposition of a metallogenic context for the dykes, the alteration and the mineralization was possible only with the integration of all the results. The main evidences lead to a same conclusion, confirming the efficiency of the chosen methods to attempt the objectives. Using the multiple evidences, it was possible to propose an evolutionary model for the studied sector of Monsabrais volcano-plutonic complex.

6.5 CONTRIBUTIONS

This study defines the Monsabrais complex as a volcano-plutonic system sourced from a unique magmatic chamber. The dykes emplacement is multi phase and continuous during the volcanism and the plutonic activities. The two major

dykes that crosscut the volcanic sequence are interpreting as magma conduits, which feed the extrusive flow event and can represent syn-volcanic faults.

6.6 ECONOMIC POTENTIAL

The Monsabrais sector presents multiple characteristics typical of volcanogenic massive sulfide settings. Unfortunately with the present knowledge, the sulfides occurrences as reported are not present in economic quantity. The erosion of the horizontal volcanic sequence imply exposure of the magmatic chamber summit, while mineralized levels are expected to occur above this, in higher levels of the volcanic sequence. However, the absence of high grade mineralization in the studied sector does not exclude the presence of mineralized zones around the Monsabrais sector or even in deeper levels.

6.7 RECOMMENDATIONS

For future studies on the Monsabrais complex, the author suggests a systematic larger mapping. The expanded area around the plutonic center could comprise the entire ring dyke, characterizing the entire dyke system.

Volcanogenic massive sulfide mineralizations commonly form stratabond deposits. In a homoclinal volcanic sequence as the Monsabrais, it is important to cover the largest area as possible, searching for evidences of alteration zones, interdigitation of the volcanic flow and the heat source as dykes that can also be

utilized as conduits for hydrothermal fluids. Geophysics techniques are also strongly recommended.

REFERENCES

Acocella, V. and Neri, M., 2009. Dike propagation in volcanic edifices: Overview and possible developments. Tectonophysics. 471(1-2): 67-77.

Anderson, E. M., 1937. Cone-sheets and ring-dykes: the dynamical explanation. *Bulletin Volcanologique.* 1 (1): 35-40.

Augustin, J., 2011. Facteurs de contrôle et processus métallogéniques des minéralisations aurifères du gisement de Wona, Mine Mana, Burkina Faso. *Mémoire de maîtrise, Université du Québec à Chicoutimi.* 220 p.

Baker, E. M. and Andrew, A. S., 1991. Geologic, fluid inclusion, and stable isotope studies of the gold-bearing breccias pipe at Kidston, Queensland, Australia. Economic Geology. 86: 810-830.

Barrett, T. J., Cattalani, S., Hoy, L., Riopel, J. and Lafleur, P. J., 1992. Massive sulfide deposits of the Noranda area, Quebec. IV. The Mobrun mine. Canadian Journal of Earth Sciences. 29:1349-1374.

Barrett, T. J. and MacLean, W. H., 1999. Volcanic sequences, lithogeochemistry, and hydrothermal alteration in some bimodal volcanic-associated massive sulfide systems. In: Barrie, C. T. and Hannington, M. D., Editors. Volcanic-Associated Massive Sulfide Systems: Processes and Examples in Modern and Ancient Settings. Reviews in Economic Geology. 8: 101-131.

Best, M. G., 2002. Igneous and metamorphic petrology. Blackwell Science Ltd, England. 729 p.

Castillo-Guimond, L., 2012. Distribution et caractérisation des faciès volcaniques et volcanoclastiques dan le secteur de Montsabrais. *Mémoire de maîtrise, Université du Québec à Chicoutimi.* 119 p.

Chadwick Jr., W. W. and Howard, K. A., 1991. The pattern of circumferential and radial eruptive fissures on the volcanoes of Femandina and Isabela Islands, Galapagos. Bulletin of Volcanology. 53: 259-275.

Côté-Mantha, O., 2009. Architecture et origine du système de minéralisation polymétallique du secteur lac Line, région de Chibougamau, Québec. *Thèse de doctorat, Université du Québec à Chicoutimi.* 485 p.

Daigneault, R., Mueller, W. U and Chown, E. H., 2004. Abitibi Greenstone belt plate tectonics: The diachrononous history of arc development, accretion and collision. In: Eriksson, P. G., Altermann, W., Nelson, D. R., Mueller, W. U. and Catuneanu, O., Editors. The Precambrian Earth: Tempos and Events. Elsevier, London. Developments in Precambrian Geology 12: 88-103.

Davis, B. K. and McPhie, J., 1996. Spherulites, quench fractures and relict perlite in a Late Devonian rhyolite dyke, Queensland, Australia. Journal of Volcanology and Geothermal Research. 71 (1): 1-11.

Dimroth, E. and Lichtblau, A. P., 1979. Metamorphic evolution of Archean hyaloclastites, Noranda area, Quebec, Canada. Part I: Comparison of Archean and Cenozoic sea-floor metamorphism. Canadian Journal of Earth Sciences. 16 (7): 1315-1340.

Dimroth, E., Imreh, L., Rocheleau, M. and Goulet, N., 1982. Evolution of the southcentral part of the Archean Abitibi Belt, Quebec. Part I. Stratigraphy and paleogeographic model. Canadian Journal of Earth Sciences. 19: 1729-1758.

Dostal, J. and Mueller, W., 1996. An Archean oceanic felsic dyke swarm in a nascent arc: the Hunter Mine Group, Abitibi greenstone belt, Canada. Journal of Volcanology and Geothermal Research. 72: 37-57.

Ernst R. E., Head, J. W., Parfitt E., Grosfils, E. and Wilson L., 1995. Giant radiating dyke swarms on Earth and Venus. Earth Science Reviews. 39: 1-58.

Fiske, R. S. and Jackson, E. D., 1972. Orientation and growth of Hawaiian rifts: The effect of regional structure and gravitational stresses. Proceedings of the Royal Society. 329: 299-326.

Fraser, R., 1993. The Lac Troilus Gold-Copper Deposit, Northwestern Quebec: A Possible Archean Porphyry System. Economic Geology. 88: 1685-1699.

Gaboury, D. and Daigneault, R., 1999. Evolution from seafloor-related to sulfide-rich quartz vein-type gold mineralization during deep submarine volcanic construction: The Géant Dormant gold mine, Archean Abitibi belt, Canada. Economic Geology. 94: 1–19.

Gaboury, D. and Daigneault, R., 2000. Flat vein formation in a transitional crustal setting by self-induced fluid pressure equilibrium – an example from the Géant Dormant gold mine, Canada. Ore Geology Reviews. 17: 155-178.

Gaboury, D., Daigneault, R. and Beaudoin, G., 2000. Volcanogenic-related origin of sulfide-rich quartz veins: Evidence from O and S Isotopes at the Géant Dormant gold mine, Abitibi belt, Canada. *Mineralium Deposita*, 35: 21-36.

Gaboury, D., Carrier, A., Crevier, M., Pelletier, C. and Sketchley, D. A., 2001. Predictive Distribution of Fault-Fill and Extensional Veins: Example from the Sigma Gold Mine, Abitibi Subprovince, Canada. Economic Geology. 96: 1397-1405.

Galley, A. G., 1993. Characteristics of semi-conformable alteration zones associated with volcanogenic massive sulphide districts. Journal of Geochemical Exploration. 48: 175-200.

Galley, A. G., Hannington, M. D. and Jonasson, I. R., 2007. Volcanogenic massive sulphide deposits. In: Goodfellow, W. D., Editor. Mineral Deposits of Canada: A Synthesis of Major Deposit-Types, District Metallogeny, the Evolution of Geological Provinces, and Exploration Methods: Geological Association of Canada, Mineral Deposits Division, Special Publication. 5: 141-161.

Genna, D., 2009. Caractérisation des altérations et des minéralisations volcanogènes du complexe volcanique du Cap d'Ours, Rouyn-Noranda, Québec. *Mémoire de maîtrise, Université du Québec à Chicoutimi.* 162 p.

Gill, J. B., 1981. Orogenic Andesites and Plate Tectonics. Reihe Minerals and Rocks 16; Springer-Verlag, Berlin New Cork. 412 p.

Goodman, S., Williams-Jones, A. E. and Carles, P, 2005. Structural controls on the Archean Troilus god-cooper deposit, Quebec, Canada. Economic Geology. 100: 577-582.

Goodwin, A. M. and Ridler, R. H., 1970. The Abitibi orogenic belt. In: Basins and geosynclines of the Canadian shield. Geological Survey of Canada. 70–40: 1–30.

Goto, Y. and McPhie, J., 1996. A Miocene basanite dyke at Stanley, northwestern Tasmania, Australia. Journal of Volcanology and Geothermal Research. 74: 111-120.

Gudmundsson, A., 1983. Form and dimensions of dykes in eastern Iceland. Tectonophysics. 95: 295-307.

Hannington, M. D., Santaguida, F., Kjarsgaard, I. M. and Cathles, L. M., 2003. Regional-scale hydrothermal alteration in the Central Blake River Group, western Abitibi subprovince, Canada: implications for VMS prospectivity. *Mineralium deposita*. 38: 393-422.

Hanson, R.E. and Schweickert, R.A., 1982. Chilling and brecciation of a Devonian rhyolite sill intruded into wet sediments, northern Sierra Nevada, California. Journal of Geology. 90: 717-724.

Humphris, S. E. and Thompson, G., 1978. Hydrothermal alteration of oceanic basalts by seawater. Geochimica et Cosmochimica Acta. 42, 1: 107–125.

Huston, D. L., Sie, S. H., Suter, G. F., Cooke, D. R. and Both, R. A., 1995. Trace elements in sulfide minerals from eastern Australian volcanic-hosted massive sulfide deposits; Part I, Proton microprobe analyses of pyrite, chalcopyrite, and sphalerite, and Part II, Selenium levels in pyrite; comparison with delta (super 34) S values and implications for the source of sulfur in volcanogenic hydrothermal systems. Economic Geology. 90:1167-1196.

Klugel, A., Walter, T. R., Schwarz, S. and Geldmacher, J., 2005. Gravitational spreading causes en-echelon diking along a rift zone of Madeira Archipelago: an experimental approach and implications for magma transport. Bulletin of Volcanology. 68: 37-46.

Lang, J. R. and Baker, T., 2001. Intrusion-related gold systems: the present level of understanding. *Mineralium Deposita*. 36: 477-489.

Legault, M. and Daigneault, R., 2006. Synvolcanic gold mineralization within a deformation zone: the Chevrier deposit, Chibougamau, Abitibi Subprovince, Canada. *Mineralium Deposita*. 41: 203–228.

MacLean, W. H., and Barret, T. J., 1993. Lithogeochemical techniques using immobile elements. Journal of Geochemical Exploration. 48: 109-133.

McNicoll et al. In: Ross, P. S., Goutier, J., McNicoll, V. J. and Dubé, B., 2008. Volcanology and geochemistry of the Monsabrais area, Blake River Group, Abitibi greenstone belt, Quebec: implications for volcanologic massive sulphide exploration. Geological Survey of Canada, Current Research. 18 p.

Middlemost, E. A. K., 1994. Naming materials in the magma/igneous system. Earth-Science Reviews. 37: 215–224.

Mueller, W. and Donaldson, J. A., 1992. A felsic dyke swarm formed under the sea: the Archean Hunter Mine Group, south-central Abitibi belt, Quebec, Canada. Bulletin of Volcanology. 54: 602-610.

Mueller, W. U., Daigneault, R., Mortensen, J. K. and Chown, E. H, 1996. Archean terrane docking: upper crust collision tectonics, Abitibi greenstone belt, Quebec, Canada. Tectonophysics. 265: 127-150.

Mueller, W. U., Moore, L. and Pilote, C., 2007. Blake River Group evolution: characteristics of the subaqueous Misema and New Senator calderas. DIVEX report. SC25: 1-9.

Mueller, W. U. and Mortensen, J. K., 2002. Age constrains and characteristics of subaqueous volcanic construction, the Archean Hunter Mine Group, Abitibi greenstone belt. Precambrian Research. 115: 119-152.

Mueller, W. U., Stix, J., Corcoran P. L. and Daigneault, R., 2009. Subaqueous calderas in the Archean Abitibi greenstone belt: An overview and new ideas. Ore Geology Reviews. 35 (no. 1): 4-46.

Mueller, W. U., Friedman, R., Daigneault, R., Moore, L. and Mortensen, J., 2012. Timing and characteristics of the Archean subaqueous Blake River Megacaldera Complex, Abitibi greenstone belt, Canada. Precambrian Research. 214–215: 1–27.

Nakamura, K., 1977. Volcanoes as possible indicators of tectonic stress orientation – principle and proposal. Journal of Volcanology and Geothermal Research. 2: 1-16.

Pearson, V. and Daigneault R., 2009. An Archean megacaldera complex: the Blake River Group, Abitibi greenstone belt. Precambrian Research. 168: 66-82.

Piché, M. and Jébrak, M., 2004. Normative minerals and alteration indices developed for mineral exploration. Journal of Geochemical Exploration. 82, 1–3: 59–77.

Pollard, D. D., 1987. Elementary fracture mechanics applied to the structural interpretation of dykes. In: H.C. Halls and W.F. Fahrig, Editors. Mafic Dyke Swarms, GAC Special Paper. 34: 5-24.

Powell, W. G., Carmichael, C. J. and Hodgson, C. J., 1993. Thermobarometry in a subgreenschist to greenschist transition in metabasites of the Abitibi

greenstone belt, Superior Province, Canada. Journal of Metamorphic Geology. 11: 165-178.

Robert, F. and Brown, A. C., 1986. Archean gold-bearing quartz veins at the Sigma mine, Abitibi greenstone belt, Quebec: Part I. Geologic relations and formation of the vein system. Economic Geology. 81: 578-592.

Rollinson, H. R., 1993. Using geochemical data: Evaluation, presentation, interpretation. Pearson Education Limited, Harlow, England. 352 p.

Ross, P. S., Goutier, J., McNicoll, V. J. and Dubé, B., 2008. Volcanology and geochemistry of the Monsabrais area, Blake River Group, Abitibi greenstone belt, Quebec: implications for volcanologic massive sulphide exploration. Geological Survey of Canada, Current Research. 18 p.

Sansfaçon, R., Grant, M. and Trudel, P., 1987. Géologie de la mine Canadian Malartic – District de Val-d'Or. *Série de Manuscrits Bruts, Gouvernement du Québec, Ministère de l'Énergie et des Ressources, Service de la géologie.* 49p.

Simons, F. S., 1962. Devitrification dykes and giant spherulites from Klondyke, Arizona. The American Mineralogist. 47: 871-885.

Sun, S. and McDonough, W.F., 1989. Chemical and isotopic systematics of oceanic basalts : implications for mantle composition and processes. In: Saunders, A. D. and Norry, M. J., Editors. Magmatism in the Ocean Basins. Geological society Special Publication. 42: 313-345.

Taylor, S. R. and McLennan, S. M., 1985. The continental crust: its composition and evolution. Blackwell, Oxford. In: **Rollinson, H. R., 1993**. Using geochemical data: Evaluation, presentation, interpretation. Pearson Education Limited, Harlow, England. 352 p.

Turcotte, D. L., Emerman, S. H. and Spence, D. A., 1987. Mechanics of dyke injection. In: Halls, H. C. and Fahrig, W. F., Editors. Mafic Dyke Swarms,GAC Special Paper. 34: 25-29.

Walker, S. D. and Cregheur, P., 1982. The Chadbourne Mine, Noranda, Quebec: A gold-bearing brecia. In: Hodder, R. W. and Petruk, W., Editors. Geology of Canadian gold deposits. Canadian Institute of Mining and Metallurgy. 24: 58-66.

Winchester, J.A. and Floyd, P.A., 1977. Geochemical discrimination of different magma series and their differentiation products using immobile elements. Chemical Geology. 20: 325-343.

Wood, D. A., 1980. The application of a Th–Hf–Ta diagram to problems of tectonomagmatic classification and to establishing the nature of crustal contamination of basaltic lavas of the British Tertiary volcanic province. Earth and Planetary Science Letters. 50: 11–30.

Yardley, B. W. D., 1990. An introduction to metamorphic petrology. Collections: Longman earth science series. Harlow, Essex: Longman Scientific & Technical; New York: J. Wiley. 248 p.

APPENDIX

Appendix 1

Table of stations descriptions.

Station	Samples	Coordinate E	Coordinate N	Unity	Geochimistry	Thin Section
LK-001A1	LK-10-001	615447	5369230	Equigranular dyke Aphanitic	yes	yes
LK-001A2	LK-10-002	615455	5369238	Porphyritic dyke	yes	yes
LK-001B		615431	5369181	Equigranular dyke Aphanitic		
LK-002A1	LK-10-003	615267	5369330	Porphyritic dyke	yes	yes
LK-002A2	LK-10-004	615275	5369338	Pillow lavas	yes	yes
LK-002A3	LK-10-005	615259	5369322	Volcaniclastic	yes	yes
LK-002B		615281	5369368	Volcaniclastic		
LK-002C		615296	5369367	Equigranular dyke Aphanitic		
LK-002D1	LK-10-072	615289	5369374	Equigranular dyke Aphanitic	yes	yes
LK-002D2	LK-10-073	615297	5369382	Porphyritic dyke	yes	yes
LK-002E1	LK-10-074	615259	5369320	Porphyritic dyke	yes	yes
LK-002E2	LK-10-075	615267	5369328	Equigranular dyke Aphanitic	no	no
LK-003A	LK-10-006	615286	5369399	Porphyritic dyke	yes	yes
LK-003B		615275	5369387	Equigranular dyke Aphanitic		
LK-004A		615344	5369533	Pillow lavas		
LK-004B		615336	5369488	Pillow lavas		
LK-004C	LK-10-007	615294	5369504	Pillow lavas	yes	yes
LK-005	LK-10-008	615310	5369418	Porphyritic dyke	yes	yes
LK-006A	LK-10-009	615484	5369293	Porphyritic dyke	yes	yes
LK-006B	LK-10-010	615492	5369301	Equigranular dyke Aphanitic	yes	yes
LK-007A	LK-10-011	615487	5369171	Equigranular dyke Aphanitic	yes	yes
LK-007B		615500	5369192	Equigranular dyke Aphanitic		
LK-008	LK-10-012	615471	5369274	Equigranular dyke Aphanitic	no	no
LK-009A		615384	5369353	Intermediate		

Station	Samples	Coordinate E	Coordinate N	Unity	Geochimistry	Thin Section
LK-009B1	LK-10-013	615391	5369378	Porphyritic dyke	yes	yes
LK-009B2	LK-10-014	615399	5369386	Volcaniclastic	yes	yes
LK-009C		615417	5369435	Intermediate		
LK-010	LK-10-015	615390	5369692	Pluton	yes	yes
LK-011	LK-10-016	615477	5369711	Pluton	yes	yes
LK-012	LK-10-017	615599	5369839	Porphyritic dyke	yes	yes
LK-013	LK-10-018	615619	5369698	Equigranular dyke Phaneritic	yes	yes
LK-014	LK-10-019	615633	5369321	Pluton	yes	yes
LK-015	LK-10-020	615671	5369799	Equigranular dyke Aphanitic	no	no
LK-016	LK-10-021	615686	5369706	Porphyritic dyke	yes	yes
LK-017	LK-10-022	615723	5369621	Pillow lavas	yes	yes
LK-018	LK-10-023	615704	5369447	Pillow lavas	yes	yes
LK-019	LK-10-024	615702	5369260	Equigranular dyke Aphanitic	no	no
LK-020A	LK-10-025	615739	5369158	Porphyritic dyke	yes	yes
LK-020B		615728	5369138	Equigranular dyke Aphanitic		
LK-021	LK-10-026	615757	5369782	Aplitic dyke	yes	yes
LK-022A	LK-10-027	615803	5369463	Pillow lavas	yes	yes
LK-022B	LK-10-028	615811	5369447	Equigranular dyke Aphanitic	yes	yes
LK-022C	LK-10-029	615834	5369351	Equigranular dyke Aphanitic	no	no
LK-023	LK-10-030	615811	5369307	Porphyritic dyke	no	yes
LK-024A	LK-10-031	615808	5369199	Porphyritic dyke	yes	yes
LK-024B	LK-10-032	615816	5369207	Porphyritic dyke	yes	yes
LK-025	LK-10-033	615892	5369512	Equigranular dyke Aphanitic	no	no
LK-026	LK-10-034	615984	5369580	Equigranular dyke Aphanitic	no	no
LK-027	LK-10-035	615983	5369510	West dyke	yes	yes
LK-028		615993	5369406	Intermediate		
LK-029A		616002	5369333	Equigranular dyke Aphanitic		

Station	Samples	Coordinate E	Coordinate N	Unity	Geochimistry	Thin Section
LK-029B	LK-10-036	616027	5369364	Equigranular dyke Aphanitic	no	no
LK-030		615922	5369281	Intermediate		
LK-031		616063	5369589	Volcaniclastic		
LK-032A		616081	5369572	Volcaniclastic		
LK-032B	LK-10-037	616085	5369572	Volcaniclastic	yes	yes
LK-033	LK-10-038	616098	5369540	Porphyritic dyke	yes	yes
LK-034	LK-10-039	616099	5369534	Equigranular dyke Aphanitic	no	no
LK-035A	LK-10-040	616138	5369532	Porphyritic dyke	yes	yes
LK-035B	LK-10-041	616146	5369540	Porphyritic dyke	yes	yes
LK-035C	LK-10-042	616130	5369524	Porphyritic dyke	yes	yes
LK-036A	LK-10-043	616142	5369473	Qtz Ca Vein	no	yes
LK-036B	LK-10-044	616150	5369481	Qtz Ca Vein	no	yes
LK-037	LK-10-045	616138	5369413	Equigranular dyke Aphanitic	no	no
LK-038	LK-10-046	616147	5369256	Equigranular dyke Aphanitic	no	no
LK-039	LK-10-047	616160	5369246	Equigranular dyke Aphanitic	no	no
LK-040	LK-10-048	616167	5369148	Equigranular dyke Aphanitic	no	no
LK-041A		616249	5369577	Equigranular dyke Aphanitic		
LK-041B		616255	5369580	Equigranular dyke Aphanitic		
LK-041C	LK-10-049	616245	5369560	Equigranular dyke Aphanitic	no	no
LK-041D		616238	5369535	Equigranular dyke Aphanitic		
LK-042A	LK-10-050	616249	5369549	Equigranular dyke Aphanitic	no	no
LK-042B		616249	5369521	Equigranular dyke Aphanitic		
LK-043A	LK-10-051	616232	5369403	Equigranular dyke Aphanitic	no	no
LK-043B		616209	5369350	Equigranular dyke Aphanitic		
LK-043C		616240	5369274	Equigranular dyke Aphanitic		
LK-044A	LK-10-057	616244	5369182	Equigranular dyke Aphanitic	no	no
LK-044B	LK-10-058	616232	5369180	Equigranular dyke Aphanitic	no	no

Station	Samples	Coordinate E	Coordinate N	Unity	Geochimistry	Thin Section
LK-044C		616231	5369191	Equigranular dyke Aphanitic		
LK-045	LK-10-052	616302	5369659	Equigranular dyke Aphanitic	no	no
LK-046	LK-10-053	616359	5369643	Equigranular dyke Aphanitic	yes	yes
LK-047	LK-10-054	616302	5369476	Equigranular dyke Aphanitic	no	no
LK-048	LK-10-055	616291	5369387	Equigranular dyke Aphanitic	no	no
LK-049	LK-10-056	616402	5369385	Equigranular dyke Aphanitic	yes	yes
LK-050		616235	5369169	Equigranular dyke Aphanitic		
LK-051		616253	5369158	Equigranular dyke Aphanitic		
LK-052A		616163	5369075	Equigranular dyke Aphanitic		
LK-052B		616168	5369063	Equigranular dyke Aphanitic		
LK-053		616226	5369098	Equigranular dyke Aphanitic		
LK-054A	LK-10-059	616257	5369116	Equigranular dyke Aphanitic	yes	yes
LK-054B	LK-10-060	616249	5369108	Equigranular dyke Aphanitic	no	no
LK-055		616495	5369703	Intermediate		
LK-056A	LK-10-061	616473	5369717	Porphyritic dyke	yes	yes
LK-056B	LK-10-062	616481	5369725	Massive flow	yes	yes
LK-057	LK-10-063	616399	5369760	Aplitic dyke	yes	yes
LK-058		616576	5369656	Equigranular dyke Aphanitic		
LK-059		616578	5369594	Equigranular dyke Aphanitic		
LK-060	LK-10-064	616792	5369820	Equigranular dyke Aphanitic	no	no
LK-061	LK-10-065	616927	5369885	Porphyritic dyke	yes	yes
LK-062A		617029	5369802	Equigranular dyke Aphanitic		
LK-062B		617038	5369817	Equigranular dyke Aphanitic		
LK-063	LK-10-066	616966	5369798	Massive flow	yes	yes
LK-064	LK-10-067	616719	5369101	Equigranular dyke Phaneritic	yes	yes
LK-065	LK-10-068	616830	5369111	Equigranular dyke Aphanitic	no	no
LK-066A		617041	5369621	Equigranular dyke Aphanitic		

Station	Samples	Coordinate E	Coordinate N	Unity	Geochimistry	Thin Section
LK-066B	LK-10-069	617045	5369611	Equigranular dyke Aphanitic	yes	yes
LK-067	LK-10-070	617175	5369716	Porphyritic dyke	yes	yes
LK-068A		617228	5369695	Equigranular dyke Aphanitic		
LK-068B		617216	5369678	Equigranular dyke Aphanitic		
LK-069		617154	5369599	Equigranular dyke Aphanitic		
LK-070		617073	5369505	Equigranular dyke Aphanitic		
LK-071		616425	5369105	Equigranular dyke Aphanitic		
LK-072A	LK-10-071	616430	5368977	Porphyritic dyke	yes	yes
LK-072B		616427	5368973	Porphyritic dyke		
LK-073A		616540	5369023	Equigranular dyke Aphanitic		
LK-073B		616538	5369047	Equigranular dyke Aphanitic		
LK-074	LK-10-076	616593	5368797	Porphyritic dyke	yes	yes
LK-075	LK-10-077	617374	5369426	Equigranular dyke Aphanitic	yes	yes
LK-076A		617413	5369270	Intermediate		
LK-076B		617421	5369278	Pillow lavas		
LK-077A	LK-10-078	617425	5369253	Equigranular dyke Aphanitic	no	no
LK-077B		617426	5369256	Equigranular dyke Aphanitic		
LK-078		617429	5369247	Equigranular dyke Aphanitic		
LK-079	LK-10-079	617302	5369120	Equigranular dyke Aphanitic	no	no
LK-080A		617315	5369204	Equigranular dyke Aphanitic		
LK-080B		617304	5369186	Equigranular dyke Aphanitic		
LK-081A		616763	5369703	Equigranular dyke Aphanitic		
LK-081B		616782	5369672	Equigranular dyke Aphanitic		
LK-082	LK-10-080	616808	5369603	Equigranular dyke Aphanitic	no	no
LK-083		616706	5369594	Pillow lavas		
LK-084A	LK-10-081	616510	5369408	Equigranular dyke Aphanitic	no	no
LK-084B		616495	5369397	Equigranular dyke Aphanitic		

Station	Samples	Coordinate E	Coordinate N	Unity	Geochimistry	Thin Section
LK-085		616603	5369284	Massive flow		
LK-086	LK-10-082	616894	5369377	Equigranular dyke Aphanitic	no	no
LK-087		616951	5369398	Volcaniclastic		
LK-088	LK-10-083	617230	5369466	Equigranular dyke Aphanitic	no	no
LK-089	LK-10-084	617239	5369430	East dyke	yes	yes
LK-090	LK-10-085	616830	5369301	Massive flow	yes	yes
LK-091A		616794	5369157	Equigranular dyke Aphanitic		
LK-091B		616797	5369161	Equigranular dyke Aphanitic		
LK-091C	LK-10-086	616807	5369204	Equigranular dyke Aphanitic	no	no
LK-091D	LK-10-087	616793	5369172	Equigranular dyke Aphanitic	yes	yes
LK-092A	LK-10-088	616684	5368936	Equigranular dyke Aphanitic	no	no
LK-092B		616672	5368920	Equigranular dyke Aphanitic		
LK-093	LK-10-089	617170	5369325	Equigranular dyke Aphanitic	no	no
LK-094A	LK-10-090	617184	5369256	East dyke	yes	yes
LK-094B	LK-10-091	617192	5369264	Equigranular dyke Aphanitic	no	no
LK-095	LK-10-092	617100	5369094	East dyke	yes	yes
LK-096		617098	5369180	Equigranular dyke Aphanitic		
LK-097		617087	5369208	Equigranular dyke Aphanitic		
LK-098		616993	5369219	Equigranular dyke Aphanitic		
LK-099		617010	5369236	Equigranular dyke Aphanitic		
LK-100		617023	5369243	Equigranular dyke Aphanitic		
LK-101		614832	5369463	Equigranular dyke Aphanitic		
LK-102A	LK-10-093	614879	5369453	Equigranular dyke Aphanitic	no	no
LK-102B	LK-10-093B	614887	5369461	Pluton	yes	yes
LK-103		614872	5369506	Coarse		
LK-104	LK-10-094	615202	5369680	Pluton	yes	yes
LK-105A		615306	5369615	Equigranular dyke Aphanitic		

Station	Samples	Coordinate E	Coordinate N	Unity	Geochimistry	Thin Section
LK-105B		615287	5369600	Equigranular dyke Aphanitic		
LK-106		615513	5369867	Massive flow		
LK-107	LK-11-095	615293	5369362	Equigranular dyke Aphanitic	yes	no
LK-108	LK-11-096	615291	5369365	Equigranular dyke Aphanitic	yes	no
LK-109	LK-11-097	615288	5369371	Equigranular dyke Aphanitic	yes	no
LK-110	LK-11-098	615258	5369334	Equigranular dyke Aphanitic	yes	no
LK-111	LK-11-099	615255	5369329	Equigranular dyke Aphanitic	yes	no
LK-112	LK-11-100	615256	5369330	Equigranular dyke Aphanitic	yes	no
LK-113	LK-11-101	615258	5369313	Equigranular dyke Aphanitic	yes	no
LK-114	LK-11-102	615259	5369314	Equigranular dyke Aphanitic	yes	no
LK-115	LK-11-103	615263	5369324	Equigranular dyke Aphanitic	yes	no
LK-116	LK-11-104	615264	5369325	Equigranular dyke Aphanitic	yes	no
LK-117		615557	5369706	Equigranular dyke Aphanitic		
MONS-01		615502	5371009	Pillow lavas		
MONS-02		615282	5369373	Pillow lavas		
MONS-03		614572	5370395	Massive flow		
MONS-04		614673	5370469	Pillow lavas		
MONS-05		615064	5371043	Pillow lavas		
MONS-06A		615622	5370028	Pillow lavas		
MONS-06B		615630	5370036	Intermediate		
MONS-07		616149	5369477	Qtz Ca Vein		
MONS-08				Intermediate		
MONS-09		615193	5369680	Intermediate		
MONS-10		615271	5369617	Intermediate		
MONS-11		615317	5369642	Intermediate		
MONS-12A		615308	5369612	Coarse		
MONS-12B		615316	5369620	Porphyritic dyke		

Station	Samples	Coordinate E	Coordinate N	Unity	Geochimistry	Thin Section
MONS-12C		615300	5369604	Equigranular dyke Aphanitic		
MONS-13A		615308	5369724	Intermediate		
MONS-13B		615316	5369732	Equigranular dyke Aphanitic		
MONS-14A		615359	5369777	Intermediate		
MONS-14B		615367	5369785	Equigranular dyke Aphanitic		
MONS-15A		615415	5369909	Intermediate		
MONS-15B		615423	5369917	Equigranular dyke Aphanitic		
MONS-16A		615222	5369791	Intermediate		
MONS-16B		615230	5369799	Equigranular dyke Aphanitic		
MONS-17A		614877	5369481	Intermediate		
MONS-17B		614885	5369489	Equigranular dyke Aphanitic		
MONS-18A		615517	5369862	Massive flow		
MONS-18B		615525	5369870	Intermediate		
MONS-18C		615509	5369854	Qtz Ca Vein		
MONS-19		615522	5369791	Pillow lavas		
MONS-20		615586	5369433	Pillow lavas		
MONS-21		615493	5369385	Coarse		
MONS-22		615490	5369387	Pillow lavas		
MONS-23		615427	5369039	Pillow lavas		
MONS-24		615451	5369063	Pillow lavas		
MONS-25A		615521	5369147	Pillow lavas		
MONS-25B		615529	5369155	Equigranular dyke Aphanitic		
MONS-26		615649	5369284	Volcaniclastic		
MONS-27A		615700	5369257	Volcaniclastic		
MONS-27B		615708	5369265	Equigranular dyke Aphanitic		
MONS-28A		615806	5369198	Volcaniclastic		
MONS-28B		615814	5369206	Equigranular dyke Aphanitic		

Station	Samples	Coordinate E	Coordinate N	Unity	Geochimistry	Thin Section
MONS-29		615827	5369289	Massive flow		
MONS-30		615833	5369328	Pillow lavas		
MONS-31		615799	5369480	Pillow lavas		
MONS-32A		615748	5369787	Volcaniclastic		
MONS-32B		615756	5369795	Coarse		
MONS-33				Volcaniclastic		
MONS-34A		616472	5368911	Volcaniclastic		
MONS-34B		614480	5368919	Massive flow		
MONS-34C		614464	5368903	Equigranular dyke Aphanitic		
MONS-35A		616456	5368947	Volcaniclastic		
MONS-35B		616464	5368955	Massive flow		
MONS-35C		616448	5368939	Equigranular dyke Aphanitic		
MONS-36A		616434	5368974	Volcaniclastic		
MONS-36B		616442	5368982	Equigranular dyke Aphanitic		
MONS-37		616613	5369226	Pillow lavas		
MONS-38		616593	5369176	Pillow lavas		
MONS-39A		616553	5369018	Volcaniclastic		
MONS-39B		616561	5369026	Equigranular dyke Aphanitic		
MONS-40		616565	5369127	Pillow lavas		
MONS-41		616575	5369167	Pillow lavas		
MONS-42		616555	5369338	Volcaniclastic		
MONS-43		616506	5369422	Volcaniclastic		
MONS-44		616410	5369438	Pillow lavas		
MONS-45A		616283	5369347	Pillow lavas		
MONS-45B		616291	5369355	Equigranular dyke Aphanitic		
MONS-46		616223	5369428	Pillow lavas		
MONS-47A		616242	5369182	Volcaniclastic		

Station	Samples	Coordinate E	Coordinate N	Unity	Geochimistry	Thin Section
MONS-47B		616250	5369190	Intermediate		
MONS-48A		616724	5369097	Volcaniclastic		
MONS-48B		616732	5369105	Intermediate		
MONS-49		616752	5369150	Pillow lavas		
MONS-50		616801	5369162	Equigranular dyke Aphanitic		
MONS-51A		616986	5369277	Pillow lavas		
MONS-51B		616994	5369285	Equigranular dyke Aphanitic		
MONS-52		617189	5369379	Equigranular dyke Aphanitic		
MONS-53		617221	5369424	Coarse		
MONS-54		617160	5369502	Equigranular dyke Aphanitic		
MONS-55		617096	5369445	Pillow lavas		
MONS-56		616601	5369302	Pillow lavas		
MONS-57A		615808	5369311	Pillow lavas		
MONS-57B		615816	5369319	Equigranular dyke Aphanitic		
MONS-58		615810	5369407	Pillow lavas		
MONS-59A		615840	5369438	Pillow lavas		
MONS-59B		615848	5369446	Volcaniclastic		
MONS-60A		615792	5369488	Pillow lavas		
MONS-60B		615800	5369496	Volcaniclastic		
MONS-61A		615809	5369467	Volcanic		
MONS-61B		615817	5369475	Equigranular dyke Aphanitic		
MONS-62		616197	5369191	Equigranular dyke Aphanitic		

Appendix 2

Table of thin sections observations.

Photo	Samples	Station	Oriented	Type	Unit	Host Rock	Amygdules	Phenocrystals	Chlorite (%)	Epidote (%)	Quartz (%)	White mica (%)	Carbonate (%)	Smectite (%)	Albite (%)
	LK-10-001	LK-001A1	no	Normal	Equigranular dyke Aphanitic	Volcaniclastic	Yes	no	20	40	5	0	0	25	0
	LK-10-002	LK-001A2	no	Normal	Porphyritic dyke	Volcaniclastic	Yes	7 Plg Ph - wm+Chl+Ep 3 (Px) Hbl Ph - Act+Chl	15	10	10	10	0	15	0
	LK-10-003	LK-002A1	no	Normal	Porphyritic dyke	Volcaniclastic		3 Act - Chl	70	15	0	10	0	5	0
	LK-10-004	LK-002A2	no	Polished	Pillow lavas	Pillow lavas	Yes	no	0	30	0	0	0	0	0
	LK-10-005	LK-002A3	no	Polished	Volcaniclastic	Volcaniclastic	Yes	no	10	30	7	0	0	0	0

Photo	Samples	Station	Oriented	Type	Unit	Host Rock	Amygdules	Phenocrystals	Chlorite (%)	Epidote (%)	Quartz (%)	White mica (%)	Carbonate (%)	Smectite (%)	Albite (%)
	LK-10-018	LK-013	yes	Normal	Equigranular dyke Phanentic	Volcaniclastic		no	15	25	5	0	0	5	0
	LK-10-019	LK-014	no	Normal	Pluton	Pluton		10 Px - Act+Chl 25 Plg - Ep+wm	15	20	15	10	0	2	0
	LK-10-021	LK-016	yes	Normal	Porphyritic dyke	Volcaniclastic	Yes	15 Plg Ph - Ep+wm	50	35	0	0	0	15	0
	LK-10-022	LK-017	no	Normal	Pillow lavas	Pillow lavas	Yes	no	0	45	60	0	0	0	0
	LK-10-023	LK-018	no	Polished	Pillow lavas	Pillow lavas	Yes	10 Plg - Qtz+Ep	15	35	25	0	0	10	0
	LK-10-025	LK-020A	yes	Normal	Porphyritic dyke	Volcaniclastic	Yes	2 (Px) Ph - Chl+Sme+wm	20	15	15	5	0	5	0
	LK-10-026	LK-021	no	Polished	Aplitic dyke	Volcaniclastic		no	3	5	30	2	2	0	0
	LK-10-027	LK-022A	yes	Polished	Pillow lavas	Pillow lavas		10 Plg - Alb+Ep+wm	10	35	30	5	0	0	20
	LK-10-028	LK-022B	yes	Normal	Equigranular dyke Aphanitic	Volcaniclastic	Yes	no	20	5	10	40	0	10	0
	LK-10-030	LK-023	yes	Normal	Porphyritic dyke	Pillow lavas	Yes	5 (Px) Ph - Chl+Ep+Act	25	20	5	40	0	5	0
	LK-10-031	LK-024A	no	Normal	Porphyritic dyke	Volcaniclastic	Yes	7 (Px) Ph - Chl	35	15	5	40	0	5	0

Photo	Samples	Station	Oriented	Type	Unit	Host Rock	Amygdules	Phenocrystals	Chlorite (%)	Epidote (%)	Quartz (%)	White mica (%)	Carbonate (%)	Smectite (%)	Albite (%)
	LK-10-032	LK-024B	no	Normal	Porphyritic dyke	Volcaniclastic	Yes	15 (Plg) Ph - Ep+ca	0	10	60	0	5	0	0
	LK-10-035	LK-027	no	Normal	West dyke	West dyke		no	25	30	5	15	0	5	0
	LK-10-037	LK-032B	yes	Normal	Volcaniclastic	Volcaniclastic	Yes	15 (Plg) Ph - Ep+wm	10	35	20	25	0	0	0
	LK-10-038	LK-033	yes	Polished	Porphyritic dyke	Volcaniclastic	Yes	2 (Px) Ph - Chl	20	25	5	10	0	10	0
	LK-10-040	LK-035A	yes	Normal	Porphyritic dyke	Volcaniclastic	Yes	20 (Plg) Ph - wm+Ep	3	10	35	15	0	0	45
	LK-10-041	LK-035B	no	Normal	Porphyritic dyke	Volcaniclastic		15 (Px) Ph - Act+Ep	5	5	5	0	0	5	70
	LK-10-042	LK-035C	no	Normal	Porphyritic dyke	Volcaniclastic	Yes	20 (Plg) Ph - wm+Ep+Chl 15 (Px) Ph - Act+Chl	3	5	10	15	3	7	45
	LK-10-043	LK-036A	no	Polished	Qtz Vein	Volcaniclastic		no	0	0	0	0	0	0	0
	LK-10-044	LK-036B	no	Polished	Qtz Vein	Volcaniclastic		no	0	0	0	0	0	0	0
	LK-10-053	LK-046	no	Polished	Equigranular dyke Aphanitic	Volcaniclastic		no	5	10	15	0	0	0	0
	LK-10-056	LK-049	yes	Normal	Porphyritic dyke	Volcaniclastic		5 (Plg) Ph - Chl	40	30	0	5	0	5	0

Photo	Samples	Station	Oriented	Type	Unit	Host Rock	Amygdules	Phenocrystals	Chlorite (%)	Epidote (%)	Quartz (%)	White mica (%)	Carbonate (%)	Smectite (%)	Albite (%)
	LK-10-059	LK-054A	no	Normal	Equigranular dyke Aphanitic	Volcaniclastic		no	45	10	25	0	0	0	0
	LK-10-061	LK-056A	no	Normal	Porphyritic dyke	Volcaniclastic		30 (Plg) Ph - Ep+wm	5	25	20	25	0	0	35
	LK-10-062	LK-056B	no	Normal	Massive flow	Massive flow	Yes	20 Plg - Ep+wm 7 (Px) Ph - Act	10	30	10	15	2	0	0
	LK-10-063	LK-057	no	Normal	Aplitic dyke	Pillow lavas	Yes	5 (Px) Act - Act	0	55	40	0	0	0	0
	LK-10-065	LK-061	yes	Normal	Porphyritic dyke	Pillow lavas	Yes	10 (Plg) Ph - Ep+Qtz	3	25	5	0	0	0	0
	LK-10-066	LK-063	no	Normal	Massive flow	Massive flow		no	0	55	40	0	0	5	0
	LK-10-067	LK-064	yes	Normal	Equigranular dyke Phanentic	Volcaniclastic		no	15	40	5	15	0	5	0
	LK-10-069	LK-066B	yes	Normal	Equigranular dyke Aphanitic	Volcaniclastic	Yes	no	35	20	15	0	0	0	0
	LK-10-070	LK-067	no	Normal	Porphyritic dyke	Pillow lavas	Yes	15 (Px) Ph - Act+Qtz+Ep	0	15	10	0	0	0	0
	LK-10-071	LK-072A	yes	Normal	Porphyritic dyke	Volcaniclastic		3 (Plg) Ph - Ep+wm	0	15	0	7	0	0	0
	LK-10-072	LK-002D1	no	Normal	Equigranular dyke Aphanitic	Volcaniclastic		no	20	10	15	50	0	0	0

Photo	Samples	Station	Oriented	Type	Unit	Host Rock	Amygdules	Phenocrystals	Chlorite (%)	Epidote (%)	Quartz (%)	White mica (%)	Carbonate (%)	Smectite (%)	Albite (%)
	LK-10-073	LK-002D2	yes	Normal	Porphyritic dyke	Volcaniclastic	Yes	20 (Plg) Ph - Ca+Sme	0	15	5	0	5	10	0
	LK-10-074	LK-002E1	no	Normal	Porphyritic dyke	Volcaniclastic		5 (Px) Act - Chl	35	20	10	0	0	5	0
	LK-10-076	LK-074	no	Normal	Porphyritic dyke	Volcaniclastic		50 (Plg) Ph - Ep+wm+Sme 10 (Px) Act - Chl+Ca	7	15	25	15	10	10	10
	LK-10-077	LK-075	no	Polished	Equigranular dyke Aphanitic	Massive flow	Yes	no	15	0	10	0	0	30	0
	LK-10-084	LK-089	no	Normal	East dyke	East dyke		30 (Px) Act - Chl	5	20	10	5	0	0	0
	LK-10-085	LK-090	no	Polished	Massive flow	Massive flow	Yes	7 (Plg) Ph - Qtz	15	30	40	0	0	0	0
	LK-10-087	LK-091D	no	Polished	Equigranular dyke Aphanitic	Volcaniclastic	Yes	no	45	15	10	30	0	0	0
	LK-10-090	LK-094A	no	Normal	East dyke	East dyke		30 (Px) Act - Chl+Ep	5	25	10	0	0	0	0
	LK-10-092	LK-095	no	Normal	East dyke	East dyke		25 (Px) Act - Chl+Ep	10	30	20	5	0	0	15
	LK-10-093b	LK-102B	no	Normal	Pluton	Pluton		no	10	60	10	20	0	0	0
	LK-10-094	LK-104	no	Normal	Pluton	Pluton		no	0	35	0	25	0	0	0

Appendix 3

Table of lithogeochemistry samples and respectively analyzed elements.

		Analysis		
		Batches		
Elements	**Method**	**1 (19 samples)**	**2 (38 samples)**	**3 (10 samples)**
Major	ME-XRF06 (%) XRF	SiO_2, Al_2O_3, Fe_2O_3, CaO, MgO, Na_2O, K_2O, Cr_2O_3, TiO_2, MnO, P_2O_5, SrO, BaO, LOI		
	ME-ICP06 (%) ICP-AES		SiO_2, Al_2O_3, Fe_2O_3, CaO, MgO, Na_2O, K_2O, Cr_2O_3, TiO_2, MnO, P_2O_5, SrO, BaO, LOI	SiO_2, Al_2O_3, Fe_2O_3, CaO, MgO, Na_2O, K_2O, Cr_2O_3, TiO_2, MnO, P_2O_5, SrO, BaO, LOI
REE and trace	ME-MS81 (ppm) ICP-MS	Ag, Ba, Ce, Co, Cr, Cs, Cu, Dy, Er, Eu, Ga, Gd, Hf, Ho, La, Lu, Mo, Nb, Nd, Ni, Pb, Pr, Rb, Sm, Sn, Sr, Ta, Tb, Th, Tl, Tm, U, V, W, Y, Yb, Zn, Zr	Ag, Ba, Ce, Co, Cr, Cs, Cu, Dy, Er, Eu, Ga, Gd, Hf, Ho, La, Lu, Mo, Nb, Nd, Ni, Pb, Pr, Rb, Sm, Sn, Sr, Ta, Tb, Th, Tl, Tm, U, V, W, Y, Yb, Zn, Zr	Ag, Ba, Ce, Co, Cr, Cs, Cu, Dy, Er, Eu, Ga, Gd, Hf, Ho, La, Lu, Mo, Nb, Nd, Ni, Pb, Pr, Rb, Sm, Sn, Sr, Ta, Tb, Th, Tl, Tm, U, V, W, Y, Yb, Zn, Zr
	ME-XRF05 (ppm) XRF	Ba, Nb, Rb, Sr, Y, Zr		
	ME-AQ81 (ppm) ICP-AES	Ag, As, Cd, Co, Cu, Hg, Mo, Ni, Pb, Zn		
	ME-ICP41 (ppm) ICP-AES			Ag, As, B, Ba, Be, Bi, Cd, Co, Cr, Cu, Ga, Hg, La, Mn, Mo, Ni, P, Pb, Sb, Sc, Sr, Th, Tl, U, V, W, Zn
	ME-ICP41 (%) ICP-AES			Al, Ca, Fe, K, Mg, Na, S, Ti
	Au-AA25 (ppm) AAS		Au	
	Ag-AA46 (ppm) AAS		Ag	
	ME-AA46 (ppm) AAS		Ag, As, Cu, Mo, Ni, Pb, Zn	
	S-OG46 (ppm) ICP-AES		S	

Appendix 4

Table of lithogeochemistry data.$_2$

Sample	SiO$_2$ %	Al$_2$O$_3$ %	Fe$_2$O$_3$ %	CaO %	MgO %	Na$_2$O %	K$_2$O %	Cr$_2$O$_3$ %	TiO$_2$ %	MnO %	P$_2$O$_5$ %	SrO %
LK-10-001	54.180	17.510	7.700	10.320	4.850	2.410	0.400	0.010	0.560	0.130	0.070	0.030
LK-10-002	52.000	17.820	7.730	9.070	6.640	1.710	0.410	0.010	0.540	0.100	0.066	0.030
LK-10-003	48.270	16.400	11.160	11.900	5.330	1.900	0.850	0.020	1.160	0.170	0.095	0.020
LK-10-004	42.870	11.430	21.320	14.490	5.020	0.450	0.380	0.010	0.460	0.270	0.076	0.020
LK-10-005	41.400	11.300	24.600	13.550	3.640	0.510	0.400	0.020	0.450	0.320	0.200	0.010
LK-10-006	48.740	17.660	10.160	10.170	5.770	1.580	1.560	0.010	1.170	0.150	0.155	0.020
LK-10-007	43.040	16.620	17.310	12.410	3.440	1.660	0.140	0.020	1.060	0.330	0.111	0.020
LK-10-008	49.380	16.880	10.120	8.800	6.220	2.180	1.380	0.010	0.980	0.160	0.083	0.020
LK-10-009	52.170	17.980	8.030	9.680	5.640	2.160	0.400	0.010	0.630	0.120	0.074	0.030
LK-10-010	56.000	17.400	6.640	9.120	4.770	3.590	0.170	0.010	0.590	0.100	0.070	0.030
LK-10-011	59.910	15.930	6.780	8.180	2.710	2.300	1.000	0.005	0.820	0.090	0.104	0.030
LK-10-013	48.560	18.240	9.250	11.410	5.740	1.990	0.640	0.010	0.900	0.130	0.089	0.020
LK-10-014	51.000	16.600	10.100	11.100	4.890	2.890	0.360	0.040	0.700	0.170	0.070	0.020
LK-10-015	65.020	15.290	6.140	3.960	1.010	4.440	0.930	0.005	0.640	0.070	0.171	0.020
LK-10-016	50.850	17.630	8.670	9.890	6.440	2.210	0.760	0.020	0.720	0.150	0.085	0.030
LK-10-017	42.870	17.180	18.980	2.910	6.390	1.400	1.130	0.010	0.690	0.090	0.047	0.010
LK-10-018	49.600	17.360	11.730	9.560	5.760	2.470	0.380	0.010	1.150	0.180	0.111	0.020
LK-10-019	50.750	17.510	8.350	9.740	6.740	1.930	0.260	0.010	0.750	0.110	0.081	0.020
LK-10-021	46.130	18.040	11.110	10.640	6.670	1.270	1.070	0.010	0.780	0.190	0.051	0.020
LK-10-022	55.400	16.400	7.300	15.950	1.440	0.160	0.010	0.060	1.200	0.100	0.240	0.050
LK-10-023	55.000	14.200	11.800	7.770	4.570	2.720	0.920	0.040	1.000	0.160	0.160	0.020
LK-10-025	51.020	17.980	9.140	7.300	6.120	2.380	0.580	0.010	0.870	0.120	0.086	0.020
LK-10-026	71.800	12.050	2.650	5.540	0.170	4.570	0.160	0.005	0.160	0.030	0.030	0.020
LK-10-027	72.200	13.450	3.530	3.510	0.670	2.890	1.310	0.005	0.200	0.020	0.040	0.020
LK-10-028	53.470	17.660	7.580	8.420	5.800	2.300	1.190	0.010	0.700	0.150	0.078	0.030
LK-10-031	51.200	15.750	9.650	9.250	7.400	1.990	1.390	0.030	0.760	0.100	0.100	0.020
LK-10-032	72.000	14.100	3.500	4.670	0.670	3.260	0.850	0.005	0.280	0.030	0.080	0.020
LK-10-035	53.700	16.450	8.700	9.470	6.080	2.360	0.600	0.020	0.880	0.110	0.100	0.030
LK-10-037	55.900	19.150	4.940	8.060	4.450	3.960	1.260	0.005	0.700	0.050	0.090	0.030
LK-10-038	48.900	16.200	12.850	10.050	6.390	2.210	0.190	0.020	1.250	0.200	0.120	0.020
LK-10-040	66.500	15.150	5.380	5.050	0.850	3.390	0.800	0.005	0.450	0.050	0.140	0.030
LK-10-041	68.100	15.050	4.180	4.620	1.220	3.730	0.810	0.005	0.440	0.060	0.140	0.030
LK-10-042	64.500	15.450	6.660	6.000	1.640	3.210	0.800	0.005	0.490	0.100	0.150	0.030
LK-10-053	56.900	18.000	6.840	2.770	3.460	7.470	0.360	0.010	0.760	0.090	0.090	0.020
LK-10-056	45.500	15.450	10.550	11.100	8.830	1.180	0.540	0.060	0.910	0.160	0.090	0.020
LK-10-059	50.200	15.850	9.850	10.350	5.860	2.610	0.800	0.030	0.730	0.180	0.070	0.020
LK-10-061	61.600	15.250	5.180	6.030	2.220	3.910	0.950	0.005	0.640	0.080	0.110	0.030
LK-10-062	54.800	16.200	8.700	7.560	3.280	2.970	1.260	0.005	0.880	0.090	0.120	0.020
LK-10-063	63.100	14.300	5.310	12.350	0.460	0.900	0.010	0.005	0.200	0.060	0.040	0.050
LK-10-065	45.700	16.000	9.660	12.950	7.280	1.070	1.580	0.040	1.060	0.160	0.160	0.020
LK-10-066	51.800	18.300	7.640	18.400	0.150	0.170	0.060	0.030	0.760	0.090	0.120	0.080
LK-10-067	44.400	15.400	13.600	10.050	7.110	1.540	1.120	0.010	1.410	0.210	0.090	0.020
LK-10-069	55.200	17.600	6.480	10.800	3.480	3.310	0.340	0.020	0.980	0.090	0.110	0.030
LK-10-070	52.500	15.000	7.590	10.650	6.950	2.340	0.770	0.050	0.630	0.120	0.070	0.020
LK-10-071	62.400	14.000	7.290	6.150	1.550	2.790	0.960	0.005	0.910	0.090	0.150	0.030
LK-10-072	55.800	15.700	9.630	6.200	2.870	3.310	1.400	0.005	1.240	0.150	0.340	0.020
LK-10-073	50.200	16.300	9.520	8.810	6.290	2.550	1.070	0.010	0.950	0.130	0.090	0.020
LK-10-074	48.100	16.500	11.600	11.900	6.150	1.830	0.440	0.020	0.920	0.170	0.070	0.020
LK-10-076	60.400	15.400	6.880	6.760	2.250	2.960	0.460	0.005	0.640	0.120	0.140	0.020
LK-10-077	55.600	14.850	9.460	6.850	4.660	4.130	0.300	0.050	1.140	0.160	0.190	0.030
LK-10-084	51.700	16.750	8.570	9.880	6.250	2.140	1.030	0.030	0.830	0.100	0.110	0.030
LK-10-085	48.200	16.150	11.050	13.400	6.010	1.430	0.800	0.040	0.870	0.190	0.090	0.020
LK-10-087	50.000	17.250	8.740	10.800	6.760	1.750	1.240	0.030	0.740	0.110	0.090	0.020
LK-10-090	52.600	16.000	10.000	10.150	5.050	2.100	0.520	0.010	0.900	0.140	0.120	0.020
LK-10-092	51.200	17.950	8.050	11.200	5.450	2.440	0.360	0.010	0.650	0.130	0.060	0.030
LK-10-093	49.800	19.650	6.410	12.150	5.760	2.740	0.230	0.010	0.450	0.120	0.040	0.030
LK-10-094	59.400	15.800	9.420	4.960	1.730	4.960	1.060	0.005	0.870	0.170	0.290	0.020
LK-11-095	51.000	15.850	9.390	9.630	6.150	2.830	0.940	0.010	0.930	0.160	0.070	0.010
LK-11-096	50.900	16.500	10.600	9.060	6.550	2.610	0.770	0.010	0.950	0.130	0.090	0.020
LK-11-097	56.800	15.550	12.000	6.930	2.230	3.760	0.460	0.005	1.220	0.220	0.330	0.020
LK-11-098	56.900	15.700	11.450	8.170	1.980	3.360	0.320	0.005	1.190	0.180	0.340	0.020
LK-11-099	47.500	17.250	12.200	11.300	5.980	1.520	1.230	0.030	0.930	0.180	0.090	0.010
LK-11-100	56.700	15.550	12.100	6.510	2.870	3.420	0.160	0.005	1.220	0.190	0.350	0.020
LK-11-101	48.800	16.550	12.100	11.050	6.140	1.820	0.500	0.030	1.050	0.180	0.090	0.010
LK-11-102	51.800	16.550	9.970	8.540	6.380	2.380	0.590	0.010	0.940	0.140	0.110	0.020
LK-11-103	49.400	17.000	12.150	11.750	6.100	1.960	0.320	0.030	1.080	0.180	0.100	0.010
LK-11-104	49.800	17.650	10.400	10.000	5.980	1.660	0.920	0.010	0.970	0.140	0.260	0.020

Sample	BaO %	LOI %	Total %	Ag (ppm)	Ba (ppm)	Ce (ppm)	Co (ppm)	Cr (ppm)	Cs (ppm)	Cu (ppm)	Dy (ppm)	Er (ppm)
LK-10-001	0.010	1.490	99.670	0.500	152.500	16.300	29.900	100.000	0.470	127.000	1.610	1.020
LK-10-002	0.005	2.650	98.780	0.500	92.500	15.700	35.300	100.000	0.660	230.000	1.570	0.980
LK-10-003	0.005	1.030	98.300	0.500	90.800	8.600	34.100	170.000	0.360	2.500	3.550	2.220
LK-10-004	0.005	1.380	98.180	1.000	43.000	12.300	65.900	110.000	0.070	6810.000	1.680	1.180
LK-10-005	0.010	1.090	97.500	0.500	42.300	60.500	59.000	120.000	0.030	13.000	3.650	1.970
LK-10-006	0.020	2.290	99.460	0.500	165.000	10.000	33.000	60.000	0.800	34.000	2.550	1.590
LK-10-007	0.005	2.460	98.620	0.500	24.500	23.600	74.200	190.000	0.060	195.000	2.920	1.700
LK-10-008	0.010	1.920	98.140	0.500	127.000	10.100	37.800	80.000	0.640	42.000	2.220	1.490
LK-10-009	0.010	2.210	99.140	0.500	144.500	17.800	34.200	100.000	0.410	116.000	1.730	1.040
LK-10-010	0.010	1.520	100.000	0.500	141.500	17.200	24.700	90.000	0.240	5.000	1.670	0.980
LK-10-011	0.030	1.570	99.450	0.500	268.000	28.800	24.200	10.000	0.830	571.000	3.150	2.000
LK-10-013	0.005	2.000	98.980	0.500	69.900	7.600	34.600	60.000	0.410	2.500	1.620	0.930
LK-10-014	0.010	1.600	99.600	0.500	74.900	13.900	42.400	270.000	0.230	75.000	1.960	1.180
LK-10-015	0.020	1.180	98.890	0.500	279.000	45.800	9.000	10.000	0.420	6.000	8.490	5.350
LK-10-016	0.010	2.220	99.680	0.500	137.500	17.600	33.800	130.000	0.430	30.000	2.600	1.580
LK-10-017	0.020	6.970	98.700	0.500	180.000	2.000	65.000	70.000	1.620	2.500	0.920	0.560
LK-10-018	0.005	1.100	99.430	0.500	64.100	10.900	39.500	100.000	0.520	11.000	2.480	1.490
LK-10-019	0.005	2.740	98.990	0.500	88.900	15.600	35.000	130.000	0.400	25.000	2.220	1.340
LK-10-021	0.020	2.210	98.210	0.500	212.000	15.100	45.200	70.000	0.550	76.000	1.330	0.790
LK-10-022	0.005	2.990	101.500	0.500	4.700	33.300	22.700	410.000	0.020	2.500	4.140	2.650
LK-10-023	0.050	2.700	101.000	0.500	405.000	28.300	65.100	300.000	0.290	159.000	3.860	2.440
LK-10-025	0.010	2.770	98.410	0.500	167.000	18.600	38.300	130.000	1.380	2.500	2.440	1.500
LK-10-026	0.005	2.790	100.000	0.500	32.100	38.400	3.500	10.000	0.120	10.000	4.700	3.230
LK-10-027	0.070	1.690	99.600	0.500	483.000	39.500	25.200	10.000	0.460	191.000	6.680	4.670
LK-10-028	0.020	2.100	99.510	2.000	238.000	17.800	35.900	130.000	0.480	13.000	2.110	1.360
LK-10-031	0.020	2.300	100.000	0.500	176.000	21.200	35.300	250.000	1.160	2.500	2.900	1.900
LK-10-032	0.030	1.580	101.000	0.500	188.000	45.100	9.300	10.000	0.550	13.000	9.980	6.900
LK-10-035	0.010	1.800	100.500	0.500	97.600	22.400	33.600	150.000	0.390	7.000	2.970	1.850
LK-10-037	0.020	2.460	101.000	0.500	142.500	25.100	22.100	30.000	0.690	6.000	3.190	1.910
LK-10-038	0.005	0.990	99.400	0.500	23.200	9.500	48.200	140.000	0.210	124.000	2.890	1.730
LK-10-040	0.030	1.880	99.700	0.500	273.000	36.600	11.500	5.000	0.580	21.000	9.430	6.080
LK-10-041	0.030	1.580	100.000	0.500	299.000	32.700	11.300	5.000	0.810	78.000	7.310	4.760
LK-10-042	0.030	1.300	100.500	0.500	223.000	23.600	12.900	20.000	0.720	34.000	4.190	2.710
LK-10-053	0.010	2.290	99.100	0.500	60.500	10.200	37.400	70.000	0.240	355.000	1.700	1.150
LK-10-056	0.020	2.800	97.200	0.500	154.500	10.500	45.900	420.000	0.460	89.000	2.370	1.420
LK-10-059	0.020	1.970	98.500	0.500	127.500	13.700	33.500	260.000	0.720	2.500	2.870	1.890
LK-10-061	0.020	1.500	97.500	0.500	173.500	22.900	13.900	10.000	0.400	7.000	3.080	2.000
LK-10-062	0.030	1.080	97.000	0.500	242.000	14.700	24.800	10.000	1.030	2.500	2.570	1.630
LK-10-063	0.005	1.690	98.500	0.500	5.900	12.000	4.100	10.000	0.030	2.500	2.060	1.390
LK-10-065	0.030	2.360	98.100	0.500	318.000	18.800	48.200	290.000	0.650	11.000	2.680	1.590
LK-10-066	0.010	1.970	99.600	0.500	26.900	21.900	6.500	270.000	0.030	11.000	3.700	2.210
LK-10-067	0.030	3.180	98.200	0.500	247.000	7.300	51.800	80.000	0.760	111.000	2.250	1.340
LK-10-069	0.010	0.900	99.400	0.500	80.900	21.700	28.200	120.000	0.130	2.500	4.110	2.490
LK-10-070	0.010	1.700	98.400	0.500	119.000	16.900	39.400	350.000	0.340	2.500	2.020	1.230
LK-10-071	0.040	1.680	98.000	0.500	400.000	38.600	16.500	5.000	1.010	43.000	4.420	2.690
LK-10-072	0.030	1.970	98.700	0.500	221.000	25.100	30.400	5.000	0.970	389.000	5.660	3.500
LK-10-073	0.020	2.470	98.400	0.500	151.500	14.600	37.600	90.000	0.520	2.500	3.080	1.850
LK-10-074	0.010	1.580	99.300	0.500	80.100	7.400	45.400	180.000	0.340	28.000	2.940	1.690
LK-10-076	0.020	3.740	99.800	0.500	215.000	20.800	14.500	5.000	0.500	18.000	2.750	1.780
LK-10-077	0.020	0.800	98.200	0.500	135.000	31.400	47.300	350.000	0.400	64.000	4.750	2.810
LK-10-084	0.020	1.780	99.200	0.500	145.500	21.200	32.900	220.000	0.800	62.000	2.560	1.570
LK-10-085	0.010	1.470	99.700	0.500	107.000	11.000	52.400	330.000	0.490	277.000	2.450	1.500
LK-10-087	0.020	2.600	100.000	0.500	161.000	16.600	35.400	250.000	0.880	75.000	2.240	1.340
LK-10-090	0.020	2.840	100.500	0.500	119.000	20.600	35.900	110.000	0.400	28.000	4.230	2.530
LK-10-092	0.010	3.000	100.500	0.500	85.700	14.500	33.000	90.000	0.300	27.000	3.050	1.860
LK-10-093	0.010	3.430	101.000	0.500	59.800	9.600	31.400	70.000	0.230	19.000	2.290	1.380
LK-10-094	0.030	1.100	99.800	0.500	299.000	42.500	14.000	5.000	0.210	2.500	9.490	5.920
LK-11-095	0.030	2.000	99.000	0.500	281.000	12.600	38.700	90.000	0.420	18.000	2.740	1.790
LK-11-096	0.010	2.500	100.500	0.500	117.000	15.800	45.300	90.000	0.460	342.000	2.920	1.860
LK-11-097	0.010	1.090	100.500	0.500	112.500	25.700	16.500	10.000	0.580	11.000	5.630	3.560
LK-11-098	0.010	1.100	100.500	0.500	87.800	25.300	16.000	10.000	0.650	62.000	5.520	3.480
LK-11-099	0.010	1.400	99.600	0.500	133.500	8.200	45.400	190.000	0.610	115.000	2.820	1.750
LK-11-100	0.010	1.090	100.000	0.500	66.300	26.800	17.300	10.000	0.480	24.000	5.600	3.520
LK-11-101	0.010	1.590	99.900	0.500	99.700	8.900	49.800	190.000	0.390	87.000	3.290	1.980
LK-11-102	0.010	2.490	99.900	0.500	132.000	15.200	41.400	90.000	0.390	2.500	2.940	1.890
LK-11-103	0.010	1.100	101.000	0.500	63.800	9.300	46.700	200.000	0.510	119.000	3.500	2.140
LK-11-104	0.020	1.790	99.600	0.500	172.500	30.900	44.000	100.000	1.030	83.000	3.350	1.990

Sample	Eu (ppm)	Ga (ppm)	Gd (ppm)	Hf (ppm)	Ho (ppm)	La (ppm)	Lu (ppm)	Mo (ppm)	Nb (ppm)	Nd (ppm)	Ni (ppm)	Pb (ppm)
LK-10-001	0.550	16.100	1.750	2.000	0.350	8.100	0.150	1.000	2.800	7.600	122.000	2.500
LK-10-002	0.610	16.100	1.800	2.200	0.330	7.900	0.150	1.000	2.600	7.500	155.000	2.500
LK-10-003	0.950	17.400	2.960	1.900	0.720	3.400	0.310	1.000	2.500	7.200	96.000	2.500
LK-10-004	2.520	20.800	1.550	1.800	0.350	6.200	0.180	1.000	2.300	6.600	87.000	8.000
LK-10-005	3.500	23.500	4.770	1.900	0.720	33.700	0.260	1.000	2.400	25.600	89.000	2.500
LK-10-006	0.770	17.000	2.330	1.500	0.540	4.400	0.240	1.000	3.000	6.700	73.000	2.500
LK-10-007	0.960	16.900	2.910	2.200	0.600	10.000	0.280	1.000	3.400	12.900	234.000	2.500
LK-10-008	0.460	17.400	1.850	2.000	0.480	4.600	0.240	1.000	2.900	5.800	160.000	2.500
LK-10-009	0.600	17.100	1.850	2.200	0.380	8.900	0.160	1.000	3.000	8.400	135.000	2.500
LK-10-010	0.720	15.300	1.850	2.000	0.340	9.000	0.140	1.000	2.800	7.800	118.000	2.500
LK-10-011	1.020	20.200	3.340	3.600	0.670	14.100	0.300	1.000	5.200	13.700	20.000	2.500
LK-10-013	0.490	15.100	1.470	0.900	0.340	3.500	0.170	1.000	1.800	4.900	82.000	2.500
LK-10-014	0.590	17.000	2.010	2.000	0.400	6.700	0.190	1.000	3.800	7.600	153.000	2.500
LK-10-015	1.770	21.000	7.740	6.400	1.780	20.200	0.810	1.000	9.400	26.800	2.500	2.500
LK-10-016	0.820	17.300	2.580	2.100	0.550	7.900	0.230	1.000	3.200	9.800	130.000	2.500
LK-10-017	0.290	19.600	0.680	0.600	0.210	0.900	0.080	1.000	1.100	1.500	100.000	2.500
LK-10-018	0.860	17.600	2.270	1.400	0.530	4.700	0.210	1.000	3.600	7.000	86.000	2.500
LK-10-019	0.710	16.700	2.220	2.100	0.480	7.300	0.200	1.000	3.200	8.300	127.000	2.500
LK-10-021	0.570	15.500	1.520	0.600	0.260	6.500	0.120	1.000	1.200	8.100	117.000	2.500
LK-10-022	1.390	28.300	4.010	3.000	0.900	14.900	0.410	1.000	5.300	18.100	151.000	2.500
LK-10-023	1.210	19.300	3.820	2.600	0.820	12.100	0.370	2.000	4.700	15.900	305.000	2.500
LK-10-025	0.690	19.000	2.620	2.300	0.520	9.100	0.230	1.000	3.400	9.400	140.000	2.500
LK-10-026	0.880	18.300	4.230	4.200	1.050	18.600	0.600	1.000	9.800	18.100	5.000	2.500
LK-10-027	1.120	17.300	5.750	4.700	1.490	18.100	0.720	1.000	8.500	22.000	2.500	2.500
LK-10-028	0.660	16.600	2.350	2.400	0.460	8.400	0.220	1.000	3.300	8.800	133.000	2.500
LK-10-031	0.650	17.800	2.720	2.200	0.620	9.700	0.300	1.000	3.300	11.600	244.000	2.500
LK-10-032	1.750	19.400	8.180	5.500	2.220	19.700	1.080	1.000	10.600	27.700	2.500	2.500
LK-10-035	0.890	18.700	2.740	2.400	0.630	10.400	0.270	1.000	4.000	12.200	63.000	2.500
LK-10-037	0.900	20.000	3.100	3.700	0.640	12.700	0.280	1.000	4.500	12.600	78.000	2.500
LK-10-038	0.840	19.000	2.720	1.500	0.610	4.100	0.250	1.000	3.200	7.600	113.000	2.500
LK-10-040	1.580	20.900	8.010	5.000	1.990	16.500	0.970	1.000	9.800	23.000	2.500	2.500
LK-10-041	0.860	19.700	6.580	5.000	1.530	14.200	0.870	1.000	9.700	20.300	7.000	2.500
LK-10-042	1.000	17.800	3.660	2.800	0.890	11.500	0.460	1.000	6.500	13.000	2.500	2.500
LK-10-053	0.520	14.200	1.350	2.000	0.370	4.900	0.200	1.000	3.700	5.000	87.000	6.000
LK-10-056	0.610	16.900	2.170	1.800	0.490	4.600	0.220	1.000	4.000	6.600	279.000	2.500
LK-10-059	0.620	19.100	2.350	2.300	0.630	7.300	0.290	1.000	3.600	7.600	215.000	2.500
LK-10-061	0.860	18.300	2.720	2.800	0.640	12.100	0.360	1.000	4.900	11.000	9.000	2.500
LK-10-062	0.750	18.600	2.390	1.800	0.530	7.500	0.260	1.000	3.600	7.800	10.000	2.500
LK-10-063	0.800	25.800	1.810	2.800	0.440	6.400	0.290	1.000	3.400	6.200	11.000	2.500
LK-10-065	0.780	17.900	2.660	1.400	0.550	8.600	0.240	1.000	3.300	10.700	186.000	2.500
LK-10-066	1.500	32.700	3.390	2.300	0.750	10.100	0.340	1.000	3.700	12.700	44.000	2.500
LK-10-067	0.730	18.000	2.060	1.200	0.470	3.200	0.200	1.000	1.900	5.300	111.000	2.500
LK-10-069	1.070	19.600	3.850	3.500	0.860	8.900	0.390	1.000	5.300	13.600	86.000	2.500
LK-10-070	0.590	15.900	1.870	2.000	0.400	8.500	0.180	1.000	3.000	8.400	320.000	2.500
LK-10-071	1.180	19.900	4.400	4.600	0.890	19.400	0.420	1.000	7.600	18.800	6.000	2.500
LK-10-072	1.560	22.400	5.200	2.900	1.180	11.400	0.530	4.000	8.000	16.500	6.000	2.500
LK-10-073	0.780	18.600	2.820	2.100	0.630	6.700	0.280	1.000	3.300	8.600	165.000	2.500
LK-10-074	0.840	18.100	2.670	1.500	0.580	3.700	0.250	1.000	2.000	6.100	175.000	2.500
LK-10-076	0.780	16.800	2.600	2.600	0.580	10.800	0.320	1.000	5.100	10.400	2.500	2.500
LK-10-077	1.300	18.600	4.610	3.300	0.980	14.600	0.430	1.000	5.600	18.400	279.000	2.500
LK-10-084	0.860	17.200	2.550	1.900	0.530	9.500	0.240	1.000	3.100	11.600	131.000	2.500
LK-10-085	0.690	16.800	2.250	1.400	0.510	4.900	0.230	1.000	3.900	7.000	196.000	2.500
LK-10-087	0.780	17.800	2.160	1.700	0.470	7.500	0.200	1.000	2.700	9.300	162.000	2.500
LK-10-090	1.060	20.000	3.840	2.800	0.860	9.200	0.380	1.000	4.300	12.700	78.000	2.500
LK-10-092	0.870	19.100	2.800	2.200	0.620	6.800	0.280	1.000	2.900	9.000	100.000	2.500
LK-10-093	0.740	18.600	1.920	1.300	0.470	4.500	0.210	1.000	1.800	5.900	121.000	2.500
LK-10-094	1.890	21.100	8.380	3.800	2.090	18.400	0.970	1.000	13.900	27.000	5.000	2.500
LK-11-095	0.600	18.100	2.410	2.200	0.600	5.600	0.280	1.000	3.400	7.400	160.000	2.500
LK-11-096	0.960	18.400	2.700	2.200	0.610	7.300	0.280	1.000	3.400	8.900	186.000	2.500
LK-11-097	1.890	23.600	5.360	3.300	1.220	10.600	0.540	1.000	8.800	17.000	2.500	2.500
LK-11-098	1.900	23.900	5.200	3.100	1.140	10.600	0.530	1.000	8.500	16.700	2.500	2.500
LK-11-099	0.710	18.300	2.660	1.600	0.600	3.500	0.250	1.000	2.200	6.100	185.000	2.500
LK-11-100	1.890	23.300	5.300	3.200	1.180	11.100	0.540	1.000	8.700	17.600	2.500	2.500
LK-11-101	0.810	18.500	2.970	1.800	0.670	3.600	0.280	1.000	2.500	6.800	151.000	2.500
LK-11-102	0.800	18.300	2.660	2.300	0.640	6.900	0.290	1.000	3.500	8.800	163.000	2.500
LK-11-103	0.880	18.800	3.190	1.900	0.740	3.700	0.300	1.000	2.600	7.200	138.000	2.500
LK-11-104	1.100	20.200	3.540	3.300	0.690	14.000	0.310	1.000	9.000	16.500	133.000	2.500

Sample	Pr (ppm)	Rb (ppm)	Sm (ppm)	Sn (ppm)	Sr (ppm)	Ta (ppm)	Tb (ppm)	Th (ppm)	Tl (ppm)	Tm (ppm)	U (ppm)	V (ppm)
LK-10-001	2.000	8.300	1.590	1.000	165.500	0.300	0.270	1.300	0.250	0.140	0.300	182.000
LK-10-002	1.870	8.700	1.620	1.000	168.000	0.300	0.270	1.300	0.250	0.150	0.300	179.000
LK-10-003	1.360	27.900	2.350	1.000	125.500	0.300	0.580	0.390	0.250	0.320	0.080	252.000
LK-10-004	1.590	1.700	1.500	5.000	114.000	0.600	0.270	1.250	0.250	0.180	0.290	112.000
LK-10-005	6.880	1.400	5.090	20.000	100.000	0.200	0.690	1.110	0.250	0.280	0.540	125.000
LK-10-006	1.460	52.000	1.990	7.000	148.500	0.300	0.410	0.590	0.250	0.240	0.140	258.000
LK-10-007	3.060	1.300	2.870	1.000	169.500	0.600	0.510	1.120	0.250	0.290	0.320	255.000
LK-10-008	1.380	41.700	1.500	2.000	137.000	0.300	0.340	0.680	0.250	0.230	0.160	237.000
LK-10-009	2.210	12.300	1.780	1.000	181.000	0.400	0.300	1.430	0.250	0.160	0.350	192.000
LK-10-010	2.030	4.200	1.750	1.000	175.500	0.300	0.280	1.290	0.250	0.150	0.350	175.000
LK-10-011	3.460	19.900	2.900	1.000	198.500	0.500	0.540	2.700	0.250	0.310	0.620	186.000
LK-10-013	1.060	20.800	1.320	1.000	205.000	0.200	0.280	0.520	0.250	0.150	0.100	233.000
LK-10-014	1.740	10.300	1.760	1.000	175.000	0.300	0.330	1.060	0.250	0.190	0.200	195.000
LK-10-015	6.260	22.900	6.860	2.000	140.000	0.800	1.400	2.710	0.250	0.820	0.550	21.000
LK-10-016	2.330	19.700	2.210	1.000	186.500	0.300	0.420	1.020	0.250	0.230	0.220	180.000
LK-10-017	0.300	42.100	0.490	1.000	40.900	0.200	0.150	0.220	0.250	0.090	0.050	205.000
LK-10-018	1.500	10.800	1.930	0.500	170.000	0.300	0.400	0.530	0.250	0.200	0.120	240.000
LK-10-019	1.980	7.600	1.990	1.000	171.000	0.300	0.370	1.060	0.250	0.210	0.250	184.000
LK-10-021	1.950	36.800	1.630	0.500	160.000	0.200	0.250	2.730	0.250	0.110	0.060	226.000
LK-10-022	4.380	0.200	3.840	1.000	451.000	0.300	0.680	1.570	0.250	0.440	0.310	245.000
LK-10-023	3.760	26.900	3.550	1.000	187.500	0.300	0.650	1.240	0.250	0.370	0.250	211.000
LK-10-025	2.320	14.800	2.240	1.000	162.500	0.400	0.420	1.470	0.250	0.220	0.340	200.000
LK-10-026	4.660	4.900	4.130	1.000	148.000	1.000	0.770	7.160	0.250	0.540	1.160	56.000
LK-10-027	5.030	49.100	5.590	0.500	150.500	0.600	1.060	2.900	0.250	0.680	0.790	2.500
LK-10-028	2.240	34.500	2.040	1.000	185.000	0.400	0.370	1.540	0.250	0.210	0.350	181.000
LK-10-031	2.690	61.800	2.820	1.000	172.500	0.300	0.460	0.970	0.250	0.280	0.230	228.000
LK-10-032	6.110	33.200	7.600	1.000	152.500	0.700	1.560	2.490	0.250	1.010	0.630	2.500
LK-10-035	2.850	18.800	2.810	1.000	223.000	0.300	0.470	1.090	0.250	0.260	0.270	222.000
LK-10-037	3.240	50.900	2.870	1.000	251.000	0.400	0.500	2.270	0.250	0.300	0.550	184.000
LK-10-038	1.560	5.300	2.170	1.000	182.500	0.200	0.450	0.270	0.250	0.250	0.070	260.000
LK-10-040	5.320	28.800	6.450	1.000	219.000	0.700	1.390	2.090	0.250	0.970	0.500	19.000
LK-10-041	4.700	28.600	5.490	1.000	208.000	0.700	1.120	2.030	0.250	0.780	0.490	20.000
LK-10-042	3.150	28.800	3.280	1.000	212.000	0.400	0.630	1.710	0.250	0.420	0.420	53.000
LK-10-053	1.300	4.800	1.200	1.000	128.500	0.300	0.260	0.940	0.250	0.190	0.270	127.000
LK-10-056	1.520	14.900	1.770	1.000	153.500	0.300	0.360	0.410	0.250	0.220	0.100	224.000
LK-10-059	1.800	29.400	1.800	1.000	164.000	0.300	0.430	1.090	0.250	0.300	0.220	210.000
LK-10-061	2.930	20.100	2.530	1.000	208.000	0.400	0.450	2.280	0.250	0.320	0.470	113.000
LK-10-062	1.920	50.600	1.950	1.000	200.000	0.300	0.390	1.340	0.250	0.250	0.340	218.000
LK-10-063	1.580	0.400	1.550	1.000	383.000	0.400	0.300	3.080	0.250	0.230	0.600	39.000
LK-10-065	2.600	58.300	2.480	1.000	199.000	0.200	0.420	0.950	0.250	0.230	0.210	273.000
LK-10-066	3.000	1.200	3.090	1.000	673.000	0.300	0.550	0.950	0.250	0.340	0.300	205.000
LK-10-067	1.120	40.200	1.570	0.500	177.500	0.100	0.330	0.260	0.250	0.200	0.070	399.000
LK-10-069	3.160	5.200	3.460	1.000	230.000	0.400	0.630	1.390	0.250	0.390	0.330	241.000
LK-10-070	2.130	21.800	1.880	1.000	179.000	0.300	0.320	1.360	0.250	0.190	0.310	193.000
LK-10-071	4.860	20.900	4.190	2.000	240.000	0.700	0.710	3.360	0.250	0.410	0.770	150.000
LK-10-072	3.680	64.100	4.330	2.000	156.500	0.500	0.860	0.900	0.250	0.540	0.220	44.000
LK-10-073	1.990	34.900	2.270	1.000	156.000	0.300	0.470	0.680	0.250	0.290	0.160	265.000
LK-10-074	1.200	14.900	1.970	1.000	131.000	0.200	0.450	0.260	0.250	0.260	0.060	230.000
LK-10-076	2.620	13.400	2.390	1.000	199.500	0.400	0.420	2.120	0.250	0.280	0.500	132.000
LK-10-077	4.470	8.000	4.400	1.000	203.000	0.400	0.750	1.440	0.250	0.430	0.320	223.000
LK-10-084	2.850	38.600	2.520	1.000	225.000	0.200	0.400	0.830	0.250	0.240	0.200	243.000
LK-10-085	1.600	25.300	1.880	1.000	200.000	0.300	0.360	0.430	0.250	0.240	0.100	251.000
LK-10-087	2.300	50.500	2.160	1.000	190.500	0.200	0.360	0.680	0.250	0.210	0.140	215.000
LK-10-090	2.900	16.800	3.320	1.000	197.500	0.300	0.650	0.920	0.250	0.390	0.210	229.000
LK-10-092	2.020	11.000	2.410	1.000	198.000	0.200	0.460	0.660	0.250	0.290	0.150	205.000
LK-10-093	1.360	6.600	1.650	0.500	226.000	0.100	0.350	0.450	0.250	0.210	0.130	180.000
LK-10-094	5.840	25.200	7.530	4.000	141.500	0.900	1.550	2.160	0.250	0.960	0.440	42.000
LK-11-095	1.600	31.100	2.050	0.500	146.500	0.200	0.400	0.610	0.250	0.260	0.190	249.000
LK-11-096	2.040	31.200	2.500	1.000	168.000	0.200	0.430	0.610	0.250	0.280	0.160	259.000
LK-11-097	3.570	17.700	4.890	0.500	168.000	0.500	0.850	0.860	0.250	0.520	0.230	38.000
LK-11-098	3.480	15.500	4.740	0.500	221.000	0.500	0.840	0.840	0.250	0.480	0.220	37.000
LK-11-099	1.180	66.500	2.050	0.500	169.500	0.100	0.410	0.250	0.250	0.240	0.070	214.000
LK-11-100	3.700	6.900	4.900	0.500	170.000	0.500	0.850	0.830	0.250	0.500	0.220	38.000
LK-11-101	1.300	21.600	2.410	0.500	125.000	0.200	0.490	0.300	0.250	0.280	0.080	246.000
LK-11-102	1.940	25.900	2.370	0.500	175.000	0.300	0.440	0.650	0.250	0.270	0.160	254.000
LK-11-103	1.370	12.300	2.600	0.500	140.500	0.200	0.520	0.320	0.250	0.310	0.080	244.000
LK-11-104	3.920	46.100	3.850	0.500	221.000	0.500	0.550	1.710	0.250	0.290	0.440	190.000

Sample	W (ppm)	Y (ppm)	Yb (ppm)	Zn (ppm)	Zr (ppm)	La/Yb	Zr/Y	Th/Yb	Eu/Eu*
LK-10-001	2.000	8.700	0.960	57.000	73.000	8.438	8.391	1.354	1.010
LK-10-002	1.000	8.400	0.870	54.000	82.000	9.080	9.762	1.494	1.094
LK-10-003	2.000	18.000	1.990	57.000	59.000	1.709	3.278	0.196	1.103
LK-10-004	5.000	9.200	1.330	137.000	69.000	4.662	7.500	0.940	5.061
LK-10-005	0.500	19.900	1.670	91.000	77.000	20.180	3.869	0.665	2.175
LK-10-006	9.000	13.300	1.500	75.000	51.000	2.933	3.835	0.393	1.095
LK-10-007	5.000	15.200	1.690	68.000	80.000	5.917	5.263	0.663	1.017
LK-10-008	2.000	12.400	1.470	83.000	71.000	3.129	5.726	0.463	0.846
LK-10-009	1.000	9.200	0.970	43.000	79.000	9.175	8.587	1.474	1.012
LK-10-010	1.000	8.500	0.900	41.000	72.000	10.000	8.471	1.433	1.225
LK-10-011	1.000	17.000	1.840	50.000	131.000	7.663	7.706	1.467	1.004
LK-10-013	1.000	8.300	0.900	55.000	32.000	3.889	3.855	0.578	1.077
LK-10-014	0.500	11.500	1.210	63.000	81.000	5.537	7.043	0.876	0.961
LK-10-015	1.000	45.700	5.090	33.000	220.000	3.969	4.814	0.532	0.744
LK-10-016	1.000	13.500	1.500	66.000	73.000	5.267	5.407	0.680	1.052
LK-10-017	2.000	4.800	0.550	51.000	19.000	1.636	3.958	0.400	1.538
LK-10-018	1.000	12.400	1.360	75.000	46.000	3.456	3.710	0.390	1.258
LK-10-019	1.000	11.900	1.320	69.000	76.000	5.530	6.387	0.803	1.034
LK-10-021	1.000	6.500	0.690	70.000	20.000	9.420	3.077	3.957	1.109
LK-10-022	0.500	23.900	2.620	40.000	112.000	5.687	4.686	0.599	1.085
LK-10-023	0.500	22.600	2.330	58.000	99.000	5.193	4.381	0.532	1.006
LK-10-025	1.000	13.000	1.380	51.000	84.000	6.594	6.462	1.065	0.872
LK-10-026	1.000	29.800	3.570	5.000	124.000	5.210	4.161	2.006	0.645
LK-10-027	1.000	46.100	4.770	31.000	182.000	3.795	3.948	0.608	0.605
LK-10-028	8.000	12.200	1.350	47.000	87.000	6.222	7.131	1.141	0.923
LK-10-031	1.000	18.100	1.830	42.000	81.000	5.301	4.475	0.530	0.719
LK-10-032	1.000	64.300	6.950	19.000	189.000	2.835	2.939	0.358	0.680
LK-10-035	1.000	17.400	1.740	52.000	97.000	5.977	5.575	0.626	0.982
LK-10-037	1.000	17.100	1.830	26.000	139.000	6.940	8.129	1.240	0.924
LK-10-038	1.000	15.600	1.640	73.000	48.000	2.500	3.077	0.165	1.059
LK-10-040	1.000	53.400	6.140	30.000	165.000	2.687	3.090	0.340	0.673
LK-10-041	1.000	42.300	5.280	36.000	174.000	2.689	4.113	0.384	0.438
LK-10-042	1.000	24.500	2.780	41.000	103.000	4.137	4.204	0.615	0.884
LK-10-053	6.000	9.100	1.200	52.000	75.000	4.083	8.242	0.783	1.251
LK-10-056	1.000	13.000	1.410	70.000	65.000	3.262	5.000	0.291	0.953
LK-10-059	1.000	17.000	1.910	61.000	85.000	3.822	5.000	0.571	0.923
LK-10-061	1.000	18.200	2.160	36.000	100.000	5.602	5.495	1.056	1.004
LK-10-062	1.000	14.300	1.630	37.000	64.000	4.601	4.476	0.822	1.064
LK-10-063	1.000	12.300	1.620	13.000	93.000	3.951	7.561	1.901	1.462
LK-10-065	1.000	14.100	1.480	88.000	51.000	5.811	3.617	0.642	0.930
LK-10-066	1.000	19.900	2.120	19.000	84.000	4.764	4.221	0.448	1.419
LK-10-067	1.000	12.100	1.330	103.000	40.000	2.406	3.306	0.195	1.243
LK-10-069	1.000	22.400	2.520	41.000	129.000	3.532	5.759	0.552	0.898
LK-10-070	1.000	11.200	1.210	47.000	75.000	7.025	6.696	1.124	0.964
LK-10-071	1.000	24.600	2.660	67.000	174.000	7.293	7.073	1.263	0.841
LK-10-072	3.000	30.100	3.420	52.000	110.000	3.333	3.654	0.263	1.007
LK-10-073	1.000	16.200	1.810	57.000	73.000	3.702	4.506	0.376	0.944
LK-10-074	1.000	15.700	1.640	70.000	45.000	2.256	2.866	0.159	1.121
LK-10-076	1.000	16.100	1.900	71.000	98.000	5.684	6.087	1.116	0.958
LK-10-077	1.000	25.700	2.670	61.000	120.000	5.468	4.669	0.539	0.884
LK-10-084	1.000	13.900	1.510	43.000	69.000	6.291	4.964	0.550	1.039
LK-10-085	1.000	13.500	1.460	67.000	49.000	3.356	3.630	0.295	1.027
LK-10-087	1.000	12.400	1.300	43.000	59.000	5.769	4.758	0.523	1.106
LK-10-090	1.000	23.000	2.470	88.000	102.000	3.725	4.435	0.372	0.909
LK-10-092	1.000	17.200	1.880	62.000	77.000	3.617	4.477	0.351	1.026
LK-10-093	1.000	12.600	1.350	44.000	42.000	3.333	3.333	0.333	1.273
LK-10-094	1.000	54.000	6.280	57.000	153.000	2.930	2.833	0.344	0.729
LK-11-095	2.000	16.900	1.740	58.000	74.000	3.218	4.379	0.351	0.827
LK-11-096	2.000	17.600	1.700	52.000	74.000	4.294	4.205	0.359	1.131
LK-11-097	1.000	33.500	3.370	60.000	112.000	3.145	3.343	0.255	1.130
LK-11-098	1.000	32.400	3.210	45.000	106.000	3.302	3.272	0.262	1.172
LK-11-099	2.000	16.800	1.600	61.000	49.000	2.188	2.917	0.156	0.931
LK-11-100	1.000	33.000	3.340	83.000	107.000	3.323	3.242	0.249	1.136
LK-11-101	2.000	19.100	1.820	69.000	56.000	1.978	2.932	0.165	0.927
LK-11-102	1.000	18.000	1.810	63.000	77.000	3.812	4.278	0.359	0.976
LK-11-103	1.000	20.500	1.940	94.000	59.000	1.907	2.878	0.165	0.936
LK-11-104	1.000	20.200	2.000	77.000	126.000	7.000	6.238	0.855	0.912

Appendix 5

A) NORMAT results calculated from the lithogeochemical analysis.

Samples	SIO2_PCT	TIO2_PCT	AL2O3_PCT	FE2O3_PCT	MNO_PCT	MGO_PCT	CAO_PCT	NA2O_PCT	K2O_PCT
LK-10-001	54.18	0.56	17.51	7.7	0.13	4.85	10.32	2.41	0.4
LK-10-002	52	0.54	17.82	7.73	0.1	6.64	9.07	1.71	0.41
LK-10-003	48.27	1.16	16.4	11.16	0.17	5.33	11.9	1.9	0.85
LK-10-004	42.87	0.46	11.43	21.32	0.27	5.02	14.49	0.45	0.38
LK-10-006	48.74	1.17	17.66	10.16	0.15	5.77	10.17	1.58	1.56
LK-10-007	43.04	1.06	16.62	17.31	0.33	3.44	12.41	1.66	0.14
LK-10-008	49.38	0.98	16.88	10.12	0.16	6.22	8.8	2.18	1.38
LK-10-009	52.17	0.63	17.98	8.03	0.12	5.64	9.68	2.16	0.4
LK-10-010	56	0.59	17.4	6.64	0.1	4.77	9.12	3.59	0.17
LK-10-011	59.91	0.82	15.93	6.78	0.09	2.71	8.18	2.3	1
LK-10-013	48.56	0.9	18.24	9.25	0.13	5.74	11.41	1.99	0.64
LK-10-015	65.02	0.64	15.29	6.14	0.07	1.01	3.96	4.44	0.93
LK-10-016	50.85	0.72	17.63	8.67	0.15	6.44	9.89	2.21	0.76
LK-10-017	42.87	0.69	17.18	18.98	0.09	6.39	2.91	1.4	1.13
LK-10-018	49.6	1.15	17.36	11.73	0.18	5.76	9.56	2.47	0.38
LK-10-019	50.75	0.75	17.51	8.35	0.11	6.74	9.74	1.93	0.26
LK-10-021	46.13	0.78	18.04	11.11	0.19	6.67	10.64	1.27	1.07
LK-10-025	51.02	0.87	17.98	9.14	0.12	6.12	7.3	2.38	0.58
LK-10-028	53.47	0.7	17.66	7.58	0.15	5.8	8.42	2.3	1.19
LK-10-005	41.4	0.45	11.3	24.6	0.32	3.64	13.55	0.51	0.4
LK-10-014	51	0.7	16.6	10.1	0.17	4.89	11.1	2.89	0.36
LK-10-022	55.4	1.2	16.4	7.3	0.1	1.44	15.95	0.16	0.01
LK-10-023	55	1	14.2	11.8	0.16	4.57	7.77	2.72	0.92
LK-10-026	71.8	0.16	12.05	2.65	0.03	0.17	5.54	4.57	0.16
LK-10-027	72.2	0.2	13.45	3.53	0.02	0.67	3.51	2.89	1.31
LK-10-031	51.2	0.76	15.75	9.65	0.1	7.4	9.25	1.99	1.39
LK-10-032	72	0.28	14.1	3.5	0.03	0.67	4.67	3.26	0.85
LK-10-035	53.7	0.88	16.45	8.7	0.11	6.08	9.47	2.36	0.6
LK-10-037	55.9	0.7	19.15	4.94	0.05	4.45	8.06	3.96	1.26
LK-10-038	48.9	1.25	16.2	12.85	0.2	6.39	10.05	2.21	0.19
LK-10-040	66.5	0.45	15.15	5.38	0.05	0.85	5.05	3.39	0.8
LK-10-041	68.1	0.44	15.05	4.18	0.06	1.22	4.62	3.73	0.81
LK-10-042	64.5	0.49	15.45	6.66	0.1	1.64	6	3.21	0.8
LK-10-053	56.9	0.76	18	6.84	0.09	3.46	2.77	7.47	0.36
LK-10-056	45.5	0.91	15.45	10.55	0.16	8.83	11.1	1.18	0.54
LK-10-059	50.2	0.73	15.85	9.85	0.18	5.86	10.35	2.61	0.8
LK-10-061	61.6	0.64	15.25	5.18	0.08	2.22	6.03	3.91	0.95
LK-10-062	54.8	0.88	16.2	8.7	0.09	3.28	7.56	2.97	1.26
LK-10-063	63.1	0.2	14.3	5.31	0.06	0.46	12.35	0.9	0.01
LK-10-065	45.7	1.06	16	9.66	0.16	7.28	12.95	1.07	1.58
LK-10-066	51.8	0.76	18.3	7.64	0.09	0.15	18.4	0.17	0.06
LK-10-067	44.4	1.41	15.4	13.6	0.21	7.11	10.05	1.54	1.12
LK-10-069	55.2	0.98	17.6	6.48	0.09	3.48	10.8	3.31	0.34
LK-10-070	52.5	0.63	15	7.59	0.12	6.95	10.65	2.34	0.77
LK-10-071	62.4	0.91	14	7.29	0.09	1.55	6.15	2.79	0.96
LK-10-072	55.8	1.24	15.7	9.63	0.15	2.87	6.2	3.31	1.4
LK-10-073	50.2	0.95	16.3	9.52	0.13	6.29	8.81	2.55	1.07
LK-10-074	48.1	0.92	16.5	11.6	0.17	6.15	11.9	1.83	0.44
LK-10-076	60.4	0.64	15.4	6.88	0.12	2.25	6.76	2.96	0.46
LK-10-077	55.6	1.14	14.85	9.46	0.16	4.66	6.85	4.13	0.3
LK-10-084	51.7	0.83	16.75	8.57	0.1	6.25	9.88	2.14	1.03
LK-10-085	48.2	0.87	16.15	11.05	0.19	6.01	13.4	1.43	0.8
LK-10-087	50	0.74	17.25	8.74	0.11	6.76	10.8	1.75	1.24
LK-10-090	52.6	0.9	16	10	0.14	5.05	10.15	2.1	0.52
LK-10-092	51.2	0.65	17.95	8.05	0.13	5.45	11.2	2.44	0.36
LK-10-094	59.4	0.87	15.8	9.42	0.17	1.73	4.96	4.96	1.06
LK-11-095	51	0.93	15.85	9.39	0.16	6.15	9.63	2.83	0.94
LK-11-096	50.9	0.95	16.5	10.6	0.13	6.55	9.06	2.61	0.77
LK-11-097	56.8	1.22	15.55	12	0.22	2.23	6.93	3.76	0.46
LK-11-098	56.9	1.19	15.7	11.45	0.18	1.98	8.17	3.36	0.32
LK-11-099	47.5	0.93	17.25	12.2	0.18	5.98	11.3	1.52	1.23
LK-11-100	56.7	1.22	15.55	12.1	0.19	2.87	6.51	3.42	0.16
LK-11-101	48.8	1.05	16.55	12.1	0.18	6.14	11.05	1.82	0.5
LK-11-102	51.8	0.94	16.55	9.97	0.14	6.38	8.54	2.38	0.59
LK-11-103	49.4	1.08	17	12.15	0.18	6.1	11.75	1.96	0.32
LK-11-104	49.8	0.97	17.65	10.4	0.14	5.98	10	1.66	0.92

Samples	P2O5_PCT	CR2O3_PCT	LOI_PCT	TOTAL_PCT	BA_PPM	CR_PPM	SR_PPM	RB_PPM	ZR_PPM
LK-10-001	0.07	0.01	1.49	99.67	150	0	166	8	8
LK-10-002	0.07	0.01	2.65	98.78	90	0	167	8	9
LK-10-003	0.1	0.02	1.03	98.3	80	0	124	27	24
LK-10-004	0.08	0.01	1.38	98.18	50	0	111	2	10
LK-10-006	0.16	0.01	2.29	99.46	160	0	148	51	23
LK-10-007	0.11	0.02	2.46	98.62	30	0	167	2	15
LK-10-008	0.08	0.01	1.92	98.14	120	0	137	41	19
LK-10-009	0.07	0.01	2.21	99.14	150	0	178	11	9
LK-10-010	0.07	0.01	1.52	100	140	0	172	4	8
LK-10-011	0.1	0.01	1.57	99.45	270	0	195	20	17
LK-10-013	0.09	0.01	2	98.98	70	0	202	20	12
LK-10-015	0.17	0.01	1.18	98.89	290	0	137	22	53
LK-10-016	0.09	0.02	2.22	99.68	140	0	184	19	16
LK-10-017	0.05	0.01	6.97	98.7	210	0	40	42	14
LK-10-018	0.11	0.01	1.1	99.43	70	0	173	11	15
LK-10-019	0.08	0.01	2.74	98.99	90	0	170	8	12
LK-10-021	0.05	0.01	2.21	98.21	230	0	160	36	14
LK-10-025	0.09	0.01	2.77	98.41	170	0	159	14	14
LK-10-028	0.08	0.01	2.1	99.51	240	0	179	32	17
LK-10-005	0.2	0.02	1.09	97.5	0	0	0	0	0
LK-10-014	0.07	0.04	1.6	99.6	0	0	0	0	0
LK-10-022	0.24	0.06	2.99	101.5	0	0	0	0	0
LK-10-023	0.16	0.04	2.7	101	0	0	0	0	0
LK-10-026	0.03	0.01	2.79	100	0	0	0	0	0
LK-10-027	0.04	0.01	1.69	99.6	0	0	0	0	0
LK-10-031	0.1	0.03	2.3	100	0	0	0	0	0
LK-10-032	0.08	0.01	1.58	101	0	0	0	0	0
LK-10-035	0.1	0.02	1.8	100.5	0	0	0	0	0
LK-10-037	0.09	0.01	2.46	101	0	0	0	0	0
LK-10-038	0.12	0.02	0.99	99.4	0	0	0	0	0
LK-10-040	0.14	0.01	1.88	99.7	0	0	0	0	0
LK-10-041	0.14	0.01	1.58	100	0	0	0	0	0
LK-10-042	0.15	0.01	1.3	100.5	0	0	0	0	0
LK-10-053	0.09	0.01	2.29	99.1	0	0	0	0	0
LK-10-056	0.09	0.06	2.8	97.2	0	0	0	0	0
LK-10-059	0.07	0.03	1.97	98.5	0	0	0	0	0
LK-10-061	0.11	0.01	1.5	97.5	0	0	0	0	0
LK-10-062	0.12	0.01	1.08	97	0	0	0	0	0
LK-10-063	0.04	0.01	1.69	98.5	0	0	0	0	0
LK-10-065	0.16	0.04	2.36	98.1	0	0	0	0	0
LK-10-066	0.12	0.03	1.97	99.6	0	0	0	0	0
LK-10-067	0.09	0.01	3.18	98.2	0	0	0	0	0
LK-10-069	0.11	0.02	0.9	99.4	0	0	0	0	0
LK-10-070	0.07	0.05	1.7	98.4	0	0	0	0	0
LK-10-071	0.15	0.01	1.68	98	0	0	0	0	0
LK-10-072	0.34	0.01	1.97	98.7	0	0	0	0	0
LK-10-073	0.09	0.01	2.47	98.4	0	0	0	0	0
LK-10-074	0.07	0.02	1.58	99.3	0	0	0	0	0
LK-10-076	0.14	0.01	3.74	99.8	0	0	0	0	0
LK-10-077	0.19	0.05	0.8	98.2	0	0	0	0	0
LK-10-084	0.11	0.03	1.78	99.2	0	0	0	0	0
LK-10-085	0.09	0.04	1.47	99.7	0	0	0	0	0
LK-10-087	0.09	0.03	2.6	100	0	0	0	0	0
LK-10-090	0.12	0.01	2.84	100.5	0	0	0	0	0
LK-10-092	0.06	0.01	3	100.5	0	0	0	0	0
LK-10-094	0.29	0.01	1.1	99.8	0	0	0	0	0
LK-11-095	0.07	0.01	2	99	0	0	0	0	0
LK-11-096	0.09	0.01	2.5	100.5	0	0	0	0	0
LK-11-097	0.33	0.01	1.09	100.5	0	0	0	0	0
LK-11-098	0.34	0.01	1.1	100.5	0	0	0	0	0
LK-11-099	0.09	0.03	1.4	99.6	0	0	0	0	0
LK-11-100	0.35	0.01	1.09	100	0	0	0	0	0
LK-11-101	0.09	0.03	1.59	99.9	0	0	0	0	0
LK-11-102	0.11	0.01	2.49	99.9	0	0	0	0	0
LK-11-103	0.1	0.03	1.1	101	0	0	0	0	0
LK-11-104	0.26	0.01	1.79	99.6	0	0	0	0	0

Samples	Y_PPM	NB_PPM	AS_PPM	CU_PPM	ZN_PPM	AG_PPM	AU_PPB	SB_PPM	PB_PPM
LK-10-001	76	3	0	0	0	0	0	0	0
LK-10-002	71	2	0	0	0	0	0	0	0
LK-10-003	58	3	0	0	0	0	0	0	0
LK-10-004	60	2	0	0	0	0	0	0	0
LK-10-006	54	3	0	0	0	0	0	0	0
LK-10-007	81	3	0	0	0	0	0	0	0
LK-10-008	71	2	0	0	0	0	0	0	0
LK-10-009	79	3	0	0	0	0	0	0	0
LK-10-010	74	3	0	0	0	0	0	0	0
LK-10-011	138	5	0	0	0	0	0	0	0
LK-10-013	36	2	0	0	0	0	0	0	0
LK-10-015	196	10	0	0	0	0	0	0	0
LK-10-016	77	3	0	0	0	0	0	0	0
LK-10-017	7	1	0	0	0	0	0	0	0
LK-10-018	48	4	0	0	0	0	0	0	0
LK-10-019	77	3	0	0	0	0	0	0	0
LK-10-021	16	2	0	0	0	0	0	0	0
LK-10-025	86	3	0	0	0	0	0	0	0
LK-10-028	90	3	0	0	0	0	0	0	0
LK-10-005	0	0	0	0	0	0	0	0	0
LK-10-014	0	0	0	0	0	0	0	0	0
LK-10-022	0	0	0	0	0	0	0	0	0
LK-10-023	0	0	0	0	0	0	0	0	0
LK-10-026	0	0	0	0	0	0	0	0	0
LK-10-027	0	0	0	0	0	0	0	0	0
LK-10-031	0	0	0	0	0	0	0	0	0
LK-10-032	0	0	0	0	0	0	0	0	0
LK-10-035	0	0	0	0	0	0	0	0	0
LK-10-037	0	0	0	0	0	0	0	0	0
LK-10-038	0	0	0	0	0	0	0	0	0
LK-10-040	0	0	0	0	0	0	0	0	0
LK-10-041	0	0	0	0	0	0	0	0	0
LK-10-042	0	0	0	0	0	0	0	0	0
LK-10-053	0	0	0	0	0	0	0	0	0
LK-10-056	0	0	0	0	0	0	0	0	0
LK-10-059	0	0	0	0	0	0	0	0	0
LK-10-061	0	0	0	0	0	0	0	0	0
LK-10-062	0	0	0	0	0	0	0	0	0
LK-10-063	0	0	0	0	0	0	0	0	0
LK-10-065	0	0	0	0	0	0	0	0	0
LK-10-066	0	0	0	0	0	0	0	0	0
LK-10-067	0	0	0	0	0	0	0	0	0
LK-10-069	0	0	0	0	0	0	0	0	0
LK-10-070	0	0	0	0	0	0	0	0	0
LK-10-071	0	0	0	0	0	0	0	0	0
LK-10-072	0	0	0	0	0	0	0	0	0
LK-10-073	0	0	0	0	0	0	0	0	0
LK-10-074	0	0	0	0	0	0	0	0	0
LK-10-076	0	0	0	0	0	0	0	0	0
LK-10-077	0	0	0	0	0	0	0	0	0
LK-10-084	0	0	0	0	0	0	0	0	0
LK-10-085	0	0	0	0	0	0	0	0	0
LK-10-087	0	0	0	0	0	0	0	0	0
LK-10-090	0	0	0	0	0	0	0	0	0
LK-10-092	0	0	0	0	0	0	0	0	0
LK-10-094	0	0	0	0	0	0	0	0	0
LK-11-095	0	0	0	0	0	0	0	0	0
LK-11-096	0	0	0	0	0	0	0	0	0
LK-11-097	0	0	0	0	0	0	0	0	0
LK-11-098	0	0	0	0	0	0	0	0	0
LK-11-099	0	0	0	0	0	0	0	0	0
LK-11-100	0	0	0	0	0	0	0	0	0
LK-11-101	0	0	0	0	0	0	0	0	0
LK-11-102	0	0	0	0	0	0	0	0	0
LK-11-103	0	0	0	0	0	0	0	0	0
LK-11-104	0	0	0	0	0	0	0	0	0

Samples	SIO2N	TIO2N	TIO2_ZR	AL2O3_TIO2	AL2O3_ZR	TIO2N_ZR	ZR_Y	MF	ACFM
LK-10-001	55.18	0.57	700	31.00	219	713	0.10	0	Chlorite
LK-10-002	54.09	0.56	600	33.00	198	624	0.10	0	Chlorite
LK-10-003	49.62	1.19	483	14.00	68	497	0.40	0	Chlorite
LK-10-004	44.29	0.48	460	25.00	114	475	0.20	0	Chlorite
LK-10-006	50.16	1.2	509	15.00	77	524	0.40	0	Chlorite
LK-10-007	44.76	1.1	707	16.00	111	735	0.20	0	Chlorite
LK-10-008	51.32	1.02	516	17.00	89	536	0.30	0	Chlorite
LK-10-009	53.82	0.65	700	29.00	200	722	0.10	0	Chlorite
LK-10-010	56.86	0.6	738	29.00	218	749	0.10	0	Chlorite
LK-10-011	61.21	0.84	482	19.00	94	493	0.10	0	Chlorite
LK-10-013	50.07	0.93	750	20.00	152	773	0.30	0	Chlorite
LK-10-015	66.54	0.65	121	24.00	29	124	0.30	0	Sericite
LK-10-016	52.18	0.74	450	24.00	110	462	0.20	0	Chlorite
LK-10-017	46.73	0.75	493	25.00	123	537	2.00	0	Sericite
LK-10-018	50.44	1.17	767	15.00	116	780	0.30	0	Chlorite
LK-10-019	52.73	0.78	625	23.00	146	649	0.20	0	Chlorite
LK-10-021	48.05	0.81	557	23.00	129	580	0.90	0	Chlorite
LK-10-025	53.35	0.91	621	21.00	128	650	0.20	0	Sericite
LK-10-028	54.89	0.72	412	25.00	104	423	0.20	0	Chlorite
LK-10-005	42.94	0.47	0	25.00	0	0	0.00	0	Chlorite
LK-10-014	52.04	0.71	0	24.00	0	0	0.00	0	Chlorite
LK-10-022	0	0	0	14.00	0	0	0.00	0	Chlorite
LK-10-023	0	0	0	14.00	0	0	0.00	0	Chlorite
LK-10-026	0	0	0	75.00	0	0	0.00	0	Sericite
LK-10-027	73.74	0.2	0	67.00	0	0	0.00	0	Sericite
LK-10-031	0	0	0	21.00	0	0	0.00	0	Chlorite
LK-10-032	72.42	0.28	0	50.00	0	0	0.00	0	Sericite
LK-10-035	54.41	0.89	0	19.00	0	0	0.00	0	Chlorite
LK-10-037	0	0	0	27.00	0	0	0.00	0	Chlorite
LK-10-038	49.69	1.27	0	13.00	0	0	0.00	0	Chlorite
LK-10-040	67.98	0.46	0	34.00	0	0	0.00	0	Sericite
LK-10-041	69.19	0.45	0	34.00	0	0	0.00	0	Sericite
LK-10-042	65.02	0.49	0	32.00	0	0	0.00	0	Sericite
LK-10-053	58.77	0.79	0	24.00	0	0	0.00	0	Sericite
LK-10-056	48.2	0.96	0	17.00	0	0	0.00	0	Chlorite
LK-10-059	52	0.76	0	22.00	0	0	0.00	0	Chlorite
LK-10-061	64.17	0.67	0	24.00	0	0	0.00	0	Chlorite
LK-10-062	57.13	0.92	0	18.00	0	0	0.00	0	Chlorite
LK-10-063	65.18	0.21	0	72.00	0	0	0.00	0	Calcite
LK-10-065	47.73	1.11	0	15.00	0	0	0.00	0	Chlorite
LK-10-066	53.06	0.78	0	24.00	0	0	0.00	0	Calcite
LK-10-067	46.73	1.48	0	11.00	0	0	0.00	0	Chlorite
LK-10-069	56.04	0.99	0	18.00	0	0	0.00	0	Chlorite
LK-10-070	54.29	0.65	0	24.00	0	0	0.00	0	Chlorite
LK-10-071	64.78	0.94	0	15.00	0	0	0.00	0	Chlorite
LK-10-072	57.69	1.28	0	13.00	0	0	0.00	0	Chlorite
LK-10-073	52.33	0.99	0	17.00	0	0	0.00	0	Chlorite
LK-10-074	49.22	0.94	0	18.00	0	0	0.00	0	Chlorite
LK-10-076	62.88	0.67	0	24.00	0	0	0.00	0	Sericite
LK-10-077	57.08	1.17	0	13.00	0	0	0.00	0	Chlorite
LK-10-084	53.07	0.85	0	20.00	0	0	0.00	0	Chlorite
LK-10-085	49.07	0.89	0	19.00	0	0	0.00	0	Chlorite
LK-10-087	0	0	0	23.00	0	0	0.00	0	Chlorite
LK-10-090	0	0	0	18.00	0	0	0.00	0	Chlorite
LK-10-092	0	0	0	28.00	0	0	0.00	0	Chlorite
LK-10-094	60.18	0.88	0	18.00	0	0	0.00	0	Chlorite
LK-11-095	52.58	0.96	0	17.00	0	0	0.00	0	Chlorite
LK-11-096	51.94	0.97	0	17.00	0	0	0.00	0	Chlorite
LK-11-097	57.14	1.23	0	13.00	0	0	0.00	0	Chlorite
LK-11-098	57.24	1.2	0	13.00	0	0	0.00	0	Chlorite
LK-11-099	48.37	0.95	0	19.00	0	0	0.00	0	Chlorite
LK-11-100	57.32	1.23	0	13.00	0	0	0.00	0	Sericite
LK-11-101	49.64	1.07	0	16.00	0	0	0.00	0	Chlorite
LK-11-102	53.18	0.96	0	18.00	0	0	0.00	0	Chlorite
LK-11-103	49.45	1.08	0	16.00	0	0	0.00	0	Chlorite
LK-11-104	50.92	0.99	0	18.00	0	0	0.00	0	Chlorite

Samples	ACTINOTE	ALBITE	ALUNITE	ANATASE	ANHYDRITE	ANKERITE	APATITE	ARSENOPYR	BORNITE
LK-10-001	4.728000164	22.31900024	0	0	0	0	0.150999993	0	0
LK-10-002	1.430999994	16.12100029	0	0	0	0	0.144999996	0	0
LK-10-003	10.4989996	17.95700073	0	0	0	0	0.209000006	0	0
LK-10-004	26.77199936	4.479000092	0	0	0	0	0.175999999	0	0
LK-10-006	4.372000217	14.88599968	0	0	0	0	0.340000004	0	0
LK-10-007	14.5	16.31100082	0	0	0	0	0.254000008	0	0
LK-10-008	4.53000021	20.61300087	0	0	0	0	0.182999998	0	0
LK-10-009	2.677999973	20.22599983	0	0	0	0	0.160999998	0	0
LK-10-010	4.285999775	32.78300095	0	0	0	0	0.149000004	0	0
LK-10-011	2.000999928	21.62400055	0	0	0	0	0.228	0	0
LK-10-013	5.599999905	18.66699982	0	0	0	0	0.194000006	0	0
LK-10-015	0	41.02199936	0	0	0	0	0.372000009	0	0
LK-10-016	4.368999958	20.52899933	0	0	0	0	0.184	0	0
LK-10-017	0	7.859000206	0	0	0	0	0.112000003	0	0
LK-10-018	4.657000065	23	0	0	0	0	0.240999997	0	0
LK-10-019	3.023999929	18.17200089	0	0	0	0	0.178000003	0	0
LK-10-021	4.762000084	12.10400009	0	0	0	0	0.112999998	0	0
LK-10-025	0	22.4640007	0	0	0	0	0.189999998	0	0
LK-10-028	2.10800004	21.36499977	0	0	0	0	0.169	0	0
LK-10-005	28.70599937	5.178999901	0	0	0	0	0.47299999	0	0
LK-10-014	10.15600014	26.89500046	0	0	0	0	0.151999995	0	0
LK-10-022	8.437999725	1.534999967	0	0	0	0	0.536000013	0	0
LK-10-023	7.593999863	25.53800011	0	0	0	0	0.349999994	0	0
LK-10-026	0	42.80599976	0	0	0	0	0.064999998	0	0
LK-10-027	0	23.55699921	0	0	0	0	0.088	0	0
LK-10-031	6.458000183	18.48500061	0	0	0	0	0.216000006	0	0
LK-10-032	0	27.69499969	0	0	0	0	0.172000006	0	0
LK-10-035	4.890999794	21.78100014	0	0	0	0	0.215000004	0	0
LK-10-037	1.335000038	35.74700165	0	0	0	0	0.188999996	0	0
LK-10-038	6.995999813	20.65800095	0	0	0	0	0.261000007	0	0
LK-10-040	0	29.53300095	0	0	0	0	0.305999994	0	0
LK-10-041	0	33.15000153	0	0	0	0	0.301999986	0	0
LK-10-042	0	29.72800064	0	0	0	0	0.324000001	0	0
LK-10-053	0	67.51999664	0	0	0	0	0.189999998	0	0
LK-10-056	7.788000107	11.36800003	0	0	0	0	0.202000007	0	0
LK-10-059	9.430999756	24.56900024	0	0	0	0	0.152999997	0	0
LK-10-061	2.117000103	36.91500092	0	0	0	0	0.241999999	0	0
LK-10-062	3.359999895	28.32799911	0	0	0	0	0.26699999	0	0
LK-10-063	9.94699955	8.737000465	0	0	0	0	0.090000004	0	0
LK-10-065	6.955999851	10.19499969	0	0	0	0	0.354999989	0	0
LK-10-066	14.23400021	1.644000053	0	0	0	0	0.270000011	0	0
LK-10-067	9.006999969	14.9460001	0	0	0	0	0.202999994	0	0
LK-10-069	6.150000095	30.45800018	0	0	0	0	0.236000001	0	0
LK-10-070	8.241999626	21.84300041	0	0	0	0	0.151999995	0	0
LK-10-071	0.907999992	26.82999992	0	0	0	0	0.335999995	0	0
LK-10-072	0.916000009	31.45100021	0	0	0	0	0.751999974	0	0
LK-10-073	5.493999958	24.09199905	0	0	0	0	0.197999999	0	0
LK-10-074	9.934000015	17.18799973	0	0	0	0	0.152999997	0	0
LK-10-076	0	26.39500046	0	0	0	0	0.312000006	0	0
LK-10-077	5.320000172	38.46500015	0	0	0	0	0.412	0	0
LK-10-084	5.360000134	19.93199921	0	0	0	0	0.238999993	0	0
LK-10-085	12.65999985	13.38399982	0	0	0	0	0.195999995	0	0
LK-10-087	6.045000076	16.2689991	0	0	0	0	0.194999993	0	0
LK-10-090	6.390999794	19.76000023	0	0	0	0	0.263000011	0	0
LK-10-092	5.169000149	22.65999985	0	0	0	0	0.129999995	0	0
LK-10-094	2.460999966	45.7859993	0	0	0	0	0.623000026	0	0
LK-11-095	8.09	26.42	0	0	0	0	0.15	0	0
LK-11-096	5.9	24.16	0	0	0	0	0.19	0	0
LK-11-097	3.58	34.99	0	0	0	0	0.71	0	0
LK-11-098	4.8	31.32	0	0	0	0	0.74	0	0
LK-11-099	8.31	14.24	0	0	0	0	0.2	0	0
LK-11-100	0	31.91	0	0	0	0	0.76	0	0
LK-11-101	8.19	17.03	0	0	0	0	0.2	0	0
LK-11-102	3.69	22.24	0	0	0	0	0.24	0	0
LK-11-103	8.8	18	0	0	0	0	0.21	0	0
LK-11-104	3.37	15.55	0	0	0	0	0.57	0	0

Samples	BRUCITE	CALCITE	CHALCOCITE	CHALCOPYR	CHL_FE	CHL_MG	CHLORITE	CHROMITE	CO2
LK-10-001	0	0	0	0	6.080999851	9.090999603	15.17199993	0.011	0
LK-10-002	0	0	0	0	8.440999985	17.2859993	25.72699928	0.012	0
LK-10-003	0	0.009	0	0	6.611999989	7.547999859	14.15999985	0.023	0.007
LK-10-004	0	1.085000038	0	0	2.312999964	1.394000053	3.707999945	0.012	0.792999983
LK-10-006	0	0	0	0	9.451000214	12.7670002	22.21800041	0.012	0
LK-10-007	0	0.009	0	0	11.73700047	5.717999935	17.45499992	0.024	0.007
LK-10-008	0	0	0	0	9.355999947	13.66399956	23.02000046	0.012	0
LK-10-009	0	0	0	0	7.929999828	13.24800014	21.1779995	0.011	0
LK-10-010	0	0	0	0	4.977000237	8.505000114	13.48099995	0.011	0
LK-10-011	0	0	0	0	6.887000084	6.558000088	13.44499969	0.006	0
LK-10-013	0	0	0	0	7.467000008	11.03199959	18.49900055	0.011	0
LK-10-015	0	0	0	0	8.11400032	3.220999956	11.33500004	0.006	0
LK-10-016	0	0	0	0	7.513999939	13.25	20.76300049	0.023	0
LK-10-017	0	2.667000055	0	0	26.22999928	22.32099915	48.54800034	0.013	1.891000032
LK-10-018	0	0	0	0	11.04800034	12.89599991	23.94400024	0.011	0
LK-10-019	0	0	0	0	8.123000145	15.62699986	23.75	0.012	0
LK-10-021	0	0	0	0	10.53999996	15.01299953	25.5529995	0.012	0
LK-10-025	0	0	0	0	11.35400009	18.11899948	29.47299957	0.012	0
LK-10-028	0	0	0	0	7.741000175	14.01399994	21.75499916	0.011	0
LK-10-005	0	0.640999973	0	0	2.671000004	1.019000053	3.690000057	0.025	0.463999987
LK-10-014	0	0.01	0	0	5.335000038	6.186999798	11.52200031	0.046	0.008
LK-10-022	0	1.488000035	0	0	3.355999947	1.587000012	4.94299984	0.07	1.100000024
LK-10-023	0	0.043000001	0	0	8.529000282	8.295000076	16.82500076	0.046	0.033
LK-10-026	0	2.654999971	0	0	3.117000103	0.513000011	3.630000114	0.006	2.019000053
LK-10-027	0	0.145999998	0	0	4.111999989	2.155999899	6.268000126	0.006	0.111000001
LK-10-031	0	0	0	0	7.181000233	13.21500015	20.39599991	0.034000002	0
LK-10-032	0	0.395999998	0	0	4.561999798	2.11500001	6.676000118	0.006	0.301999986
LK-10-035	0	0	0	0	7.065999985	11.80000019	18.86599922	0.023	0
LK-10-037	0	0.240999997	0	0	4.835000038	10.42700005	15.26200008	0.006	0.188999996
LK-10-038	0	0	0	0	10.35299969	12.68999958	23.04299927	0.023	0
LK-10-040	0	0.31099999	0	0	7.135000229	2.729000092	9.86400032	0.006	0.237000003
LK-10-041	0	0.142000005	0	0	5.517000198	3.867000103	9.383999825	0.006	0.108999997
LK-10-042	0	0	0	0	8.097999573	4.813000202	12.91100025	0.006	0
LK-10-053	0	0.272000015	0	0	7.708000183	9.713000298	17.42099953	0.011	0.216999993
LK-10-056	0	0	0	0	7.876999855	15.76000023	23.63699913	0.071000002	0
LK-10-059	0	0.006	0	0	5.670000076	8.06400013	13.73400021	0.035	0.005
LK-10-061	0	0	0	0	4.895999908	4.999000072	9.895000458	0.006	0
LK-10-062	0	0	0	0	8.43599987	7.611999989	16.04700089	0.006	0
LK-10-063	0	0.879000008	0	0	0	0	0	0.006	0.658999979
LK-10-065	0	0	0	0	3.242000103	5.826000214	9.06799984	0.046999998	0
LK-10-066	0	2.171000004	0	0	0	0	0	0.035	1.603000045
LK-10-067	0	0	0	0	10.71899986	13.625	24.34399986	0.012	0
LK-10-069	0	0	0	0	3.571000099	4.580999851	8.152000427	0.023	0
LK-10-070	0	0	0	0	3.624000072	7.923999786	11.54800034	0.057	0
LK-10-071	0	0.003	0	0	8.361000061	4.282000065	12.64299965	0.006	0.002
LK-10-072	0	0	0	0	10.90799999	7.960999966	18.86899948	0.006	0
LK-10-073	0	0	0	0	7.940999985	12.50399971	20.44499969	0.012	0
LK-10-074	0	0.007	0	0	7.473999977	9.451999664	16.9260006	0.023	0.005
LK-10-076	0	2.002000093	0	0	9.465999603	7.354000092	16.81999969	0.006	1.498000026
LK-10-077	0	0	0	0	6.855000019	8.81099987	15.66600037	0.057	0
LK-10-084	0	0	0	0	6.644000053	11.63399982	18.27700043	0.034000002	0
LK-10-085	0	0.014	0	0	4.802000046	6.294000149	11.09599972	0.046	0.011
LK-10-087	0	0	0	0	6.412000179	11.85999966	18.27099991	0.034000002	0
LK-10-090	0	0.165000007	0	0	7.880000114	9.486000061	17.36700058	0.012	0.125
LK-10-092	0	0.407999992	0	0	6.210999966	10.00500011	16.2159996	0.011	0.312999994
LK-10-094	0	0	0	0	9.25	4.179999828	13.43099976	0.006	0
LK-11-095	0	0	0	0	5.97	9.3	15.27	0.01	0
LK-11-096	0	0	0	0	8.73	12.88	21.61	0.01	0
LK-11-097	0	0	0	0	11.67	5.31	16.98	0.01	0
LK-11-098	0	0	0	0	10.32	4.35	14.67	0.01	0
LK-11-099	0	0	0	0	9.26	10.81	20.07	0.03	0
LK-11-100	0	0	0	0	12.85	7.4	20.25	0.01	0
LK-11-101	0	0	0	0	9.17	11.1	20.27	0.03	0
LK-11-102	0	0	0	0	9.56	14.57	24.13	0.01	0
LK-11-103	0	0	0	0	8.58	10.27	18.85	0.03	0
LK-11-104	0	0	0	0	10.32	14.13	24.44	0.01	0

Samples	DENSITE	DIASPORE	DOLOMITE	EPIDOTE	FERAT_CALC	GAF	GALENE	H2OM	H2OP
LK-10-001	2.970999956	0	0	33.97399902	0.159999996	0	0	0.017999999	2.471999884
LK-10-002	2.940999985	0	0	33.5340004	0.141000003	0	0	0.021	3.309000015
LK-10-003	3.059999943	0	0	33.76800156	0.170000002	0	0	0.02	2.654000044
LK-10-004	3.355000019	0	0	34.67599869	0.287999988	-0.017000001	0	0.018999999	2.042999983
LK-10-006	2.986999989	0	0	32.60599899	0.157000005	0	0	0.021	3.147000074
LK-10-007	3.155999899	0	0	38.50400162	0.172999993	-0.001	0	0.022	2.977999926
LK-10-008	2.957000017	0	0	27.50900078	0.156000003	0	0	0.021	3.135999918
LK-10-009	2.957000017	0	0	34.02500153	0.150000006	0	0	0.02	2.960000038
LK-10-010	2.928999901	0	0	28.58300018	0.158000007	0	0	0.016000001	2.223999977
LK-10-011	2.898000002	0	0	28.95400047	0.158999994	0	0	0.014	2.058000088
LK-10-013	3.017999887	0	0	36.81399918	0.158999994	0	0	0.021	2.928999901
LK-10-015	2.778000116	0	0	13.55300045	0.184	0	0	0.01	1.501999974
LK-10-016	2.971999884	0	0	31.6420002	0.153999999	0	0	0.02	2.994999886
LK-10-017	2.888000011	0	0	0.015	0.185000002	-0.002	0	0.032000002	5.298999786
LK-10-018	2.980000019	0	0	30.04800034	0.158000007	0	0	0.022	3.259000063
LK-10-019	2.967000008	0	0	33.19300079	0.147	0	0	0.021	3.236999989
LK-10-021	3.016000032	0	0	36.08300018	0.156000003	0	0	0.023	3.506000042
LK-10-025	2.901000023	0	0	27.56999969	0.182999998	0	0	0.022	3.507999897
LK-10-028	2.917999983	0	0	28.97900009	0.148000002	0	0	0.018999999	2.905999899
LK-10-005	3.414999962	0	0	34.51499939	0.317000002	-0.033	0	0.017999999	1.953999996
LK-10-014	3.02699995	0	0	31.52700043	0.170000002	0	0	0.017999999	2.309000015
LK-10-022	3.08100009	0	0	50.17300034	0.177000001	0	0	0.015	1.848999977
LK-10-023	2.96600008	0	0	20.29999924	0.162	-0.001	0	0.017000001	2.54399991
LK-10-026	2.732000113	0	0	11.70800018	0.170000002	0	0	0.005	0.638000011
LK-10-027	2.765000105	0	0	13.22299957	0.158000007	-0.001	0	0.009	1.230999947
LK-10-031	2.971999884	0	0	25.47299957	0.156000003	0	0	0.02	2.97300005
LK-10-032	2.769999981	0	0	16.25200081	0.180000007	0	0	0.009	1.230000019
LK-10-035	2.960000038	0	0	28.61700058	0.156000003	0	0	0.018999999	2.785000086
LK-10-037	2.869999886	0	0	26.5189991	0.141000003	0	0	0.015	2.263999939
LK-10-038	3.025000095	0	0	28.94799995	0.156000003	-0.001	0	0.022	3.263000011
LK-10-040	2.796999931	0	0	17.65500069	0.180000007	0	0	0.011	1.60800004
LK-10-041	2.779000044	0	0	16.35199928	0.180999994	0	0	0.01	1.460000038
LK-10-042	2.832000017	0	0	22.40299988	0.180000007	0	0	0.012	1.769999981
LK-10-053	2.752000093	0	0	7.389999866	0.180999994	0	0	0.012	2.094000101
LK-10-056	3.049999952	0	0	31.5890007	0.156000003	0	0	0.024	3.50999999
LK-10-059	3.012000084	0	0	28.34900093	0.166999996	0	0	0.017999999	2.487999916
LK-10-061	2.829999924	0	0	20.40699959	0.159999996	0	0	0.011	1.559999943
LK-10-062	2.90199995	0	0	25.19799995	0.159999996	0	0	0.016000001	2.313999891
LK-10-063	2.996999979	0	0	42.25299835	0.181999996	0	0	0.011	1.080000043
LK-10-065	3.111000061	0	0	40.15100098	0.349999994	-0.003	0	0.02	2.671000004
LK-10-066	3.140000105	0	0	59.08399963	0.181999996	0	0	0.015	1.508000016
LK-10-067	3.052000046	0	0	27.45499992	0.160999998	0	0	0.023	3.479000092
LK-10-069	2.97300005	0	0	33.05899811	0.167999998	0	0	0.015	1.879999995
LK-10-070	3.003999949	0	0	27.73500061	0.165999994	0	0	0.017000001	2.325000048
LK-10-071	2.84800005	0	0	21.84700012	0.160999998	0	0	0.012	1.802000046
LK-10-072	2.871000051	0	0	19.6609993	0.156000003	0	0	0.015	2.424999952
LK-10-073	2.957000017	0	0	25.97400093	0.157000005	0	0	0.02	2.928999901
LK-10-074	3.061000109	0	0	34.32300186	0.165999994	0	0	0.021	2.898000002
LK-10-076	2.819999933	0	0	17.89500046	0.182999998	0	0	0.014	2.253000021
LK-10-077	2.923000097	0	0	17.3939991	0.150000006	-0.003	0	0.015	2.28399992
LK-10-084	2.974999905	0	0	29.82299995	0.156000003	0	0	0.018999999	2.786000013
LK-10-085	3.105999947	0	0	36.76900101	0.171000004	0	0	0.02	2.519000053
LK-10-087	3.002000093	0	0	32.57699966	0.157000005	0	0	0.02	2.880000114
LK-10-090	2.986000061	0	0	30.76799965	0.162	0	0	0.018999999	2.760999918
LK-10-092	2.99000001	0	0	34.95800018	0.158999994	0	0	0.018999999	2.690999985
LK-10-094	2.838999987	0	0	14.28499985	0.165999994	0	0	0.012	1.81099999
LK-11-095	2.98	0	0	25.64	0.17	0	0	0.02	2.57
LK-11-096	2.97	0	0	26.07	0.16	0	0	0.02	3.05
LK-11-097	2.92	0	0	20.42	0.17	0	0	0.02	2.32
LK-11-098	2.94	0	0	24.74	0.17	0	0	0.01	2.21
LK-11-099	3.04	0	0	33.98	0.16	0	0	0.02	3.09
LK-11-100	2.92	0	0	21.48	0.23	0	0	0.02	2.57
LK-11-101	3.04	0	0	32.5	0.16	0	0	0.02	3.1
LK-11-102	2.94	0	0	26.98	0.15	0	0	0.02	3.18
LK-11-103	3.05	0	0	33.77	0.17	0	0	0.02	3.02
LK-11-104	2.98	0	0	32.9	0.15	0	0	0.02	3.29

Samples	HAL_SYLV	HEMATITE	IAB	ICD	ICHLO	IFRAIS	IOR	IPAF	IPARA
LK-10-001	0	0	22.6420002	0	0	100	2.47300005	-31.83417702	0
LK-10-002	0	0	15.78600025	0	0	86.04799652	2.49000001	-14.46421623	12.05099964
LK-10-003	0	0	19.05900002	0.035999998	0	100	5.610000134	-69.56665802	0
LK-10-004	0	0	6.477000237	10.00699997	0	100	3.598999977	-84.46888733	0
LK-10-006	0	0	14.71800041	0	0	96.09700012	9.562000275	-20.91511917	2.365999937
LK-10-007	0	0	16.43099976	0.033	0	100	0.912	-16.85852432	0
LK-10-008	0	0	21.24600029	0	0	96.09300232	8.848999977	-30.38743019	2.757999897
LK-10-009	0	0	19.76300049	0	0	93.20600128	2.407999992	-18.94295692	6.056000233
LK-10-010	0	0	33.94100189	0	0	100	1.057999969	-25.93208694	0
LK-10-011	0	0	23.75200081	0	0	95.88600159	6.795000076	-16.76708221	3.198999882
LK-10-013	0	0	17.94799995	0	0	100	3.798000097	-26.06163597	0
LK-10-015	0	0	47.29999924	0	0	86.74299622	6.519000053	-14.39348984	11.65100002
LK-10-016	0	0	20.62199974	0	0	97.77400208	4.665999889	-20.7837162	1.815000057
LK-10-017	0	0	7.361999989	0	31.125	20.29899979	3.910000086	18.97299957	31.72699928
LK-10-018	0	0	23.40600014	0	0	94.90499878	2.368999958	-54.18421173	4.626999855
LK-10-019	0	0	18.13199997	0	0	92.38600159	1.606999993	-11.29417515	6.993999958
LK-10-021	0	0	11.58100033	0	0	95.04100037	6.420000076	-29.32823944	3.190000057
LK-10-025	0	0	21.67200089	0	0	75.48799896	3.474999905	-14.72384644	21.125
LK-10-028	0	0	21.42499924	0	0	91.40599823	7.294000149	-21.16342354	6.410999775
LK-10-005	0	0	7.425000191	12.55000019	0	100	3.832000017	-85.72494507	0
LK-10-014	0	0	28.63999939	0.043000001	0	100	2.346999884	-36.94343567	0
LK-10-022	0	0	1.605000019	0	0	100	0.066	9.187999725	0
LK-10-023	0	0	31.51099968	0	0	100	7.013000011	0.335000008	0
LK-10-026	0	0	62.34700012	18.59000015	0	100	1.43599999	25.78300095	0
LK-10-027	0	0	30.59700012	0	0	83.34300232	9.126000404	3.34800005	12.82999992
LK-10-031	0	0	20.78499985	0	0	100	9.55300045	-20.53439713	0
LK-10-032	0	0	34.98699951	0	0	92.99299622	6.001999855	7.289999962	5.980999947
LK-10-035	0	0	23.60099983	0	0	99.88500214	3.947999954	-29.33226585	0.098999999
LK-10-037	0	0	34.01800156	0	0	95.8730011	7.122000217	2.163000107	3.411999941
LK-10-038	0	0	22.44199944	0	0	99.7009964	1.269999981	-62.42522049	0.282999992
LK-10-040	0	0	34.13100052	0	0	87.01000214	5.300000191	5.360000134	11.24400043
LK-10-041	0	0	39.06800079	0	0	87.09100342	5.581999779	2.687999964	11.29500008
LK-10-042	0	0	34.09600067	0	0	90.81800079	5.59100008	-20.86184311	7.888999939
LK-10-053	0	0	68.14900208	2.721999884	0	89.52500153	2.161000013	4.806000233	10.15299988
LK-10-056	0	0	12.56400013	0	0	100	3.782999992	-15.24239159	0
LK-10-059	0	0	27.0890007	0.025	0	100	5.462999821	-23.40512848	0
LK-10-061	0	0	42.17900085	0	0	98.36100006	6.743000031	-1.591775656	1.412999988
LK-10-062	0	0	30.15999985	0	0	96.94599915	8.418999672	-39.99927139	2.387000084
LK-10-063	0	0	10.35400009	5.157000065	0	100	0.075999998	-1.621822	0
LK-10-065	0	0	11.0010024	6.184000015	0	100	10.68900013	-35.89516068	0
LK-10-066	0	0	1.527999997	9.086000443	0	100	0.354999989	-27.73618507	0
LK-10-067	0	0	16.45100021	0	0	100	7.872000217	-6.52964735	0
LK-10-069	0	0	30.93899918	0	0	100	2.09100008	-58.7816925	0
LK-10-070	0	0	25.66300011	0	0	100	5.556000233	-30.86332893	0
LK-10-071	0	0	32.7840004	0.022	0	94.13200378	7.421999931	-5.614369869	4.78399992
LK-10-072	0	0	34.68299866	0	0	89.93599701	9.652000427	-16.20565796	7.873000145
LK-10-073	0	0	25.73600006	0	0	99.98200226	7.105000019	-11.94190693	0.014
LK-10-074	0	0	18.24500084	0.026000001	0	100	2.885999918	-51.09640121	0
LK-10-076	0	0	29.47900009	0	0	91.60700226	3.013999939	18.6590004	7.613999844
LK-10-077	0	0	45.7519989	0	0	100	2.187000036	-58.20770645	0
LK-10-084	0	0	21.01799965	0	0	100	6.656000137	-30.06604385	0
LK-10-085	0	0	14.56599998	0.050000001	0	100	5.361999989	-56.26460648	0
LK-10-087	0	0	16.68899918	0	0	100	7.781000137	-8.476998329	0
LK-10-090	0	0	21.59199905	0	0	100	3.517999887	1.166000009	0
LK-10-092	0	0	22.36199951	0	0	100	2.171000004	2.746000051	0
LK-10-094	0	0	51.64300156	0	0	95.41000366	7.262000084	-31.01849937	4.024000168
LK-11-095	0	0	29.37	0.01	0	100	6.42	-21.99	0
LK-11-096	0	0	26.02	0	0	99.62	5.05	-15.37	0.32
LK-11-097	0	0	39.78	0	0	94.57	3.2	-41.78	5.03
LK-11-098	0	0	35.21	0.02	0	98.06	2.21	-39.06	1.83
LK-11-099	0	0	14.5	0.01	0	100	7.72	-55.78	0
LK-11-100	0	0	36.08	4.41	0	85.72	1.11	-44.98	13.86
LK-11-101	0	0	18.09	0.01	0	100	3.27	-42.11	0
LK-11-102	0	0	23.66	0	0	93.18	3.86	-17.39	5.86
LK-11-103	0	0	18.97	0.02	0	100	2.04	-61.68	0
LK-11-104	0	0	15.47	0	0	92.27	5.64	-35.6	5.67

Samples	IPYRO	ISER	K_CANCRIN	MAGNESITE	MAGNETITE	MANGANITE	MILLERITE	MOLYBDEN	NA_CANCRIN
LK-10-001	0	0	0	0	0	0	0	0	0
LK-10-002	0	1.901000023	0	0	0	0	0	0	0
LK-10-003	0	0	0	0	0.086000003	0	0	0	0
LK-10-004	0	0	0	0	5.440999985	0	0	0	0
LK-10-006	0	1.536999941	0	0	0	0	0	0	0
LK-10-007	0	0	0	0	1.116999984	0	0	0	0
LK-10-008	0	1.149000049	0	0	0	0	0	0	0
LK-10-009	0	0.737999976	0	0	0	0	0	0	0
LK-10-010	0	0	0	0	0	0	0	0	0
LK-10-011	0	0.915000021	0	0	0	0	0	0	0
LK-10-013	0	0	0	0	0	0	0	0	0
LK-10-015	0	1.605999947	0	0	0.097999997	0	0	0	0
LK-10-016	0	0.411000013	0	0	0	0	0	0	0
LK-10-017	0	16.85000038	0	0	1.773000002	0	0	0	0
LK-10-018	0	0.467999995	0	0	0	0	0	0	0
LK-10-019	0	0.620000005	0	0	0	0	0	0	0
LK-10-021	0	1.769000053	0	0	0	0	0	0	0
LK-10-025	0	3.387000084	0	0	0	0	0	0	0
LK-10-028	0	2.183000088	0	0	0	0	0	0	0
LK-10-005	0	0	0	0	7.554999828	0	0	0	0
LK-10-014	0	0	0	0	0.050999999	0	0	0	0
LK-10-022	0	0	0	0	0	0	0	0	0
LK-10-023	0	0	0	0	0.633000016	0	0	0	0
LK-10-026	0	0	0	0	0	0	0	0	0
LK-10-027	0	3.826999903	0	0	0	0	0	0	0
LK-10-031	0	0	0	0	0	0	0	0	0
LK-10-032	0	1.026000023	0	0	0	0	0	0	0
LK-10-035	0	0.016000001	0	0	0	0	0	0	0
LK-10-037	0	0.713999987	0	0	0	0	0	0	0
LK-10-038	0	0.016000001	0	0	0.138999999	0	0	0	0
LK-10-040	0	1.746000051	0	0	0	0	0	0	0
LK-10-041	0	1.613999963	0	0	0	0	0	0	0
LK-10-042	0	1.29400003	0	0	0	0	0	0	0
LK-10-053	0	0.321999997	0	0	0.430000007	0	0	0	0
LK-10-056	0	0	0	0	0	0	0	0	0
LK-10-059	0	0	0	0	0.075000003	0	0	0	0
LK-10-061	0	0.225999996	0	0	0	0	0	0	0
LK-10-062	0	0.666000009	0	0	0	0	0	0	0
LK-10-063	0	0	0	0	0	0	0	0	0
LK-10-065	0	0	0	0	1.789000034	0	0	0	0
LK-10-066	0	0	0	0	0	0	0	0	0
LK-10-067	0	0	0	0	0.463999987	0	0	0	0
LK-10-069	0	0	0	0	0	0	0	0	0
LK-10-070	0	0	0	0	0	0	0	0	0
LK-10-071	0	1.082999945	0	0	0	0	0	0	0
LK-10-072	0	2.190999985	0	0	0.172999993	0	0	0	0
LK-10-073	0	0.004	0	0	0	0	0	0	0
LK-10-074	0	0	0	0	0	0	0	0	0
LK-10-076	0	0.778999984	0	0	0	0	0	0	0
LK-10-077	0	0	0	0	0.252000004	0	0	0	0
LK-10-084	0	0	0	0	0	0	0	0	0
LK-10-085	0	0	0	0	0.015	0	0	0	0
LK-10-087	0	0	0	0	0	0	0	0	0
LK-10-090	0	0	0	0	0	0	0	0	0
LK-10-092	0	0	0	0	0	0	0	0	0
LK-10-094	0	0.565999985	0	0	0.606000006	0	0	0	0
LK-11-095	0	0	0	0	0.03	0	0	0	0
LK-11-096	0	0.06	0	0	0	0	0	0	0
LK-11-097	0	0.41	0	0	0.7	0	0	0	0
LK-11-098	0	0.11	0	0	0.5	0	0	0	0
LK-11-099	0	0	0	0	0	0	0	0	0
LK-11-100	0	0.43	0	0	1.47	0	0	0	0
LK-11-101	0	0	0	0	0.03	0	0	0	0
LK-11-102	0	0.96	0	0	0	0	0	0	0
LK-11-103	0	0	0	0	0.01	0	0	0	0
LK-11-104	0	2.07	0	0	0	0	0	0	0

Samples	ORTHOSE	PAF_100	PAF_CALC	PAF_MAX	PAF_MIN	PARAGONITE	PENTLAND	PSILOMELAN	PYRITE
LK-10-001	2.437000036	1.506999969	2.49000001	0	2.49000001	0	0	0	0
LK-10-002	2.542999983	2.704999924	3.33100009	0	3.33100009	0	0	0	0
LK-10-003	5.285999775	1.059999943	2.680999994	0	2.680999994	0	0	0	0
LK-10-004	2.489000082	1.437000036	2.838000059	0	2.838000059	0	0	0	0
LK-10-006	9.670999527	2.326999903	3.167999983	0	3.167999983	0	0	0	0
LK-10-007	0.904999971	2.539999962	3.006000042	0	3.006000042	0	0	0	0
LK-10-008	8.585000038	1.976999998	3.157000065	0	3.157000065	0	0	0	0
LK-10-009	2.464999914	2.247999907	2.979000092	0	2.979000092	0	0	0	0
LK-10-010	1.021000028	1.529999971	2.24000001	0	2.24000001	0	0	0	0
LK-10-011	6.18599987	1.590000033	2.072000027	0	2.072000027	0	0	0	0
LK-10-013	3.950000048	2.039999962	2.948999882	0	2.948999882	0	0	0	0
LK-10-015	5.653999805	1.200999975	1.511999965	0	1.511999965	0.57099998	0	0	0
LK-10-016	4.644999981	2.246999979	3.015000105	0	3.015000105	0	0	0	0
LK-10-017	4.173999786	7.203000069	7.218999863	17.18000031	4.867000103	9.031999588	0	0	0
LK-10-018	2.328000069	1.120000005	3.279999971	0	3.279999971	0	0	0	0
LK-10-019	1.610999942	2.792000055	3.257999897	0	3.257999897	0	0	0	0
LK-10-021	6.710000038	2.27699995	3.529000044	0	3.529000044	0	0	0	0
LK-10-025	3.601999998	2.842000008	3.529000044	0	3.529000044	0.150000006	0	0	0
LK-10-028	7.272999763	2.128000021	2.924999952	0	2.924999952	0	0	0	0
LK-10-005	2.673000097	1.146999955	2.414000034	0	2.414000034	0	0	0	0
LK-10-014	2.203999996	1.623999953	2.36500001	0	2.36500001	0	0	0	0.021
LK-10-022	0.063000001	2.974999905	2.974999905	16.36300087	1.620000005	0	0	0	0.009
LK-10-023	5.683000088	2.703999996	2.782000065	14.79500008	2.663000107	0	0	0	0.166999996
LK-10-026	0.986000001	2.799000025	2.812000036	6.21600008	1.611999989	0.041000001	0	0	0.136000007
LK-10-027	7.026000023	1.703999996	1.723999977	6.130000114	1.550999999	5.120999813	0	0	0.337000012
LK-10-031	8.49600029	2.323999882	3.013000011	0	3.013000011	0	0	0	0.017999999
LK-10-032	4.750999928	1.569000006	1.57099998	6.712999821	1.164999962	3.377000093	0	0	0.027000001
LK-10-035	3.644000053	1.81099999	2.812999964	0	2.812999964	0	0	0	0.009
LK-10-037	7.484000206	2.447000027	2.471999884	13.24400043	2.207999945	0	0	0	0.004
LK-10-038	1.16900003	1.008999944	3.582000017	0	3.582000017	0	0	0	0.263999999
LK-10-040	4.585999966	1.896999955	1.906999946	7.960000038	1.55400002	3.246000051	0	0	0.045000002
LK-10-041	4.736999989	1.588000059	1.610000009	7.449999809	1.425999999	2.023000002	0	0	0.027000001
LK-10-042	4.875	1.304999948	1.861999989	0	1.861999989	0.101999998	0	0	0.071999997
LK-10-053	2.141000032	2.328000069	2.361999989	8.838000298	2	0.167999998	0	0	0.035
LK-10-056	3.423000097	2.913000107	3.555000067	0	3.555000067	0	0	0	0.018999999
LK-10-059	4.954999924	2.019999981	2.530999899	0	2.530999899	0	0	0	0.012
LK-10-061	5.901000023	1.547000051	1.58099997	0	1.58099997	0	0	0	0.009
LK-10-062	7.907999992	1.123999953	2.339999914	0	2.339999914	0	0	0	0.009
LK-10-063	0.064000003	1.725999951	1.754999995	0	1.754999995	0	0	0	0.005
LK-10-065	9.906000137	2.431999922	2.709000111	0	2.709000111	0	0	0	0
LK-10-066	0.381999999	1.995000005	3.135999918	0	3.135999918	0	0	0	0.009
LK-10-067	7.15199995	3.286999941	3.542999983	0	3.542999983	0	0	0	0.029999999
LK-10-069	2.059000015	0.912	1.904999971	0	1.904999971	0	0	0	0.009
LK-10-070	4.729000092	1.741999984	2.352999926	0	2.352999926	0	0	0	0.009
LK-10-071	6.073999882	1.728000045	1.878000021	0	1.878000021	0	0	0	0.056000002
LK-10-072	8.753000259	2.01699996	2.592999935	0	2.592999935	0	0	0	0.131999999
LK-10-073	6.65199995	2.535000086	2.953999996	0	2.953999996	0	0	0	0.005
LK-10-074	2.719000101	1.610000014	2.934000015	0	2.934000015	0	0	0	0.002
LK-10-076	2.698999882	3.775000095	3.775000095	11.21399975	2.069000006	2.683000088	0	0	0.009
LK-10-077	1.838000059	0.823000014	2.859999895	0	2.859999895	0	0	0	0.5
LK-10-084	6.311999798	1.81099999	2.835000038	0	2.835000038	0	0	0	0.027000001
LK-10-085	4.926000118	1.491000056	2.660000086	0	2.660000086	0	0	0	0.093000002
LK-10-087	7.585000038	2.619999886	2.910000086	0	2.910000086	0	0	0	0.009
LK-10-090	3.220000029	2.855999947	2.914999962	16.54500008	2.694999933	0	0	0	0.009
LK-10-092	2.200000048	3.009000063	3.032000065	17.23900032	2.607000113	0	0	0	0.009
LK-10-094	6.438000202	1.113000035	1.827000022	0	1.827000022	0	0	0	0.001
LK-11-095	5.78	2.04	2.59	0	2.59	0	0	0	0
LK-11-096	4.69	2.51	3.07	0	3.07	0	0	0	0
LK-11-097	2.82	1.1	2.34	0	2.34	0	0	0	0
LK-11-098	1.96	1.11	2.22	0	2.22	0	0	0	0
LK-11-099	7.58	1.42	3.12	0	3.12	0	0	0	0
LK-11-100	0.98	1.1	2.59	0	2.59	0.13	0	0	0
LK-11-101	3.08	1.61	3.13	0	3.13	0	0	0	0
LK-11-102	3.63	2.52	3.2	0	3.2	0	0	0	0
LK-11-103	1.93	1.1	3.04	0	3.04	0	0	0	0
LK-11-104	5.67	1.82	3.31	0	3.31	0	0	0	0

Samples	PYROPHIL	PYRRHOTITE	QUARTZ	RODOCHROS	S	SERICITE	SERPENTINE	SIDERITE	SMAG_CALC
LK-10-001	0.064999998	0	12.86699963	0	0	0	0	0	0
LK-10-002	0.068999998	0	16.3010006	0	0	0	0	0	0
LK-10-003	0.180999994	0	3.282999992	0	0	0	0	0	0.838
LK-10-004	0.02	0	0.275000006	0	0	0	0	0	50.86000061
LK-10-006	0.088	0	7.334000111	0	0	0	0	0	0
LK-10-007	0.217999995	0	1.213999987	0	0	0	0	0	10.61400032
LK-10-008	0.088	0	6.68900013	0	0	0	0	0	0
LK-10-009	0.07	0	13.3380003	0	0	0	0	0	0
LK-10-010	0.055	0	11.05200005	0	0	0	0	0	0
LK-10-011	0.057999998	0	23.79700089	0	0	0	0	0	0
LK-10-013	0.079000004	0	5.947000027	0	0	0	0	0	0
LK-10-015	0	0	25.92099953	0	0	0.079000004	0	0	0.967999995
LK-10-016	0.075000003	0	8.508999825	0	0	0	0	0	0
LK-10-017	0.007	0	19.36300087	0	0	4.796999931	0	0	16.06900024
LK-10-018	0.115999997	0	7.727000237	0	0	0	0	0	0
LK-10-019	0.074000001	0	12.52700043	0	0	0	0	0	0
LK-10-021	0.097999997	0	6.052999973	0	0	0	0	0	0
LK-10-025	0	0	14.59500027	0	0	0.024	0	0	0
LK-10-028	0.067000002	0	12.94200039	0	0	0	0	0	0
LK-10-005	0.02	0.02	0.992999971	0	0.01	0	0	0	69.97699738
LK-10-014	0.155000001	0.012	3.953999996	0	0.029999999	0	0	0	0.537999988
LK-10-022	0.046	0	26.02700043	0	0.01	0	0	0	0
LK-10-023	0.174999997	0.01	13.06400013	0	0.189999998	0	0	0	6.162000179
LK-10-026	0	0	37.61600113	0	0.150999993	0.001	0	0	0
LK-10-027	0	0	42.26300049	0	0.372999996	1.52699995	0	0	0
LK-10-031	0.085000001	0	6.81099987	0	0.02	0	0	0	0
LK-10-032	0	0	39.4659996	0	0.029999999	0.578999996	0	0	0
LK-10-035	0.074000001	0	11.82499981	0	0.01	0	0	0	0
LK-10-037	0.041999999	0	8.819000244	0	0.005	0	0	0	0
LK-10-038	0.241999999	0.014	6.947999954	0	0.298000008	0	0	0	1.38499999
LK-10-040	0	0	32.95999908	0	0.050000001	0.504000008	0	0	0
LK-10-041	0	0	32.63700104	0	0.029999999	0.289000005	0	0	0
LK-10-042	0	0	28.50399971	0	0.079999998	0.017000001	0	0	0
LK-10-053	0	0.001	2.815000057	0	0.041000001	0.005	0	0	4.372000217
LK-10-056	0.093000002	0	4.18900013	0	0.021	0	0	0	0
LK-10-059	0.167999998	0.012	3.486999989	0	0.02	0	0	0	0.768999994
LK-10-061	0.044	0	20.89599991	0	0.01	0	0	0	0
LK-10-062	0.082999997	0	13.80900002	0	0.01	0	0	0	0
LK-10-063	0	0	35.50699997	0	0.005	0	0	0	0
LK-10-065	0	0.037	0	0	0.02	0	2.345000029	0	17.66900063
LK-10-066	0	0	19.78899956	0	0.01	0	0	0	0
LK-10-067	0.248999998	0.014	1.485999942	0	0.041000001	0	0	0	4.514999866
LK-10-069	0.050000001	0	9.815999985	0	0.01	0	0	0	0
LK-10-070	0.061999999	0	6.229000092	0	0.01	0	0	0	0
LK-10-071	0.07	0	28.72500038	0	0.061999999	0	0	0	0
LK-10-072	0.189999998	0.011	15.67399979	0	0.152999997	0	0	0	1.720000029
LK-10-073	0.085000001	0	6.302999973	0	0.005	0	0	0	0
LK-10-074	0.119000003	0.015	4.017000198	0	0.01	0	0	0	0.044
LK-10-076	0	0	29.47900009	0	0.01	0.273999989	0	0	0
LK-10-077	0.159999996	0.009	10.61699963	0	0.564999998	0	0	0	2.503999949
LK-10-084	0.072999999	0	8.737000465	0	0.029999999	0	0	0	0
LK-10-085	0.158000007	0.013	2.14199996	0	0.109999999	0	0	0	0.180999994
LK-10-087	0.074000001	0	6.157000065	0	0.01	0	0	0	0
LK-10-090	0.089000002	0	12.29300022	0	0.01	0	0	0	0
LK-10-092	0.068000004	0	8.43900013	0	0.01	0	0	0	0
LK-10-094	0.136000007	0.008	13.23900032	0	0.005	0	0	0	6.007999897
LK-11-095	0.17	0	3.82	0	0	0	0	0	0.29
LK-11-096	0.11	0	6.51	0	0	0	0	0	0
LK-11-097	0.18	0	15.34	0	0	0	0	0	6.82
LK-11-098	0.17	0	16.49	0	0	0	0	0	4.84
LK-11-099	0.13	0	3.73	0	0	0	0	0	0.05
LK-11-100	0	0	19.35	0	0	0	0	0	14.13
LK-11-101	0.23	0	6.24	0	0	0	0	0	0.33
LK-11-102	0.09	0	11.33	0	0	0	0	0	0
LK-11-103	0.12	0	5.41	0	0	0	0	0	0.07
LK-11-104	0.09	0	10.67	0	0	0	0	0	0

Samples	SPHALERITE	SPHENE	TALC	TOTAL	TREMOLITE
LK-10-001	0	1.207000017	0	100	7.06799984
LK-10-002	0	1.184999943	0	100	2.930999994
LK-10-003	0	2.552000046	0	100	11.98600006
LK-10-004	0	1.065999985	3.661000013	100	16.13999939
LK-10-006	0	2.565999985	0	100	5.907000065
LK-10-007	0	2.424999952	0	100	7.06400013
LK-10-008	0	2.157000065	0	100	6.614999771
LK-10-009	0	1.373000026	0	100	4.473999977
LK-10-010	0	1.253999949	0	100	7.323999882
LK-10-011	0	1.794999957	0	100	1.906000018
LK-10-013	0	1.965000033	0	100	8.272999763
LK-10-015	0	1.389999986	0	100	0
LK-10-016	0	1.557000041	0	100	7.703999996
LK-10-017	0	1.64199996	0	100	0
LK-10-018	0	2.493000031	0	100	5.43599987
LK-10-019	0	1.644000053	0	100	5.815999985
LK-10-021	0	1.730000019	0	100	6.782999992
LK-10-025	0	1.921000004	0	100	0
LK-10-028	0	1.514000058	0	100	3.816999912
LK-10-005	0	1.06400001	3.490999937	100	10.95300007
LK-10-014	0	1.516000032	0	100	11.77999973
LK-10-022	0	2.680999994	0	100	3.989000082
LK-10-023	0	2.184999943	0	100	7.386000156
LK-10-026	0	0.349000007	0	100	0
LK-10-027	0	0.437999994	0	100	0
LK-10-031	0	1.643000007	0	100	11.88399982
LK-10-032	0	0.601999998	0	100	0
LK-10-035	0	1.891000032	0	100	8.168000221
LK-10-037	0	1.470999956	0	100	2.880000114
LK-10-038	0	2.720000029	0	100	8.574999809
LK-10-040	0	0.984000027	0	100	0
LK-10-041	0	0.949999988	0	100	0
LK-10-042	0	1.059000015	0	100	0
LK-10-053	0	1.601999998	0	100	0
LK-10-056	0	2.040999889	0	100	15.57999992
LK-10-059	0	1.600000024	0	100	13.41399956
LK-10-061	0	1.406999946	0	100	2.161000013
LK-10-062	0	1.953999996	0	100	3.030999899
LK-10-063	0	0.451999992	0	100	2.059999943
LK-10-065	0	2.351000071	4.298999786	100	12.50199986
LK-10-066	0	1.710999966	0	100	0.66900003
LK-10-067	0	3.184999943	0	100	11.44999981
LK-10-069	0	2.098999977	0	100	7.889999866
LK-10-070	0	1.368999958	0	100	18.02499962
LK-10-071	0	2.036999941	0	100	0.465000004
LK-10-072	0	2.743000031	0	100	0.66900003
LK-10-073	0	2.088999987	0	100	8.651000023
LK-10-074	0	2.010999918	0	100	12.56200027
LK-10-076	0	1.424999952	0	100	0
LK-10-077	0	2.470999956	0	100	6.839000225
LK-10-084	0	1.799999952	0	100	9.38599968
LK-10-085	0	1.894999981	0	100	16.59300041
LK-10-087	0	1.600999951	0	100	11.18200016
LK-10-090	0	1.970999956	0	100	7.69299984
LK-10-092	0	1.404999971	0	100	8.324999809
LK-10-094	0	1.868999958	0	100	1.111999989
LK-11-095	0	2.02	0	100	12.6
LK-11-096	0	2.05	0	100	8.7
LK-11-097	0	2.64	0	100	1.63
LK-11-098	0	2.58	0	100	2.02
LK-11-099	0	2.03	0	100	9.7
LK-11-100	0	2.66	1	100	0
LK-11-101	0	2.29	0	100	9.91
LK-11-102	0	2.04	0	100	5.63
LK-11-103	0	2.31	0	100	10.53
LK-11-104	0	2.11	0	100	4.62

B) NORMAT results from Castillo-Guimond (2012) lithogeochemistry analysis.

Samples	SIO2_PCT	TIO2_PCT	AL2O3_PCT	FE2O3_PCT	MNO_PCT	MGO_PCT	CAO_PCT	NA2O_PCT	K2O_PCT	P2O5_PCT	CR2O3_PCT
LC-10-002	50.85	0.71	17.65	8.51	0.12	5.32	11	2.07	0.44	0.09	0.02
LC-10-003	56.69	0.65	16.58	7.32	0.12	4.3	8	4.63	0.47	0.1	0.02
LC-10-004	54.74	0.7	17.28	7.11	0.11	4.96	8.5	3.19	0.5	0.1	0.02
LC-10-006	53.04	0.65	15.88	9.29	0.14	4.04	11.41	2.52	0.18	0.1	0.02
LC-10-007	48.41	1.11	17.46	10.67	0.21	6.03	10.25	1.96	0.39	0.16	0.01
LC-10-008	56.57	0.72	17.56	5.66	0.09	3.93	9.3	3.92	0.41	0.11	0.03
LC-10-010	57.2	0.86	15.85	7.99	0.12	5.05	7.15	2.79	0.36	0.1	0.01
LC-10-011	54.42	1.02	17.89	7.06	0.14	3.87	9.73	3.23	0.26	0.13	0.03
LC-10-012	51.97	1.06	18.4	8.91	0.14	4.52	10.18	3	0.51	0.12	0.02
LC-10-013	53.02	0.61	16.18	8.56	0.14	4.64	10.83	3.13	0.23	0.09	0.02
LC-10-015	44.75	1.3	18.43	11.58	0.15	7.11	9.43	1.85	0.89	0.15	0.03
LC-10-016	57.3	1.08	14.77	9.12	0.13	2.84	9.15	2.76	0.31	0.16	0.03
LC-10-017	57.29	1.07	14.91	8.27	0.13	4.08	7.97	3.55	0.29	0.17	0.03
LC-10-018	58.73	1.05	15.35	7.71	0.16	3.36	6.52	4.1	0.53	0.16	0.03
LC-10-019	54.36	1.11	15.99	9.5	0.15	5.45	6.56	2.71	0.76	0.17	0.04
LC-10-020	69.04	0.29	14.55	4.19	0.03	0.68	3.25	4.25	0.88	0.1	0.01
LC-10-021	56.17	0.77	16.59	9.12	0.05	3.83	6.94	1.75	1.42	0.14	0.01
LC-10-025	63.14	0.9	12.45	7.35	0.13	3.74	6.85	2.75	0.22	0.14	0.03
LC-10-026A	62.5	0.49	15.92	6.81	0.11	1.74	6.33	2.63	0.28	0.14	0.01
LC-10-026B	64.19	0.47	15.6	5.49	0.07	1.44	6.75	2.95	0.3	0.15	0.01
LC-10-028	53.97	0.7	18.27	6.61	0.11	4.19	7.45	4.3	0.85	0.11	0.01
LC-10-030	54	1.06	14.76	6.38	0.16	3.53	13.39	4.03	0.31	0.15	0.03
LC-10-031	53.8	1.12	15.21	9.61	0.2	4.87	9.52	3.91	0.29	0.17	0.03
LC-10-032	47.63	1.15	16.23	9.38	0.25	3.48	15.21	2.83	0.24	0.18	0.03
LC-10-033	57.61	1.25	14.79	11.81	0.18	2.63	5.81	3.88	0.55	0.32	0.01
LC-10-034	51.5	1.04	14.29	10.4	0.18	6.78	9.7	2.18	0.93	0.15	0.03
LC-10-035	52.79	0.96	14.64	8.8	0.12	6	9.92	3.66	0.5	0.14	0.03
LC-10-036	51.66	0.88	18.43	7.89	0.09	3.75	10.99	2.7	1.27	0.1	0.01
LC-10-039	55.94	0.67	17.42	6.5	0.12	4.26	8.15	3.03	0.94	0.1	0.01
LC-10-040	59.5	0.49	15.7	5.22	0.1	3.45	9.4	3.08	0.53	0.08	0.01
LC-10-043	54.29	0.71	17.51	7.22	0.12	4.67	8.76	4.46	0.77	0.11	0.03
LC-10-044	51.17	0.68	17.52	8.48	0.2	5.11	10.25	3.11	1.06	0.11	0.03
LC-10-045	56.42	0.6	15.03	8.07	0.14	3.46	8.81	2.9	0.51	0.1	0.02
LC-10-046	50.93	0.88	18.14	8.68	0.1	6.34	7.4	2.01	0.75	0.11	0.02
LC-10-047	50.21	0.95	14.3	9.6	0.26	3.39	15.2	3.39	0.24	0.13	0.03
LC-10-048	41.6	0.7	9.42	25.8	0.37	3.31	15.96	0.58	0.61	0.12	0.05
LC-10-049B	51.77	1.01	14.96	12.33	0.16	3.58	10.25	2.58	0.57	0.12	0.03
LC-10-050	53.6	1.23	16.02	9.36	0.14	4.43	9.64	2.62	0.85	0.18	0.03
LC-10-051	53.63	0.7	18.88	6.79	0.11	4.22	9.16	2.97	0.62	0.1	0.01
LC-10-053	49.77	0.86	16.59	8.65	0.16	6.39	10.77	2.28	1.14	0.08	0.02
LC-10-056	55.97	0.66	17.27	6.64	0.12	4.08	8.11	3.45	1.14	0.1	0.02
LC-10-058	55.81	0.63	17.31	6.07	0.09	3.71	7.83	4.23	0.3	0.09	0.02
LC-10-062	50.89	0.77	18.48	7.4	0.12	4.38	10.85	3.49	0.73	0.11	0.03

Samples	LOI_PCT	TOTAL_PCT	BA_PPM	CR_PPM	SR_PPM	RB_PPM	ZR_PPM	Y_PPM	NB_PPM	AS_PPM	CU_PPM
LC-10-002	1.65	98.45	100	0	185	12	13	84	3	0	0
LC-10-003	0.81	99.73	150	0	170	8	12	89	3	0	0
LC-10-004	0.99	98.24	170	0	198	13	13	95	3	0	0
LC-10-006	1.12	98.42	40	0	202	2	10	87	3	0	0
LC-10-007	1.52	98.2	70	0	149	11	17	57	3	0	0
LC-10-008	0.68	99.02	90	0	283	4	12	97	4	0	0
LC-10-010	1.52	99.03	140	0	135	10	16	94	4	0	0
LC-10-011	0.5	98.31	100	0	187	5	15	81	4	0	0
LC-10-012	1.18	100.05	160	0	217	8	16	84	3	0	0
LC-10-013	0.98	98.46	70	0	182	3	11	82	3	0	0
LC-10-015	2.88	98.59	200	0	126	27	24	105	4	0	0
LC-10-016	1.02	98.7	60	0	236	3	26	108	4	0	0
LC-10-017	0.79	98.58	70	0	218	6	22	113	4	0	0
LC-10-018	1.31	99.05	180	0	158	12	22	103	5	0	0
LC-10-019	1.99	98.87	480	0	268	16	25	122	4	0	0
LC-10-020	1.39	98.68	180	0	166	27	63	184	12	0	0
LC-10-021	2.48	99.31	200	0	166	46	26	116	4	0	0
LC-10-025	0.54	98.27	100	0	206	4	15	91	4	0	0
LC-10-026A	1.61	98.59	110	0	193	7	24	109	6	0	0
LC-10-026B	1.29	98.73	100	0	186	7	25	110	7	0	0
LC-10-028	2.27	98.89	220	0	171	22	15	97	4	0	0
LC-10-030	0.42	98.25	100	0	252	4	21	111	4	0	0
LC-10-031	0.52	99.3	100	0	319	2	21	126	4	0	0
LC-10-032	1.95	98.6	70	0	249	6	21	109	5	0	0
LC-10-033	1.31	100.15	170	0	158	8	43	185	10	0	0
LC-10-034	1.38	98.6	120	0	212	37	29	107	4	0	0
LC-10-035	1.32	98.9	60	0	121	15	23	99	4	0	0
LC-10-036	1.36	99.17	120	0	211	24	24	109	4	0	0
LC-10-039	1.7	98.89	270	0	173	24	13	90	3	0	0
LC-10-040	0.72	98.31	170	0	130	9	10	67	3	0	0
LC-10-043	1.26	99.95	130	0	225	25	16	98	4	0	0
LC-10-044	1.65	99.42	250	0	194	30	17	93	3	0	0
LC-10-045	2.49	98.58	110	0	182	16	12	86	3	0	0
LC-10-046	3.11	98.49	150	0	105	29	16	93	3	0	0
LC-10-047	0.94	98.68	90	0	217	4	21	95	4	0	0
LC-10-048	0.51	99.06	60	0	77	3	20	60	3	0	0
LC-10-049B	1.46	98.85	80	0	234	16	23	102	4	0	0
LC-10-050	1.22	99.35	90	0	164	26	28	126	5	0	0
LC-10-051	1.54	98.77	130	0	210	15	13	102	3	0	0
LC-10-053	1.61	98.37	210	0	198	32	22	88	3	0	0
LC-10-056	1.42	99.04	320	0	223	29	17	94	3	0	0
LC-10-058	2.36	98.49	210	0	231	7	11	96	3	0	0
LC-10-062	1.65	98.95	130	0	292	23	21	113	4	0	0

Samples	ZN_PPM	AG_PPM	AU_PPB	SB_PPM	PB_PPM	SIO2N	TIO2N	TIO2_ZR	AL2O3_TIO2	AL2O3_ZR	TIO2N_ZR
LC-10-002	0	0	0	0	0	52.53	0.73	546	25.00	136	564
LC-10-003	0	0	0	0	0	57.31	0.66	542	26.00	138	548
LC-10-004	0	0	0	0	0	56.29	0.72	538	25.00	133	554
LC-10-006	0	0	0	0	0	54.51	0.67	650	24.00	159	668
LC-10-007	0	0	0	0	0	50.07	1.15	653	16.00	103	675
LC-10-008	0	0	0	0	0	57.52	0.73	600	24.00	146	610
LC-10-010	0	0	0	0	0	58.66	0.88	538	18.00	99	551
LC-10-011	0	0	0	0	0	55.64	1.04	680	18.00	119	695
LC-10-012	0	0	0	0	0	52.56	1.07	663	17.00	115	670
LC-10-013	0	0	0	0	0	54.39	0.63	555	27.00	147	569
LC-10-015	0	0	0	0	0	46.76	1.36	542	14.00	77	566
LC-10-016	0	0	0	0	0	58.66	1.11	415	14.00	57	425
LC-10-017	0	0	0	0	0	58.58	1.09	486	14.00	68	497
LC-10-018	0	0	0	0	0	60.09	1.07	477	15.00	70	488
LC-10-019	0	0	0	0	0	56.11	1.15	444	14.00	64	458
LC-10-020	0	0	0	0	0	70.96	0.3	46	50.00	23	47
LC-10-021	0	0	0	0	0	58.01	0.8	296	22.00	64	306
LC-10-025	0	0	0	0	0	64.61	0.92	600	14.00	83	614
LC-10-026A	0	0	0	0	0	64.45	0.51	204	32.00	66	211
LC-10-026B	0	0	0	0	0	65.88	0.48	188	33.00	62	193
LC-10-028	0	0	0	0	0	55.86	0.72	467	26.00	122	483
LC-10-030	0	0	0	0	0	55.2	1.08	505	14.00	70	516
LC-10-031	0	0	0	0	0	54.46	1.13	533	14.00	72	540
LC-10-032	0	0	0	0	0	49.28	1.19	548	14.00	77	567
LC-10-033	0	0	0	0	0	58.29	1.26	291	12.00	34	294
LC-10-034	0	0	0	0	0	52.97	1.07	359	14.00	49	369
LC-10-035	0	0	0	0	0	54.1	0.98	417	15.00	64	428
LC-10-036	0	0	0	0	0	52.82	0.9	367	21.00	77	375
LC-10-039	0	0	0	0	0	57.56	0.69	515	26.00	134	530
LC-10-040	0	0	0	0	0	60.97	0.5	490	32.00	157	502
LC-10-043	0	0	0	0	0	55.01	0.72	444	25.00	109	450
LC-10-044	0	0	0	0	0	52.34	0.7	400	26.00	103	409
LC-10-045	0	0	0	0	0	58.72	0.62	500	25.00	125	520
LC-10-046	0	0	0	0	0	53.4	0.92	550	21.00	113	577
LC-10-047	0	0	0	0	0	51.37	0.97	452	15.00	68	463
LC-10-048	0	0	0	0	0	42.21	0.71	350	13.00	47	355
LC-10-049B	0	0	0	0	0	53.16	1.04	439	15.00	65	451
LC-10-050	0	0	0	0	0	54.62	1.25	439	13.00	57	448
LC-10-051	0	0	0	0	0	55.16	0.72	538	27.00	145	554
LC-10-053	0	0	0	0	0	51.44	0.89	391	19.00	75	404
LC-10-056	0	0	0	0	0	57.33	0.68	388	26.00	102	398
LC-10-058	0	0	0	0	0	58.06	0.66	573	27.00	157	596
LC-10-062	0	0	0	0	0	52.3	0.79	367	24.00	88	377

Samples	ZR_Y	MF	ACFM	ACTINOTE	ALBITE	ALUNITE	ANATASE	ANHYDRITE	ANKERITE	APATITE	ARSENOPYR
LC-10-002	0.20	0	Chlorite	5.370999813	19.46899986	0	0	0	0	0.194999993	0
LC-10-003	0.10	0	Chlorite	6.355999947	41.95500183	0	0	0	0	0.200000003	0
LC-10-004	0.10	0	Chlorite	3.115999937	29.59399986	0	0	0	0	0.204999998	0
LC-10-006	0.10	0	Chlorite	10.52400017	23.76000023	0	0	0	0	0.228	0
LC-10-007	0.30	0	Chlorite	4.270999908	18.54800034	0	0	0	0	0.354999989	0
LC-10-008	0.10	0	Chlorite	4.581999779	35.78099823	0	0	0	0	0.238000005	0
LC-10-010	0.20	0	Chlorite	1.628000021	26.05900002	0	0	0	0	0.219999999	0
LC-10-011	0.20	0	Chlorite	3.526000023	29.9279995	0	0	0	0	0.280999988	0
LC-10-012	0.20	0	Chlorite	4.376999855	27.56599998	0	0	0	0	0.254999995	0
LC-10-013	0.10	0	Chlorite	9.588000298	29.15200043	0	0	0	0	0.202000007	0
LC-10-015	0.20	0	Chlorite	2.290999889	17.6060009	0	0	0	0	0.330000013	0
LC-10-016	0.20	0	Chlorite	7.370999813	26.12100029	0	0	0	0	0.342000008	0
LC-10-017	0.20	0	Chlorite	5.859000206	33.07799911	0	0	0	0	0.368999988	0
LC-10-018	0.20	0	Chlorite	3.526000023	38.09899902	0	0	0	0	0.342000008	0
LC-10-019	0.20	0	Chlorite	0.777999997	25.53899956	0	0	0	0	0.370999992	0
LC-10-020	0.30	0	Sericite	0	36.66400146	0	0	0	0	0.214000002	0
LC-10-021	0.20	0	Sericite	0	16.57099915	0	0	0	0	0.300000012	0
LC-10-025	0.20	0	Chlorite	5.045000076	25.93400002	0	0	0	0	0.303000003	0
LC-10-026A	0.20	0	Sericite	0	24.25499916	0	0	0	0	0.312999994	0
LC-10-026B	0.20	0	Sericite	0	27.74900055	0	0	0	0	0.324999988	0
LC-10-028	0.20	0	Chlorite	2.372999907	39.75899887	0	0	0	0	0.232999995	0
LC-10-030	0.20	0	Calcite	11.38199997	37.17300034	0	0	0	0	0.324000001	0
LC-10-031	0.20	0	Calcite	10.25599957	35.9129982	0	0	0	0	0.358999997	0
LC-10-032	0.20	0	Calcite	16.99699974	26.80699921	0	0	0	0	0.386000007	0
LC-10-033	0.20	0	Chlorite	2.799000025	36.2859993	0	0	0	0	0.68599999	0
LC-10-034	0.30	0	Chlorite	9.225999832	20.48500061	0	0	0	0	0.333000004	0
LC-10-035	0.20	0	Chlorite	10.63599968	33.81200027	0	0	0	0	0.293000013	0
LC-10-036	0.20	0	Chlorite	6.357999802	25.07999992	0	0	0	0	0.209999993	0
LC-10-039	0.10	0	Chlorite	2.207000017	28.18600082	0	0	0	0	0.209999993	0
LC-10-040	0.10	0	Chlorite	5.802999973	28.62100029	0	0	0	0	0.174999997	0
LC-10-043	0.20	0	Chlorite	6.21999979	40.37400055	0	0	0	0	0.231999993	0
LC-10-044	0.20	0	Chlorite	7.327000141	28.71800041	0	0	0	0	0.245000005	0
LC-10-045	0.10	0	Chlorite	5.818999767	27.63199997	0	0	0	0	0.213	0
LC-10-046	0.20	0	Sericite	0	18.95599937	0	0	0	0	0.244000003	0
LC-10-047	0.20	0	Calcite	16.9489994	31.72999954	0	0	0	0	0.282999992	0
LC-10-048	0.30	0	Calcite	45.00500107	5.795000076	0	0	0	0	0.270000011	0
LC-10-049B	0.20	0	Chlorite	12.38300037	24.58099937	0	0	0	0	0.275000006	0
LC-10-050	0.20	0	Chlorite	6.514999866	24.45999908	0	0	0	0	0.388999999	0
LC-10-051	0.10	0	Chlorite	1.504999995	27.5890007	0	0	0	0	0.223000005	0
LC-10-053	0.30	0	Chlorite	7.653999805	21.32699966	0	0	0	0	0.180999994	0
LC-10-056	0.20	0	Chlorite	3.555999994	31.87400055	0	0	0	0	0.209000006	0
LC-10-058	0.10	0	Chlorite	2.575999975	39.45800018	0	0	0	0	0.197999999	0
LC-10-062	0.20	0	Chlorite	6.767000198	32.25600052	0	0	0	0	0.238999993	0

Samples	BORNITE	BRUCITE	CALCITE	CHALCOCITE	CHALCOPYR	CHL_FE	CHL_MG	CHLORITE	CHROMITE	CO2	DENSITE
LC-10-002	0	0	0	0	0	6.743000031	10.04399967	16.78700066	0.023	0	3.002000093
LC-10-003	0	0	0.005	0	0	4.366000175	6.096000195	10.46199989	0.022	0.004	2.905999899
LC-10-004	0	0	0	0	0	6.441999912	10.69299984	17.13500023	0.023	0	2.917000055
LC-10-006	0	0	0.014	0	0	4.34100008	4.492000103	8.833000183	0.023	0.011	3.028000116
LC-10-007	0	0	0	0	0	10.26799965	13.72799969	23.99600029	0.012	0	2.996000051
LC-10-008	0	0	0	0	0	3.611000061	5.972000122	9.583000183	0.033	0	2.924000025
LC-10-010	0	0	0	0	0	8.55700016	12.86400032	21.42099953	0.011	0	2.885999918
LC-10-011	0	0	0	0	0	6.130000114	7.965000153	14.09399986	0.034000002	0	2.944999933
LC-10-012	0	0	0	0	0	7.660999775	9.241999626	16.90299988	0.022	0	2.969000101
LC-10-013	0	0	0.012	0	0	3.946000099	5.083000183	9.029000282	0.023	0.009	3.005000114
LC-10-015	0	0	0	0	0	12.66699982	18.55599976	31.22299957	0.035	0	2.980000019
LC-10-016	0	0	0.008	0	0	6.178999901	4.622000217	10.80099964	0.035	0.006	2.959000111
LC-10-017	0	0	0.002	0	0	6.027999878	7.111999989	13.14099979	0.034000002	0.002	2.917999983
LC-10-018	0	0	0	0	0	6.945000172	7.190999985	14.13599968	0.034000002	0	2.867000103
LC-10-019	0	0	0	0	0	11.03600025	15.07400036	26.11100006	0.046	0	2.881000042
LC-10-020	0	0	0.138999999	0	0	5.587999821	2.176000118	7.763999939	0.006	0.107000001	2.743999958
LC-10-021	0	0	0	0	0	11.52299976	11.63199997	23.15500069	0.012	0	2.884000063
LC-10-025	0	0	0.001	0	0	5.585000038	6.785999775	12.37100029	0.035	0.001	2.88499999
LC-10-026A	0	0	0	0	0	9.331999779	5.662000179	14.99400043	0.006	0	2.851000071
LC-10-026B	0	0	0	0	0	7.06400013	4.416999817	11.48099995	0.006	0	2.845000029
LC-10-028	0	0	0.008	0	0	6.328000069	9.524999619	15.85200024	0.011	0.006	2.878000021
LC-10-030	0	0	2.875	0	0	0	0	0	0.034000002	2.209000111	2.986999989
LC-10-031	0	0	0.006	0	0	4.357999802	5.367000103	9.725000381	0.034000002	0.005	2.99000001
LC-10-032	0	0	2.851000071	0	0	0	0	0	0.035	2.154999971	3.105000019
LC-10-033	0	0	0	0	0	11.92199993	6.552999973	18.47500038	0.006	0.001	2.890000105
LC-10-034	0	0	0.001	0	0	6.329999924	9.954999924	16.28499985	0.034000002	0	3.006000042
LC-10-035	0	0	0.007	0	0	3.165999889	5.272999763	8.437999725	0.034000002	0.005	3.002000093
LC-10-036	0	0	0	0	0	5.190999985	5.892000198	11.08399963	0.011	0	2.989000082
LC-10-039	0	0	0	0	0	6.368999958	9.892999649	16.26199913	0.011	0	2.898000002
LC-10-040	0	0	0	0	0	2.426000118	3.796999931	6.22300005	0.011	0	2.933999922
LC-10-043	0	0	0	0	0	4.297999859	6.612999916	10.90999985	0.033	0	2.924999952
LC-10-044	0	0	0	0	0	5.31400013	7.556000233	12.86999989	0.034000002	0	2.980999947
LC-10-045	0	0	0.579999983	0	0	6.092999935	6.202000141	12.29500008	0.023	0.442999989	2.926000118
LC-10-046	0	0	0	0	0	10.93000031	19.07500076	30.00499916	0.023	0	2.903000116
LC-10-047	0	0	3.710999966	0	0	0	0	0	0.034000002	2.799999952	3.066999912
LC-10-048	0	0	6.005000114	0	0	0	0	0	0.061000001	4.152999878	3.36500001
LC-10-049B	0	0	0.008	0	0	6.436999798	4.609000206	11.04699993	0.035	0.006	3.04399991
LC-10-050	0	0	0.005	0	0	6.96600008	7.852000237	14.81900024	0.034000002	0.004	2.969000101
LC-10-051	0	0	0	0	0	7.156000137	10.56599998	17.72100067	0.011	0	2.923000097
LC-10-053	0	0	0	0	0	5.385000229	9.432999611	14.81799984	0.023	0	3.006999969
LC-10-056	0	0	0	0	0	5.572999954	8.126999855	13.69999981	0.023	0	2.900000095
LC-10-058	0	0	0.363999993	0	0	5.586999893	8.133999825	13.72099972	0.023	0.282999992	2.878999949
LC-10-062	0	0	0	0	0	4.322000027	6.086999893	10.4099985	0.034000002	0	2.986000061

Samples	DIASPORE	DOLOMITE	EPIDOTE	FERAT_CALC	GAF	GALENE	H2OM	H2OP	HAL_SYLV	HEMATITE	IAB
LC-10-002	0	0	36.04700089	0.158999994	0	0	0.018999999	2.71600008	0	0	19.29299927
LC-10-003	0	0	21.57699966	0.165999994	0	0	0.014	1.888000011	0	0	45.93899918
LC-10-004	0	0	27.91300011	0.152999997	0	0	0.017000001	2.503000021	0	0	30.36899948
LC-10-006	0	0	33.60800171	0.173999995	0	0	0.016000001	2.059999943	0	0	26.1060009
LC-10-007	0	0	33.41199875	0.157000005	0	0	0.022	3.319000006	0	0	18.46699905
LC-10-008	0	0	28.40800095	0.163000003	0	0	0.014	1.871999979	0	0	36.72399902
LC-10-010	0	0	24.30900002	0.150000006	0	0	0.017999999	2.753999949	0	0	28.95700073
LC-10-011	0	0	31.89000017	0.159999996	0	0	0.016000001	2.315000057	0	0	29.70100021
LC-10-012	0	0	32.54299927	0.159999996	0	0	0.017999999	2.631999969	0	0	26.8220005
LC-10-013	0	0	30.57799911	0.172000006	0	0	0.016000001	2.042000055	0	0	31.8239994
LC-10-015	0	0	31.99900055	0.150000006	0	0	0.025	3.915999889	0	0	16.51300049
LC-10-016	0	0	27.35499954	0.170000002	0	0	0.015	1.993999958	0	0	30.74099922
LC-10-017	0	0	21.99399948	0.165000007	0	0	0.015	2.132999897	0	0	39.16799927
LC-10-018	0	0	19.0739994	0.163000003	0	0	0.014	2.061000109	0	0	43.93999863
LC-10-019	0	0	22.1760006	0.149000004	0	0	0.018999999	3.142999887	0	0	27.88100052
LC-10-020	0	0	11.52000046	0.180999994	0	0	0.009	1.317999959	0	0	44.27099991
LC-10-021	0	0	26.22500038	0.180999994	0	0	0.017999999	2.842000008	0	0	17.23500061
LC-10-025	0	0	19.20199966	0.164000005	0	0	0.013	1.927999973	0	0	36.3370018
LC-10-026A	0	0	24.41799927	0.182999998	0	0	0.014	2.04399991	0	0	26.31999969
LC-10-026B	0	0	25.97100067	0.182999998	0	0	0.012	1.69799954	0	0	31.00900078
LC-10-028	0	0	24.65999985	0.153999999	0	0	0.015	2.346999884	0	0	38.7179985
LC-10-030	0	0	25.17499924	0.185000002	0	0	0.011	1.182999969	0	0	44.91600037
LC-10-031	0	0	22.33600044	0.172999993	0	0	0.015	2.032999992	0	0	42.29000092
LC-10-032	2.414999962	0	30.7688991	0.185000002	0	0	0.014	1.77100028	0	0.063000001	28.68499947
LC-10-033	0	0	16.36499977	0.164000005	0	0	0.015	2.371999979	0	0	43.1570015
LC-10-034	0	0	23.77099991	0.165000007	0	0	0.018999999	2.68600109	0	0	25.09600067
LC-10-035	0	0	21.88400078	0.172999993	0	0	0.015	2.002000093	0	0	41.1269989
LC-10-036	0	0	34.82899857	0.165999994	0	0	0.016000001	2.177000046	0	0	24.10000038
LC-10-039	0	0	28.05200005	0.152999997	0	0	0.016000001	2.35800004	0	0	28.61400032
LC-10-040	0	0	28.82600021	0.171000004	0	0	0.012	1.565999985	0	0	32.27299881
LC-10-043	0	0	24.06200027	0.165000007	0	0	0.015	2.005000114	0	0	41.90200043
LC-10-044	0	0	29.81900024	0.166999996	0	0	0.017000001	2.329999924	0	0	29.20199966
LC-10-045	0	0	26.21999931	0.165999994	0	0	0.015	2.094000101	0	0	31.74099922
LC-10-046	0	0	27.90800095	0.181999996	0	0	0.022	3.563999891	0	0	18.07500076
LC-10-047	0	0	27.73600006	0.185000002	0	0	0.012	1.307999969	0	0	38.99900055
LC-10-048	5.515999794	0	11.49400043	0.182999998	-0.013	0	0.017000001	2.203999996	0	0.024	10.12899971
LC-10-049B	0	0	28.13199997	0.172999993	0	0	0.017000001	2.191999912	0	0	28.37100029
LC-10-050	0	0	27.8409996	0.165000007	0	0	0.017000001	2.436000109	0	0	26.90399933
LC-10-051	0	0	33.05500031	0.150999993	0	0	0.017000001	2.562000036	0	0	25.87899971
LC-10-053	0	0	30.3560009	0.164000005	0	0	0.018999999	2.608999968	0	0	22.60899925
LC-10-056	0	0	26.04800034	0.158999994	0	0	0.015	2.142999887	0	0	32.86299896
LC-10-058	0	0	25.14100075	0.155000001	0	0	0.014	2.128000021	0	0	40.2000076
LC-10-062	0	0	32.83599854	0.166999996	0	0	0.016000001	2.135999918	0	0	31.06800079

Samples	ICD	ICHLO	IFRAIS	IOR	IPAF	IPARA	IPYRO	ISER	K_CANCRIN	MAGNESITE	MAGNETITE
LC-10-002	0	0	100	2.697999954	-31.06211472	0	0	0	0	0	0
LC-10-003	0.026000001	0	100	3.068000078	-59.12763596	0	0	0	0	0	0
LC-10-004	0	0	96.89499664	3.131999969	-46.65918732	2.815000057	0	0.289999992	0	0	0
LC-10-006	0.061999999	0	100	1.226999998	-54.35243225	0	0	0	0	0	0
LC-10-007	0	0	94.6230011	2.417999983	-42.07942963	4.755000114	0	0.621999979	0	0	0
LC-10-008	0	0	100	2.52699995	-66.42284393	0	0	0	0	0	0
LC-10-010	0	0	89.23699951	2.457999945	-33.9085083	9.920999527	0	0.842000008	0	0	0
LC-10-011	0	0	99.05999756	1.572999954	-70.75311279	0.893000007	0	0.046999998	0	0	0
LC-10-012	0	0	98.98999786	3	-42.23004532	0.907999992	0	0.101999998	0	0	0
LC-10-013	0.052999999	0	100	1.539000034	-59.10498428	0	0	0	0	0	0
LC-10-015	0	0	85.47499847	5.227000237	-15.97915554	11.03299999	0	3.492000103	0	0	0.115999997
LC-10-016	0.045000002	0	100	2.272000074	-52.26973343	0	0	0	0	0	0.059999999
LC-10-017	0.013	0	100	2.105000019	-56.32789612	0	0	0	0	0	0.039999999
LC-10-018	0	0	98.12799835	3.736999989	-27.83048439	1.725000024	0	0.147	0	0	0
LC-10-019	0	0	82.76000214	5.144999981	-28.28632327	14.5539999	0	2.666000109	0	0	0
LC-10-020	0	0	84.91500092	6.031000137	3.595999956	13.27600002	0	1.809000015	0	0	0
LC-10-021	0	0	79.11299896	9.201999864	-8.6980896	13.61699963	0	7.269999981	0	0	0
LC-10-025	0.008	0	100	1.912999888	-64.47677612	0	0	0	0	0	0.059
LC-10-026A	0	0	80.53700256	1.843999982	-13.8183651	18.18899918	0	1.274000049	0	0	0
LC-10-026B	0	0	92.27899933	2.075000048	-15.64500618	7.236999989	0	0.483999997	0	0	0
LC-10-028	0	0	96.2460022	5.035999775	0.068000004	3.322000027	0	0.432000011	0	0	0
LC-10-030	13.35099983	0	100	2.273000002	-59.68192673	0	0	0	0	0	0.135000005
LC-10-031	0.027000001	0	100	2.063999891	-75.97740936	0	0	0	0	0	0.446999997
LC-10-032	11.08699989	0	100	1.600999951	-46.46712112	0	0	0	0	0	0.437999994
LC-10-033	0	0	91.80999756	4.025000095	-36.89257431	7.491000175	0	0.699000001	0	0	0
LC-10-034	0.002	0	100	7.044000149	-47.34615326	0	0	0	0	0	0.785000026
LC-10-035	0.028999999	0	100	3.697000027	-37.18411636	0	0	0	0	0	0.282999992
LC-10-036	0	0	100	7.459000111	-43.16924286	0	0	0	0	0	0.361999989
LC-10-039	0	0	95.26300049	5.84100008	-20.46155548	3.934000015	0	0.802999973	0	0	0
LC-10-040	0	0	100	3.654000044	-62.76743698	0	0	0	0	0	0
LC-10-043	0	0	100	4.760000229	-42.40502167	0	0	0	0	0	0
LC-10-044	0	0	100	6.548999786	-34.98730469	0	0	0	0	0	0
LC-10-045	0.044	0	100	3.673000097	4.833000183	0	0	0	0	0	0
LC-10-046	14.48799992	0	71.65399933	4.438000202	-8.442141533	22.75900078	0	5.587999821	0	0	0
LC-10-047	15.53800011	0	100	1.817000031	-54.08493805	0	0	0	0	0	0.691999972
LC-10-048	0	0	100	7.008999825	-95.38038635	0	0	0	0	0	4.934999943
LC-10-049B	0.037	0	100	4.124000072	-37.82597351	0	0	0	0	0	0.730000019
LC-10-050	0.023	0	100	5.743000031	-44.88012695	0	0	0	0	0	0
LC-10-051	0	0	93.08399963	3.555000067	-28.45751572	6.080999851	0	0.834999979	0	0	0
LC-10-053	0	0	100	7.438000202	-43.26870728	0	0	0	0	0	0
LC-10-056	0	0	99.57900238	7.144999981	-25.99720192	0.345999986	0	0.075000003	0	0	0
LC-10-058	0	0	99.5510025	1.876000047	3.434999943	0.42899999	0	0.02	0	0	0
LC-10-062	0	0	100	4.276000023	-30.42764091	0	0	0	0	0	0

Samples	MANGANITE	MILLERITE	MOLYBDEN	NA_CANCRIN	ORTHOSE	PAF_100	PAF_CALC	PAF_MAX	PAF_MIN	PARAGONITE	PENTLAND
LC-10-002	0	0	0	0	2.72300005	1.690999985	2.734999895	0	2.734999895	0	0
LC-10-003	0	0	0	0	2.802000046	0.819000006	1.904999971	0	1.904999971	0	0
LC-10-004	0	0	0	0	3.052000046	1.016000032	2.519999981	0	2.519999981	0	0
LC-10-006	0	0	0	0	1.116999984	1.149000049	2.086999893	0	2.086999893	0	0
LC-10-007	0	0	0	0	2.427999973	1.565000057	3.342000008	0	3.342000008	0	0
LC-10-008	0	0	0	0	2.461999893	0.690999985	1.886000037	0	1.886000037	0	0
LC-10-010	0	0	0	0	2.211999893	1.547999978	2.770999908	0	2.770999908	0	0
LC-10-011	0	0	0	0	1.585000038	0.512000024	2.33100009	0	2.33100009	0	0
LC-10-012	0	0	0	0	3.082999945	1.190999985	2.650000095	0	2.650000095	0	0
LC-10-013	0	0	0	0	1.409999967	1.003999949	2.066999912	0	2.066999912	0	0
LC-10-015	0	0	0	0	5.572999954	2.957000017	3.940999985	0	3.940999985	0	0
LC-10-016	0	0	0	0	1.929999948	1.042999983	2.015000105	0	2.015000105	0	0
LC-10-017	0	0	0	0	1.777999997	0.808000028	2.150000095	0	2.150000095	0	0
LC-10-018	0	0	0	0	3.240999937	1.333999991	2.073999882	0	2.073999882	0	0
LC-10-019	0	0	0	0	4.712999821	2.03399992	3.161999941	0	3.161999941	0	0
LC-10-020	0	0	0	0	4.994999886	1.414999962	1.434000015	5.853000164	1.248999953	4.383999825	0
LC-10-021	0	0	0	0	8.847000122	2.522000074	2.859999895	0	2.859999895	0.158999994	0
LC-10-025	0	0	0	0	1.36500001	0.55400002	1.942000031	0	1.942000031	0	0
LC-10-026A	0	0	0	0	1.699000001	1.644999981	2.058000088	0	2.058000088	1.105000019	0
LC-10-026B	0	0	0	0	1.856999993	1.31400001	1.710000038	0	1.710000038	0.125	0
LC-10-028	0	0	0	0	5.171000004	2.312000036	2.368999958	13.25199986	2.305000067	0	0
LC-10-030	0	0	0	0	1.881000042	0.430000007	3.403000116	0	3.403000116	0	0
LC-10-031	0	0	0	0	1.753000021	0.528999984	2.052000046	0	2.052000046	0	0
LC-10-032	0	0	0	0	1.496000051	1.998000026	3.940999985	0	3.940999985	0	0
LC-10-033	0	0	0	0	3.384000063	1.324000001	2.387000084	0	2.387000084	0	0
LC-10-034	0	0	0	0	5.75	1.414999962	2.70600009	0	2.70600009	0	0
LC-10-035	0	0	0	0	3.039000034	1.347000003	2.023000002	0	2.023000002	0	0
LC-10-036	0	0	0	0	7.762000084	1.383000016	2.194000006	0	2.194000006	0	0
LC-10-039	0	0	0	0	5.752999783	1.730999947	2.374000072	0	2.374000072	0	0
LC-10-040	0	0	0	0	3.240999937	0.736999989	1.578999996	0	1.578999996	0	0
LC-10-043	0	0	0	0	4.585999966	1.269999981	2.019000053	0	2.019000053	0	0
LC-10-044	0	0	0	0	6.440000057	1.674999952	2.346999884	0	2.346999884	0	0
LC-10-045	0	0	0	0	3.197000027	2.548000097	2.552000046	13.92500019	1.970000029	0	0
LC-10-046	0	0	0	0	4.653999805	3.186000109	3.585999966	0	3.585999966	0.225999996	0
LC-10-047	0	0	0	0	1.478000045	0.962000012	4.119999886	0	4.119999886	0	0
LC-10-048	0	0	0	0	4.010000229	0.528999984	6.361000061	0	6.361000061	0	0
LC-10-049B	0	0	0	0	3.572999954	1.496000051	2.214999914	0	2.214999914	0	0
LC-10-050	0	0	0	0	5.221000195	1.24000001	2.457000017	0	2.457000017	0	0
LC-10-051	0	0	0	0	3.789999962	1.57099998	2.578999996	0	2.578999996	0	0
LC-10-053	0	0	0	0	7.015999794	1.65199995	2.627000093	0	2.627000093	0	0
LC-10-056	0	0	0	0	6.929999828	1.444000006	2.157999992	0	2.157999992	0	0
LC-10-058	0	0	0	0	1.840999961	2.411999941	2.42600018	12.94799995	2.036999941	0	0
LC-10-062	0	0	0	0	4.43900013	1.680999994	2.15199995	0	2.15199995	0	0

Samples	PSILOMELAN	PYRITE	PYROPHIL	PYRRHOTITE	QUARTZ	RODOCHROS	S	SERICITE	SERPENTINE	SIDERITE	SMAG_CALC
LC-10-002	0	0	0.072999999	0	9.758000374	0	0	0	0	0	0
LC-10-003	0	0	0.07	0	6.303999901	0	0	0	0	0	0
LC-10-004	0	0	0.061000001	0	12.2159996	0	0	0	0	0	0
LC-10-006	0	0	0.079999998	0	9.494000435	0	0	0	0	0	0
LC-10-007	0	0	0.093000002	0	8.729000092	0	0	0	0	0	0
LC-10-008	0	0	0.046	0	9.758000374	0	0	0	0	0	0
LC-10-010	0	0	0.07	0	19.75399971	0	0	0	0	0	0
LC-10-011	0	0	0.059999999	0	11.81099987	0	0	0	0	0	0
LC-10-012	0	0	0.074000001	0	7.630000114	0	0	0	0	0	0
LC-10-013	0	0	0.074000001	0	6.260000229	0	0	0	0	0	0
LC-10-015	0	0	0.103	0	4.603000164	0	0	0	0	0	0
LC-10-016	0	0	0.141000003	0	17.88899994	0	0	0	0	0	1.131000042
LC-10-017	0	0	0.150000006	0	14.30300045	0	0	0	0	0	0.588999987
LC-10-018	0	0	0.150999993	0	15.43500042	0	0	0	0	0	0.398999989
LC-10-019	0	0	0.083999999	0	16.68400002	0	0	0	0	0	0
LC-10-020	0	0	0	0	33.08399963	0	0	0.597000003	0	0	0
LC-10-021	0	0	0	0	22.93700027	0	0	0.085000001	0	0	0
LC-10-025	0	0	0.137999997	0	27.44300079	0	0	0	0	0	0.572000027
LC-10-026A	0	0	0	0	32.04700089	0	0	0.077	0	0	0
LC-10-026B	0	0	0	0	31.44599915	0	0	0.008	0	0	0
LC-10-028	0	0	0.057	0	6.796999931	0	0	0	0	0	0
LC-10-030	0	0	0.167999998	0	3.555999994	0	0	0	0	0	1.325000048
LC-10-031	0	0	0.123000003	0	4.021999836	0	0	0	0	0	4.429999828
LC-10-032	0	0	0	0	0	0	0	0	0	0	4.232999802
LC-10-033	0	0	0.179000005	0	16.77499962	0	0	0	0	0	7.617000103
LC-10-034	0	0	0.178000003	0	6.870999813	0	0	0	0	0	2.769000053
LC-10-035	0	0	0.111000001	0	1.603999972	0	0	0	0	0	3.605999947
LC-10-036	0	0	0.063000001	0	5.482999802	0	0	0	0	0	0
LC-10-039	0	0	0.057	0	14.38199997	0	0	0	0	0	0
LC-10-040	0	0	0.039999999	0	16.91600037	0	0	0	0	0	0
LC-10-043	0	0	0.057	0	2.457999945	0	0	0	0	0	0
LC-10-044	0	0	0.068999998	0	2.596999884	0	0	0	0	0	0
LC-10-045	0	0	0.075000003	0	16.69009998	0	0	0	0	0	0
LC-10-046	0	0	0	0	15.98099995	0	0	0.055	0	0	0
LC-10-047	0	0	0.185000002	0	0.493000001	0	0	0	0	0	6.671999931
LC-10-048	0	0	0	0	0	0	0	0	0	0	43.64199829
LC-10-049B	0	0	0.144999996	0	7.984000206	0	0	0	0	0	7.084000111
LC-10-050	0	0	0.092	0	10.6079998	0	0	0	0	0	0
LC-10-051	0	0	0.059	0	12.31099987	0	0	0	0	0	0
LC-10-053	0	0	0.071999997	0	3.273000002	0	0	0	0	0	0
LC-10-056	0	0	0.056000002	0	11	0	0	0	0	0	0
LC-10-058	0	0	0.052000001	0	11.50599957	0	0	0	0	0	0
LC-10-062	0	0	0.059	0	1.774000049	0	0	0	0	0	0

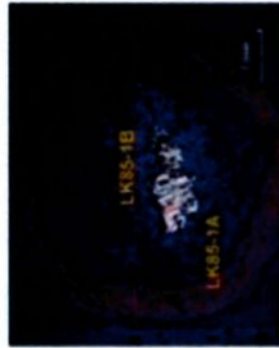| Samples	SPHALERITE	SPHENE	TALC	TOTAL	TREMOLITE
LC-10-002	0	1.55400002	0	100	8
LC-10-003	0	1.371000051	0	100	8.876000404
LC-10-004	0	1.511999965	0	100	5.171999931
LC-10-006	0	1.427000046	0	100	10.8920002
LC-10-007	0	2.444999933	0	100	5.710000038
LC-10-008	0	1.529999971	0	100	7.578000069
LC-10-010	0	1.870000005	0	100	2.447000027
LC-10-011	0	2.200000048	0	100	4.581999779
LC-10-012	0	2.2609996	0	100	5.28000021
LC-10-013	0	1.322999954	0	100	12.35099983
LC-10-015	0	2.880000114	0	100	3.355999947
LC-10-016	0	2.378999949	0	100	5.513000011
LC-10-017	0	2.321000099	0	100	6.912000179
LC-10-018	0	2.270999908	0	100	3.651000023
LC-10-019	0	2.434999943	0	100	1.062999964
LC-10-020	0	0.632000029	0	100	0
LC-10-021	0	1.708999991	0	100	0
LC-10-025	0	1.975999951	0	100	6.129000187
LC-10-026A	0	1.085999966	0	100	0
LC-10-026B	0	1.031999946	0	100	0
LC-10-028	0	1.506999969	0	100	3.572000027
LC-10-030	0	2.27600023	0	100	15.02099991
LC-10-031	0	2.394999981	0	100	12.63199997
LC-10-032	0	2.536000013	0	100	15.20800018
LC-10-033	0	2.720999956	0	100	1.537999988
LC-10-034	0	2.275000095	0	100	14.50899982
LC-10-035	0	2.063999891	0	100	17.7159996
LC-10-036	0	1.902999997	0	100	7.217000008
LC-10-039	0	1.450999975	0	100	3.427999973
LC-10-040	0	1.059999943	0	100	9.083999634
LC-10-043	0	1.496000051	0	100	9.569999695
LC-10-044	0	1.462000012	0	100	10.41800022
LC-10-045	0	1.33099997	0	100	5.922999859
LC-10-046	0	1.947999954	0	100	0
LC-10-047	0	2.069999933	0	100	14.63799953
LC-10-048	0	1.628000021	0	100	15.25699997
LC-10-049B	0	2.24000001	0	100	8.866999626
LC-10-050	0	2.673000097	0	100	7.342999935
LC-10-051	0	1.514000058	0	100	2.221999884
LC-10-053	0	1.873000026	0	100	13.40699959
LC-10-056	0	1.41900003	0	100	5.184999943
LC-10-058	0	1.368000031	0	100	3.750999928
LC-10-062	0	1.656999946	0	100	9.529999733

Appendix 6

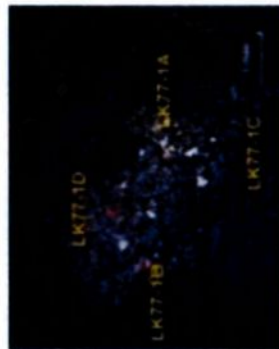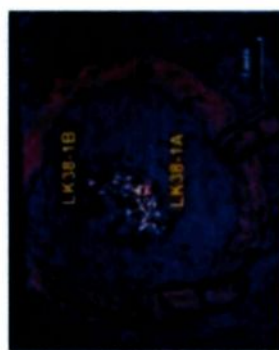Thin sections and photomicrographs from the minerals analyzed by LA-ICP-MS.

LK-10-087

LK-10-053

LK-10-043

LK-10-027

LK-10-085

LK-10-077
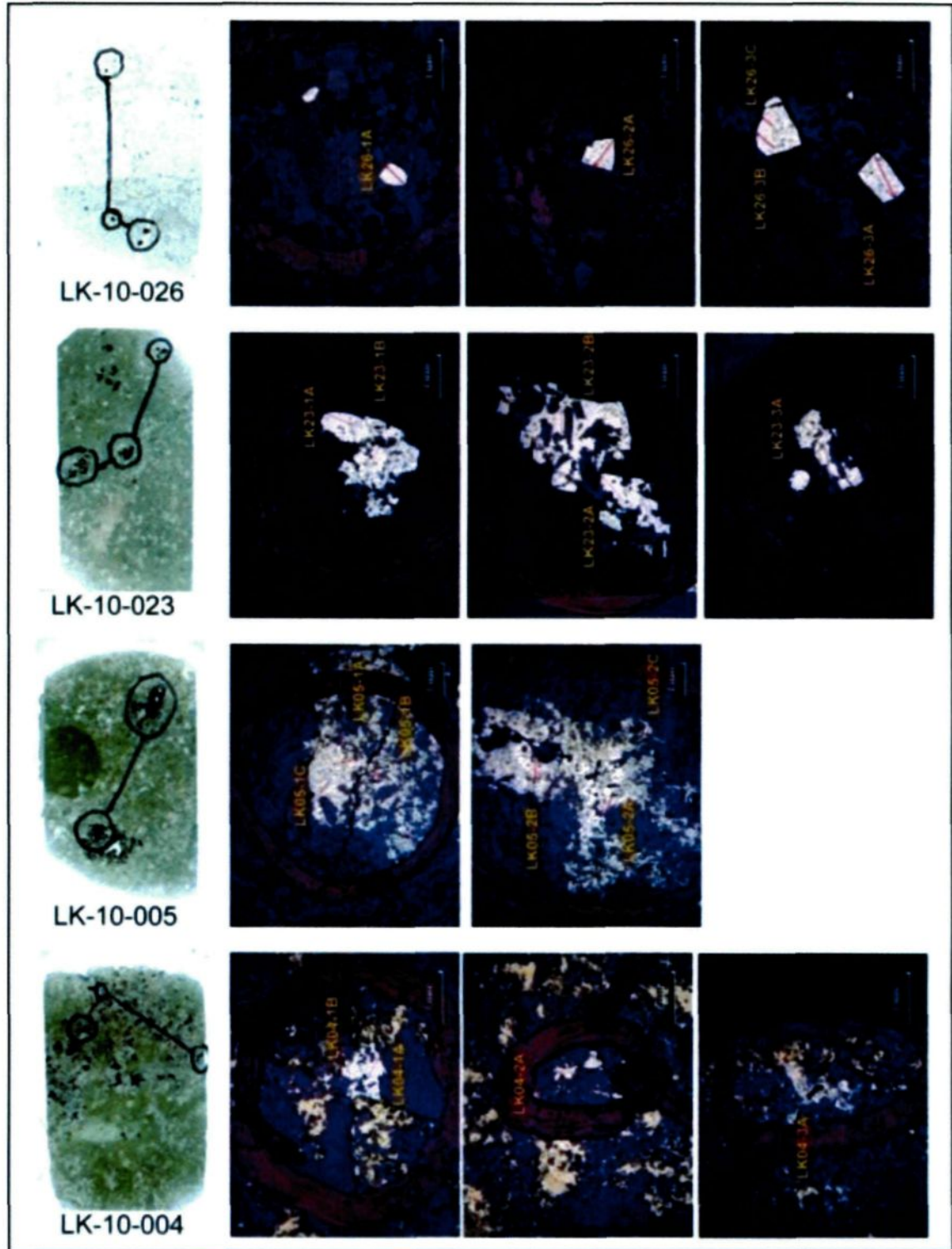
LK-10-038

LK-10-007

LK-10-026

LK-10-023

LK-10-005

LK-10-004

Appendix 7

A) Pyrites elemental data analyzed by the LA-ICP-MS.

Sample	Source	^{33}S (ppm)	^{34}S (ppm)	^{51}V (ppm)	^{52}Cr (ppm)	^{53}Cr (ppm)	^{55}Mn (ppm)	^{59}Co (ppm)	^{60}Ni (ppm)	^{65}Cu (ppm)	^{66}Zn (ppm)
LK04-1A	Monsabrais-Py1	57023.75	541376.5	814.625	0.246715	0.488775	10.161865	34.0746	67.963	202.958	763.42
LK04-3A	Monsabrais-Py1	400330	693595	15454.6	2.4206	3.812445	11.96335	66.5665	1959.755	6610.1	1917.86
LK04-2A	Monsabrais-Py1	125219.5	727576.5	11172	0.80066	2.10406	10.84615	40.54505	1303.4	85.652	140.1155
LLK04-1B	Monsabrais-Py1	394278.5	519498	619115	2.006305	2.257675	11.96335	70.756	24.206	351.918	1382.535
LK05-1A	Monsabrais-Py1	141512	631218	18620	0.609805	1.61994	11.31165	54.3704	34.447	64.7045	8.14625
LK05-1B	Monsabrais-Py1	1033410	599098.5	190855	3.64952	9.44965	19.2717	195.9755	526.015	325.85	58.653
LK05-1C	Monsabrais-Py1	457121	608408.5	684285	5.91185	9.91515	18.75965	112.1855	65.17	122.892	48.8775
LK05-2A	Monsabrais-Py1	114047.5	595840	2141.3	0.572565	1.326675	11.08821	41.47605	95.4275	134.995	875.14
LK05-2B	Monsabrais-Py1	814625	593512.5	16106.3	3.77055	7.30835	16.9442	157.339	202.4925	215.5265	1242.885
LK05-2C	Monsabrais-Py1	150822	613529	6051.5	1.81545	2.28095	12.42885	46.78275	12.8478	25.137	17.689
LK23-1A	Monsabrais-Py1	49343	553945	1019.445	0.526015	1.065995	11.09752	35.378	744.3345	1596.665	2.481115
LK23-2A	Monsabrais-Py1	43710.45	597236.5	959.3955	0.3058335	0.721525	10.18514	33.00395	884.45	2062.165	5.3998
LK23-2B	Monsabrais-Py1	48272.35	569772	884.45	0.339815	0.647045	9.984975	33.84185	6349.42	746.662	5.9584
LK23-3A	Monsabrais-Py1	51670.5	621908	954.275	0.408709	0.786695	10.7065	35.2849	1419.775	1024.1	21.413
LK23-1B	Monsabrais-Py1	46596.55	569306.5	1457.015	0.333298	0.516705	10.38065	34.30735	6870.78	381.71	2.574215
LK43-1C	Monsabrais-Py1	170373	702439.5	3365.565	0.511119	1.44305	9.69171	37.3331	809.97	10380.65	3239.88
LK43-1D	Monsabrais-Py1	65635.5	656820.5	2248.365	0.447811	0.861175	9.770845	34.49355	246.715	19737.2	2918.685
LK43-3B	Monsabrais-Py1	688940	737817.5	4422.25	0.91238	9.91515	10.40858	40.8709	605.15	293.265	456.19
LK26-1A	Monsabrais-Py2	73083.5	645183	2788.345	0.4091745	1.335985	10.23169	31.97985	122.892	350.987	6.9825
LK26-2A	Monsabrais-Py2	637735	516239.5	796005	36.82105	30.21095	39.0089	81.4625	1470.98	597.702	12.103
LK26-3A	Monsabrais-Py2	433380.5	523687.5	549290	19.03895	16.99075	26.02145	61.9115	470.155	287.2135	10.6134
LK26-3B	Monsabrais-Py2	381710	508326	2886100	49.343	9.8686	18.4338	36.6814	5492.9	1727.005	6.37735
LK26-3C	Monsabrais-Py2	323057	464103.5	307230	13.73225	34.9125	41.4295	54.8359	763.42	409.64	6.3308
LK27-1A	Monsabrais-Py2	111720	732231.5	4841.2	0.721525	2.33681	10.506335	38.31065	485.051	9961.7	13.4995
LK27-1B	Monsabrais-Py2	83324.5	780643.5	2983.855	0.639597	2.853515	10.04549	35.89005	50.7395	5595.31	9.6824
LK27-1C	Monsabrais-Py2	108927	713611.5	4943.61	0.879795	2.713865	10.17583	37.19345	62.88905	5492.9	24.99735
LK43-1AA	Monsabrais-Py2	44501.8	522291	698.25	0.2080785	0.898415	10.59478	36.6814	62.8425	78.6695	7.6342
LK43-1B	Monsabrais-Py2	37053.8	591185	1475.635	0.3905545	0.96824	9.407755	32.07295	82.859	17.17695	4.166225
LK43-2A	Monsabrais-Py2	38357.2	600029.5	1152.578	0.3765895	0.67032	9.575335	31.5609	4.23605	148.96	2.70921
LK43-3A	Monsabrais-Py2	155942.5	768075	3230.57	0.7136115	4.89706	9.957045	41.47605	32.1195	92.6345	33.0505
LK53-1A	Monsabrais-Py2	1415120	544169.5	7168.7	112.651	3.21195	12.14955	146.6325	12289.2	34353.9	1261.505
LK53-1B	Monsabrais-Py2	837900	513446.5	7541.1	39.5675	6.00495	13.54605	116.8405	2560.25	1484.945	1889.93
LK53-2A	Monsabrais-Py2	29792	578616.5	344.47	0.202027	0.49343	11.2651	35.98315	5632.55	29792	1103.235
LK77-1A	Monsabrais-Py2	229491.5	524153	18620	6.4239	3.86365	13.5926	56.791	17549.35	105.203	418.95
LK77-1B	Monsabrais-Py2	85652	522291	2653.35	1.53615	1.559425	11.77715	41.7088	11730.6	19.13205	26.5335
61-1A	Chadbourne	116840.5	647976	563255	5.3998	0.6139945	9.277415	36.0297	11.87025	14.06741	4.361735
61-1B	Chadbourne	772730	606081	1070650	10.65995	0.62377	9.333275	40.07955	115.444	20.1096	8.70485
61-1C	Chadbourne	572565	652631	14896	12.52195	0.823935	9.26345	35.23835	449.673	2881.445	61.9115
61-3A	Chadbourne	133598.5	576289	181545	4.88775	1.07996	10.11997	34.447	59.1185	34.2608	3.70538
HB2-2A	Bouchard-Hébert	42826	585133.5	1610.63	1.044582	0.67032	8.88174	31.23505	38.6365	2.751105	1596.665
HB2-4A	Bouchard-Hébert	54929	537652.5	1275.47	0.8886395	0.97755	9.00277	35.9366	26.30075	1.56408	544.635

Sample	Source	^{71}Ga (ppm)	^{72}Ge (ppm)	^{75}As (ppm)	^{82}Se (ppm)	^{95}Mo (ppm)	^{98}Mo (ppm)	^{107}Ag (ppm)	^{111}Cd (ppm)	^{115}In (ppm)	^{118}Sn (ppm)
LK04-1A	Monsabrais-Py1	23.88015	0.043757	5.44635	0.526015	106.5064	0.075411	143.374	10.7996	0.69825	0.4538625
LK04-3A	Monsabrais-Py1	9.2169	0.330505	5.80944	1.317365	137.788	0.2592835	251.37	32.81775	0.71687	0.0972895
LK04-2A	Monsabrais-Py1	6.8894	0.07867	5.87461	37.7055	210.8715	0.056791	41.895	1.34995	0.0442225	0.0014431
LLK04-1B	Monsabrais-Py1	33.0505	0.080532	5.497555	0.57722	128.478	0.1214955	229.026	15.12875	1.07065	0.86583
LK05-1A	Monsabrais-Py1	4.14295	0.069825	4.38501	5.26015	40.26575	0.00931	0.04655	0.145236	0.100548	0.0071222
LK05-1B	Monsabrais-Py1	40.033	0.296058	4.426905	26.5335	45.3397	0.023275	13.034	1.16375	0.60515	0.056791
LK05-1C	Monsabrais-Py1	17.689	0.213665	4.33846	4.585175	48.5051	0.0851865	0.3724	0.628425	0.0898415	0.0127082
LK05-2A	Monsabrais-Py1	13.4995	0.078204	4.2826	7.02905	34.0746	0.0093566	117.7715	0.702905	0.16758	0.0071222
LK05-2B	Monsabrais-Py1	17.2235	0.44688	4.408285	9.91515	37.3331	0.066101	97.2895	1.34995	0.265335	0.028861
LK05-2C	Monsabrais-Py1	9.7755	0.144305	4.40363	8.14625	34.0746	0.00931	14.4305	0.159201	0.11172	0.014896
LK23-1A	Monsabrais-Py1	6.19115	0.061446	5.460315	32.35225	54.23075	0.0619115	6.00495	0.0069825	0.0702905	0.001862
LK23-2A	Monsabrais-Py1	69.3595	0.035518	5.25084	70.2905	69.1733	0.0105669	31.1885	0.0553945	0.162925	0.0256025
LK23-2B	Monsabrais-Py1	11.6375	0.064705	5.24153	337.953	65.5424	0.0131271	13.034	0.06517	0.28861	0.006936
LK23-3A	Monsabrais-Py1	158.27	0.144305	5.586	41.1502	51.5774	0.070756	42.826	0.423605	4.70155	0.20482
LK23-1B	Monsabrais-Py1	0.79135	0.033516	5.329975	519.498	46.1776	0.0026534	13.034	0.0498085	0.056791	0.001862
LK43-1C	Monsabrais-Py1	165.2525	0.082859	5.869955	2090.095	38.96235	0.159201	493.8955	14.2443	6.7032	6.251665
LK43-1D	Monsabrais-Py1	269.99	0.078204	5.767545	1647.87	37.56585	0.0442225	451.0695	12.9409	9.6824	10.56685
LK43-3B	Monsabrais-Py1	25.6025	0.127082	5.832715	130.8055	18.8993	0.31654	36.7745	9.07725	0.805315	0.395675
LK26-1A	Monsabrais-Py2	15.827	0.057722	5.80944	1.605975	0.82859	0.0237405	10.7065	0.0330505	0.24206	0.017689
LK26-2A	Monsabrais-Py2	6.47045	0.70756	5.460315	13.3133	1.29409	0.0218785	26.5335	0.2434565	0.0833245	0.0053067
LK26-3A	Monsabrais-Py2	4.5619	0.44176	5.255495	9.2169	1.065995	0.0339815	16.15285	0.154546	0.088445	0.006005
LK26-3B	Monsabrais-Py2	7.5411	0.246715	5.32532	35.378	2.6999	0.036309	27.93	0.1429085	0.237405	0.04655
LK26-3C	Monsabrais-Py2	7.7273	0.35378	4.82258	7.49455	0.40964	0.0265335	12.5685	0.116375	0.265335	0.05586
LK27-1A	Monsabrais-Py2	32.585	0.161994	6.21908	16.1994	29.55925	0.1112545	44.688	0.358435	3.1654	0.149891
LK27-1B	Monsabrais-Py2	28.861	0.114513	6.25632	2.5137	35.79695	0.072618	26.999	0.218785	1.72235	0.0619115
LK27-1C	Monsabrais-Py2	80.066	0.30723	5.84668	11.7306	22.76295	0.170373	32.585	0.339815	3.58435	0.1522185
LK43-1AA	Monsabrais-Py2	29.792	0.047947	4.529315	33.516	9.31	0.0190855	8.9376	0.052136	0.78204	0.062377
LK43-1B	Monsabrais-Py2	1.010135	0.032725	5.64186	29.18685	18.7131	0.0080532	-0.32585	0.0205286	0.0600495	0.0035378
LK43-2A	Monsabrais-Py2	12.7547	0.032725	5.39049	161.5285	35.378	0.0544635	17.64245	0.035378	0.19551	0.0042826
LK43-3A	Monsabrais-Py2	20.482	0.086583	5.879265	180.1485	24.3922	0.0349125	17.689	0.8379	0.498085	0.01862
LK53-1A	Monsabrais-Py2	200.165	16.52525	5.441695	148.4945	188.993	0.11172	126.1505	3.91951	0.88445	0.154546
LK53-1B	Monsabrais-Py2	102.41	3.39815	4.417595	591.185	194.1135	0.1438395	142.443	3.3516	2.00165	0.0488775
LK53-2A	Monsabrais-Py2	9.7755	0.063774	4.42225	44.2225	151.2875	-0.0061772	162.925	2.28095	0.0321195	0.0190855
LK77-1A	Monsabrais-Py2	10.241	0.206217	4.175535	21.413	11.68405	0.015827	111.72	0.442225	0.043757	0.0064239
LK77-1B	Monsabrais-Py2	22.344	0.077273	4.184845	26.5335	10.84615	0.004655	3.724	0.080066	0.039102	0.0033516
61-1A	Chadbourne	-0.03259	0.432915	7.00112	2.46715	27.51105	0.089376	39.102	0.1112545	0.1047375	0.0031654
61-1B	Chadbourne	2.37405	0.944965	6.894055	2.713865	40.91745	0.1084615	81.4625	0.460845	0.094031	0.0037706
61-1C	Chadbourne	48.8775	2.099405	6.8894	37.19345	64.19245	1.969065	35.8435	2.37405	0.95893	0.0470155
61-3A	Chadbourne	1.12651	0.563255	6.624065	2.36474	28.5817	0.097755	64.7045	0.1233575	0.0851865	0.054929
HB2-2A	Bouchard-Hébert	302.575	0.358435	7.09422	112.651	68.894	0.0740145	386.365	68.4285	1.62925	0.451535
HB2-4A	Bouchard-Hébert	7.7273	0.053998	6.92664	57.2565	28.0231	0.0591185	86.583	9.4031	0.1559425	0.0889105

Sample	Source	121Sb (ppm)	125Te (ppm)	182W (ppm)	184W (ppm)	195Pt (ppm)	197Au (ppm)	200Hg (ppm)	202Hg (ppm)	208Pb (ppm)	209Bi (ppm)
LK04-1A	Monsabrais-Py1	0.043292	0.058188	2.50439	0.0060981	0.0045619	-0.0035378	0.0099617	0.488775	9216.9	111.72
LK04-3A	Monsabrais-Py1	0.24206	0.096359	3.77055	0.025137	0.0162925	-0.0010707	0.0330505	0.7448	20621.65	404.985
LK04-2A	Monsabrais-Py1	0.096359	0.038171	80.066	0.023275	0.0190855	0.023275	0.14896	0.526015	32.585	20.0165
LLK04-1B	Monsabrais-Py1	0.200165	0.085187	2.10406	0.032585	0.047481	0	0.004655	0.516705	17270.05	157.339
LK05-1A	Monsabrais-Py1	0.094497	0.081928	1.7735555	0.029792	0.0358435	0.006517	0.0088445	0.674975	5.1205	11.12545
LK05-1B	Monsabrais-Py1	0.302575	0.23275	13.6857	0.17689	0.190855	0.007448	0.432915	0.68894	64.7045	39.14855
LK05-1C	Monsabrais-Py1	0.8379	0.278835	3.831065	0.35378	0.41895	0	0.017689	0.33516	36.7745	36.82105
LK05-2A	Monsabrais-Py1	0.078204	0.106134	3.170055	0.01862	0.0144305	0.0031189	0.17689	0.44688	21.8785	17.5959
LK05-2B	Monsabrais-Py1	0.40964	0.349125	6.56355	0.041895	0.038171	-0.0069825	0.1335985	0.349125	66.5665	29.8851
LK05-2C	Monsabrais-Py1	0.134995	0.047481	2.93265	0.010241	0.013965	0.0023275	0.0265335	0.377055	4.1895	6.9825
LK23-1A	Monsabrais-Py1	-0.00047	0.010893	1.21961	-0.000791	-0.0053998	-0.0015827	0.0017224	0.58653	6.0515	0.386365
LK23-2A	Monsabrais-Py1	0.064239	0.088445	1.75959	0.0058188	-0.000372	0.0039102	0.0053998	0.609805	59.1185	0.628425
LK23-2B	Monsabrais-Py1	0.040033	0.056791	19.03895	0.0020948	0.012103	0.0054464	0.0073084	0.507395	46.55	1.540805
LK23-3A	Monsabrais-Py1	0.22344	0.87514	1.49891	0.11172	0.073549	0.0079135	0.013965	0.516705	242.06	0.98686
LK23-1B	Monsabrais-Py1	0.004655	0.033516	1.252195	0.0013034	0.0016758	-0.0010241	0.0077273	0.49343	13.4995	2.28095
LK43-1C	Monsabrais-Py1	3.5378	10.1479	2.732485	0.013965	0.034447	0.0032585	0.300713	0.563255	81.4625	247.1805
LK43-1D	Monsabrais-Py1	8.70485	8.8445	2.99782	0.020482	0.019551	0.00135	0.37655895	0.44688	75.411	242.991
LK43-3B	Monsabrais-Py1	0.460845	0.81928	5.53945	0.1280125	0.120099	0.019551	0.0628425	0.94962	20.482	40.964
LK26-1A	Monsabrais-Py2	0.072153	0.051205	1.43374	0.016758	0.0153615	0.0013965	0.010241	0.553945	32.585	0.21413
LK26-2A	Monsabrais-Py2	0.432915	0.064705	1.862	1.1172	1.056685	-0.0062377	0.0228095	0.581875	14.896	16.1063
LK26-3A	Monsabrais-Py2	0.39102	0.047016	1.754935	0.498085	0.507395	-0.0040033	0.0137788	0.53067	22.8095	12.1961
LK26-3B	Monsabrais-Py2	1.01479	0.049809	1.782865	3.39815	3.4447	0.0004655	0.011172	0.526015	32.1195	5.8653
LK26-3C	Monsabrais-Py2	0.200165	0.079135	1.401155	0.404985	0.432915	-0.00027	0.014896	0.265335	11.6375	12.80125
LK27-1A	Monsabrais-Py2	0.79135	0.33516	5.711685	0.072618	0.080997	0.0153615	0.0175028	0.600495	163.856	1.05203
LK27-1B	Monsabrais-Py2	0.516705	0.228095	14.75635	0.063308	0.034447	0.005586	0.014896	0.553945	125.685	0.69825
LK27-1C	Monsabrais-Py2	0.64239	0.414295	11.3582	0.0749455	0.06517	0.014384	0.019551	0.3849685	293.265	1.88993
LK43-1AA	Monsabrais-Py2	0.040499	0.084256	2.46715	0.0097755	0.0451535	0.0047947	0.000931	1.894585	60.515	0.57722
LK43-1B	Monsabrais-Py2	0.003724	0.015222	2.555595	0.0041895	0.005074	-0.0025603	0.0033982	0.656355	0.13965	0.137788
LK43-2A	Monsabrais-Py2	0.012103	0.024206	3.21195	0.0007914	0.0055395	-0.0052136	0.0014431	0.544635	7.30835	0.244853
LK43-3A	Monsabrais-Py2	0.169442	0.13965	3.570385	0.0768075	0.081928	0.005586	0.021413	0.82859	49.343	6.19115
LK53-1A	Monsabrais-Py2	0.758765	0.12103	18.0614	0.0931	0.11172	-0.012103	0.1214955	1.17306	29.792	8.8445
LK53-1B	Monsabrais-Py2	0.591185	0.172235	11.3582	0.0833245	0.134995	0.0041895	0.0423605	0.982205	55.3945	5.8653
LK53-2A	Monsabrais-Py2	0.023275	0.067498	31.9333	0.0088445	0	-0.0067265	0.12103	1.04272	79.135	23.7405
LK77-1A	Monsabrais-Py2	0.049809	0.057257	82.3935	0.020482	0.003724	0.0162925	0.0870485	0.265335	30.723	7.1687
LK77-1B	Monsabrais-Py2	0.053998	0.033051	8.89105	0.0041895	0.011172	-0.0074294	0.011172	0.40033	12.103	0.851865
61-1A	Chadbourne	0.118703	0.04655	7.1687	0.488775	0.442225	-0.0033982	0.0358435	0.94962	-0.2793	5.106535
61-1B	Chadbourne	0.221578	0.147564	15.7339	0.99617	0.92169	-0.0023741	0.2145955	0.7448	5.91185	9.0307
61-1C	Chadbourne	0.179683	0.26068	26.39385	0.120099	0.091238	-0.004655	1.07065	0.879795	170.8385	9.31
61-3A	Chadbourne	0.109858	0.064239	7.40145	0.34447	0.209475	-0.0027465	0.031654	0.58653	1.2103	4.2826
HB2-2A	Bouchard-Hébert	4.259325	7.1687	2.98851	0.2229745	0.208544	0.0060515	0.91238	2.5137	451.535	70.756
HB2-4A	Bouchard-Hébert	0.368676	3.26781	1.42443	0.63308	0.69825	-0.0004655	0.3724	2.890755	76.342	32.07295

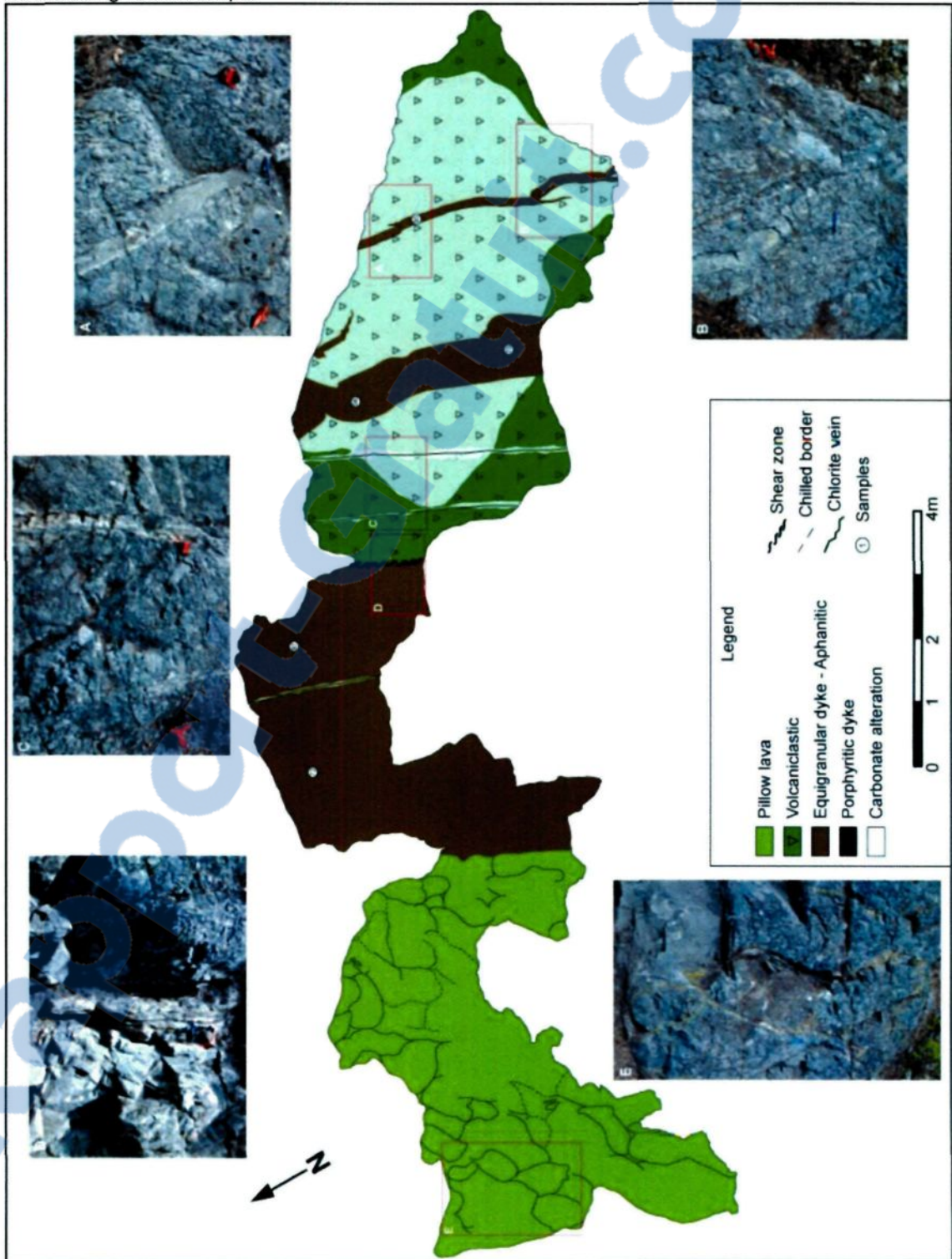B) Pyrrhotites elemental data analyzed by the LA-ICP-MS.

Sample	Source	^{33}S (ppm)	^{34}S (ppm)	^{51}V (ppm)	^{52}Cr (ppm)	^{53}Cr (ppm)	^{55}Mn (ppm)	^{59}Co (ppm)	^{60}Ni (ppm)	^{65}Cu (ppm)	^{66}Zn (ppm)
LK85-1A	Monsabrais	1533318	590888.4	6918.63	4.92407	22.62579	29.54442	188.2366	816.523	10596.1	66.6931
LK85-1B	Monsabrais	2169084	587148.6	8975.52	6.48232	30.29238	31.60131	232.4909	461.8653	6046.01	57.9669
LK85-2A	Monsabrais	40015.86	438179.9	184.4968	0.1651745	1.938463	13.7126	48.43041	351.5412	8595.307	3.209995
LK85-2B	Monsabrais	80405.7	578422.4	2181.55	1.140639	17.88871	17.01609	78.5358	346.5548	7697.755	14.46056
LK85-3A	Monsabrais	417611	577175.8	3029.238	2.873413	19.9456	21.25453	137.7493	428.8304	6600.747	29.66908
LK07-1A	Monsabrais	330349	474954.6	1477.221	18.0757	4.79941	15.64483	76.6659	795.9541	4724.614	1.62058
LK07-1B	Monsabrais	188236.6	473084.7	141489.1	5.11106	6.73164	17.95104	133.3862	590.8884	6108.34	2.74252
LK07-2A	Monsabrais	33097.23	465605.1	292.951	0.2281278	2.156618	13.89959	48.49274	658.2048	5192.089	5.17339
LK07-3A	Monsabrais	39766.54	446282.8	181.3803	0.274252	2.212715	13.77493	52.41953	798.4473	4001.586	1.315163
LK77-1C	Monsabrais	723028	418857.6	28048.5	69.1863	54.2271	61.7067	386.446	215.0385	11905.03	2.55553
LK77-1D	Monsabrais	984814	428830.4	40265.18	68.563	37.64732	47.43313	421.3508	438.8032	17701.72	11.90503
LK77-2A	Monsabrais	81652.3	527935.1	1832.502	3.80213	19.63395	21.00521	110.3241	530.4283	11905.03	23.93472
LK38-1A	Monsabrais	43007.7	394548.9	828.989	1.520852	2.231414	15.45784	52.91817	1065.843	10222.12	5.04873
LK38-1B	Monsabrais	35777.42	441296.4	7043.29	1.283998	2.18155	14.46056	53.66613	370.8635	8788.53	2.393472
LK38-2A	Monsabrais	92871.7	410131.4	6233	7.60426	8.7262	19.75861	63.63893	484.3041	7030.824	6.35766
LK87-1A	Monsabrais	230621	610210.7	1682.91	18.699	4.73708	15.27085	292.951	710.562	35590.43	177.6405
MM-22-1A	Géant Dormant	66069.8	576552.5	461.8653	0.49864	24.3087	26.8019	46.80983	1569.4694	4699.682	0.473708
MM-22-1B	Géant Dormant	83522.2	548504	673.164	0.4780711	6.60698	16.95376	44.44129	1636.7858	4693.449	2.000793
MM-22-2A	Géant Dormant	75730.95	547880.7	408.8848	0.4662284	6.66931	14.77221	43.25702	1614.347	4045.217	0.772892

Sample	Source	^{71}Ga (ppm)	^{72}Ge (ppm)	^{75}As (ppm)	^{82}Se (ppm)	^{95}Mo (ppm)	^{98}Mo (ppm)	^{107}Ag (ppm)	^{111}Cd (ppm)	^{115}In (ppm)	^{118}Sn (ppm)
LK85-1A	Monsabrais	5.11106	0.785358	6.320262	239.9705	84.1455	1.527085	0	0.573436	0.205689	0.0193223
LK85-1B	Monsabrais	13.0893	0.947416	5.952515	331.5956	72.17814	1.988327	4.42543	0.193223	0.168291	0.0180757
LK85-2A	Monsabrais	2.36854	0.028672	5.354147	0.704329	54.60108	0.0280485	0	0.1078309	0.0168291	0.0011843
LK85-2B	Monsabrais	24.3087	0.180757	5.460108	2.05689	72.11581	0.1097008	4.3631	0.405145	0.180757	0.0052357
LK85-3A	Monsabrais	5.17339	0.866387	5.634632	42.3844	81.15366	0.691863	4.23844	0.0928717	0.149592	0.0118427
LK07-1A	Monsabrais	2.61786	1.62058	5.54737	0.804057	18.699	0.211922	4.3631	0.417611	0.0031165	0.0099728
LK07-1B	Monsabrais	8.7262	0.153332	5.210788	0.654465	20.63123	-0.0024309	0.99728	0.2094288	0.193223	-0.001995
LK07-2A	Monsabrais	0.274252	0.065447	5.260652	0.548504	16.95376	0.523572	1.2466	0.1427357	0.0305417	0.0006233
LK07-3A	Monsabrais	0.698096	0.045501	4.92407	0.878853	20.00793	0.0529805	1.62058	0.255553	0.105961	0.006233
LK77-1C	Monsabrais	28.6718	3.86446	5.85902	0.660698	7.54193	0	10.5961	0.367747	-0.024932	0.0230621
LK77-1D	Monsabrais	25.74229	2.331142	5.578535	0.660698	10.53377	0.0641999	0	0.766659	0.0461242	0.0218155
LK77-2A	Monsabrais	5.6097	0.342815	5.241953	2.050657	11.65571	0.405145	0	0.255553	0.031165	0.0081029
LK38-1A	Monsabrais	3.1165	0.061083	5.067429	0.822756	58.15389	0.286718	-1.050261	0.635766	-0.009973	-0.001995
LK38-1B	Monsabrais	3.55281	0.081652	5.135992	0.492407	60.52243	0.0118427	4.42543	0.473708	0.342815	0.0014959
LK38-2A	Monsabrais	3.92679	0.218155	4.843041	0.704329	59.71214	0.180757	0	0.49864	0.087262	0.0011843
LK87-1A	Monsabrais	16.8291	0.723028	4.61242	0.43631	138.3726	0.068563	0	221.2715	2.30621	0.0317883
MM-22-1A	Géant Dormant	13.0893	0.057344	8.464414	3.041704	45.62556	0.155825	-0.99728	0.461242	0.224388	0.0013713
MM-22-1B	Géant Dormant	105.961	0.066693	7.884745	2.661491	47.9941	0.0430077	1.18427	0.56097	0.741727	0.0041138
MM-22-2A	Géant Dormant	58.5902	0.046124	8.389618	2.381006	53.22982	0.299184	2.99184	0.1957162	0.236854	0.0043008

Sample	Source	^{121}Sb (ppm)	^{125}Te (ppm)	^{182}W (ppm)	^{184}W (ppm)	^{195}Pt (ppm)	^{197}Au (ppm)	^{200}Hg (ppm)	^{202}Hg (ppm)	^{208}Pb (ppm)	^{209}Bi (ppm)
LK85-1A	Monsabrais	2.019492	0.710562	1.944696	0.37398	0.330349	0.0268019	0.0018699	1.49592	25.5553	2.711355
LK85-1B	Monsabrais	1.68291	0.536038	1.202969	0.355281	0.2786151	0.0021816	0	1.290231	33.0349	3.203762
LK85-2A	Monsabrais	0.115311	0.041138	0.099728	0.0087262	0.0105961	0.0105961	0.0063577	2.175317	1.74524	0.947416
LK85-2B	Monsabrais	0.330349	0.218155	2.80485	0.0236854	0.0031165	-0.0239347	0.0043631	1.30893	6.233	2.74252
LK85-3A	Monsabrais	0.604601	0.336582	1.439823	0.0991047	0.0860154	0.0074796	0.0034905	1.470988	14.9592	0.81029
LK07-1A	Monsabrais	0.517339	0.06794	0.93495	0	0.0037398	0	-0.006856	1.37126	94.7416	2.592928
LK07-1B	Monsabrais	0.06046	0.046124	0.679397	0.0081029	-0.000249	0.0037398	0	1.18427	44.8776	1.43359
LK07-2A	Monsabrais	0.093495	0.044254	0.149592	0.0099728	-0.003634	0.0292951	-0.001608	1.49592	1.2466	0.922484
LK07-3A	Monsabrais	0.193223	0.06981	0.330349	-0.000623	0.0174524	0.0211922	-0.003927	1.763939	11.8427	2.80485
LK77-1C	Monsabrais	0.504873	0.018076	1.37126	0.0031165	-0.015022	0	0	2.18155	4.3631	3.945489
LK77-1D	Monsabrais	0.779125	0.064823	1.015979	-0.002007	-0.002493	0.0261786	0.0112194	1.115707	99.728	3.291024
LK77-2A	Monsabrais	0.455009	0.268019	2.43087	0.0330349	0.0723028	-0.0023062	0.0056097	0.87262	2.4932	2.36854
LK38-1A	Monsabrais	0.130893	0.057344	0.87262	0	0.0012466	-0.0211922	0.0006233	1.43359	-2.05689	7.4796
LK38-1B	Monsabrais	0.155825	0.087262	0.361514	0.006233	-0.012466	-0.037024	-0.00331	1.30893	-5.79669	2.74252
LK38-2A	Monsabrais	0.174524	0.05672	1.676677	0	-0.001589	-0.0137126	0	1.62058	-1.375075	10.28445
LK87-1A	Monsabrais	0.174524	0.037398	-0.87262	-0.002917	0	0.043631	0.018699	1.12194	2754.986	21.75317
MM-22-1A	Géant Dormant	0.004363	0.035528	-0.04363	0.0299184	0.0069186	0.0162058	0.006233	3.085335	22.4388	1.153105
MM-22-1B	Géant Dormant	-0.01434	0.067316	-0.5485	0.0087262	0.0056097	0.0292951	0.0037398	1.358794	0.99728	2.966908
MM-22-2A	Géant Dormant	0.129646	0.051111	0.673164	0.0243087	0.0074796	0.0074796	-0.009038	1.93223	12.466	0.866387

Appendix 8

A) Detailed map of a small area on the Monsabrais sector, showing the dykes and volcanic rock crosscutting relationships.

B) Detailed map of a small area on the Monsabrais sector, showing the dyke crosscutting relationships.

Legend

Volcaniclastic	Chilled borders
Equigranular dyke - Aphanitic	Chlorite veins
Porphyritic dyke	Samples
Carbonate alteration	

0 1 2 4m